

Article

# On the Resonant Vibrations Control of the Nonlinear Rotor Active Magnetic Bearing Systems

Nasser A. Saeed <sup>1,\*</sup> , Sabry M. El-Shourbagy <sup>2</sup>, Magdi Kamel <sup>1</sup>, Kamal R. Raslan <sup>3</sup>, Jan Awrejcewicz <sup>4</sup>   
and Khaled A. Gepreel <sup>5</sup> 

<sup>1</sup> Department of Physics and Engineering Mathematics, Faculty of Electronic Engineering, Menoufia University, Menouf 32952, Egypt

<sup>2</sup> Department of Basic Science, Higher Technological Institute, Tenth of Ramadan City 44629, Egypt

<sup>3</sup> Mathematics Department, Faculty of Science, Al-Azhar University, Nasr City 11651, Egypt

<sup>4</sup> Department of Automation, Biomechanics and Mechatronics, Faculty of Mechanical Engineering, Lodz University of Technology, 90924 Lodz, Poland

<sup>5</sup> Department of Mathematics, College of Science, Taif University, P.O. Box 11099, Taif 21944, Saudi Arabia

\* Correspondence: nasser.a.saeed@el-eng.menofia.edu.eg

**Abstract:** Nonlinear vibration control of the twelve-poles electro-magnetic suspension system was tackled in this study, using a novel control strategy. The introduced control algorithm was a combination of three controllers: the proportional-derivative (*PD*) controller, the integral resonant controller (*IRC*), and the positive position feedback (*PPF*) controller. According to the presented control algorithm, the mathematical model of the controlled twelve-poles rotor was established as a nonlinear four-degree-of-freedom dynamical system coupled to two first-order filters. Then, the derived nonlinear dynamical system was analyzed using perturbation analysis to extract the averaging equations of motion. Based on the extracted averaging equations of motion, the efficiency of different control strategies (i.e., *PD*, *PD + IRC*, *PD + PPF*, and *PD + IRC + PPF*) for mitigating the rotor's undesired vibrations and improving its catastrophic bifurcation was investigated. The acquired analytical results demonstrated that both the *PD* and *PD + IRC* controllers can force the rotor to respond as a linear system; however, the controlled system may exhibit the maximum oscillation amplitude at the perfect resonance condition. In addition, the obtained results demonstrated that the *PD + PPF* controller can eliminate the rotor nonlinear oscillation at the perfect resonance, but the system may suffer from high oscillation amplitudes when the resonance condition is lost. Moreover, we report that the combined control algorithm (*PD + IRC + PPF*) has all the advantages of the individual control algorithms (i.e., *PD*, *PD + IRC*, *PD + PPF*), while avoiding their drawbacks. Finally, the numerical simulations showed that the *PD + IRC + PPF* controller can eliminate the twelve-poles system vibrations regardless of both the excitation force magnitude and the resonant conditions at a short transient time.

**Keywords:** nonlinear vibration control; rotor electro-magnetic suspension system; *PD*-control algorithm; *IRC*-control algorithm; *PPF*-control algorithm; forward whirling motion; rub/impact force



**Citation:** Saeed, N.A.; El-Shourbagy, S.M.; Kamel, M.; Raslan, K.R.; Awrejcewicz, J.; Gepreel, K.A. On the Resonant Vibrations Control of the Nonlinear Rotor Active Magnetic Bearing Systems. *Appl. Sci.* **2022**, *12*, 8300. <https://doi.org/10.3390/app12168300>

Academic Editor: Fabio La Foresta

Received: 4 July 2022

Accepted: 16 August 2022

Published: 19 August 2022

**Publisher's Note:** MDPI stays neutral with regard to jurisdictional claims in published maps and institutional affiliations.



**Copyright:** © 2022 by the authors. Licensee MDPI, Basel, Switzerland. This article is an open access article distributed under the terms and conditions of the Creative Commons Attribution (CC BY) license (<https://creativecommons.org/licenses/by/4.0/>).

## 1. Introduction

Vibration analysis and control of the electro-magnetic suspension system are among the most important research topics for scientists and engineers worldwide. The importance of this suspension system is due to its many industrial applications, including its use in rotor dynamics and in the automobile industries. The rotor electro-magnetic suspension system is a special type of active bearing that is used to support the rotating shafts without any physical contact with the stator parts of the system. The working principle of rotor electro-magnetic suspension is the application of controllable electro-magnetic attractive forces to support the rotating shafts in their hovering positions via compensating for the external loads that are exerted on these shafts. The operation of the rotating shafts

without physical contact with the stators gives this suspension system many preferable features when compared with conventional bearings systems, such as less maintenance, no need for lubrication between the rotors and stators, a clean working environment, high operational speed, high reliability, and high durability. Accordingly, many research articles have investigated the dynamical characteristics of different configurations of the rotor electro-magnetic suspension system.

Different control algorithms have been proposed to enhance the vibratory characteristics and eliminate the undesired nonlinear bifurcation behaviors of this suspension system. Ji et al. [1] studied the nonlinear dynamics and motion bifurcations of a rotor electro-magnetic suspension system consisting of a four-poles configuration. They established the mathematical model that governs the rotor lateral vibrations as a two-degree-of-freedom nonlinear dynamical system. Then, they investigated the derived equations of motion using the multiple-time scales perturbation method. Based on their analysis, they reported that the rotor system may lose its stability either via saddle-node or Hopf bifurcations.

Saeed et al [2] investigated the vibratory characteristics of a rotor supported by a six-poles electro-magnetic suspension system. They introduced two control strategies utilizing the *PD*-control algorithm. The first control technique was established based on the Cartesian displacements and velocities of the rotor in the horizontal and vertical directions, while the second control technique was designed according to the radial oscillations of the rotor in the direction of the six poles. Based on their analysis, they reported that the rotor system may lose its stability and exhibit unbounded oscillation in the case of the radial control technique at a specific value of the proportional gain. In addition, they showed that the system may perform either a quasi-periodic or chaotic response in the case of the Cartesian control strategy at a strong excitation force.

Ji and Hansen [3,4] studied the nonlinear dynamics of a rotor supported by an eight-poles electro-magnetic suspension system. They applied the Cartesian *PD*-control strategy to improve the vibratory characteristics of that system at both primary [3] and super-harmonic resonance conditions [4]. They reported that the eight-poles system has bi-stable and tri-stable solutions. In addition, they showed that the system may be exposed to a multi-jump when the rotor angular speed crosses its first critical speed.

El-Shourbagy et al. [5] introduced a nonlinear *PD*-control algorithm to enhance the nonlinear lateral vibrations of a rotor supported by an eight-poles electro-magnetic suspension system. Saeed et al. [6] explored numerically the motion bifurcations of a rotor system supported by the eight poles when the rub-impact force between the rotor and stator occurs. They illustrated that the rotor may execute either full annular rub mode or rub-impact motion, depending on both the impact stiffness and the dynamic friction coefficients. In addition, Zhang et al. [7–12] introduced detailed investigations of the eight-poles electro-magnetic suspension system with variable stiffness coefficients. The nonlinear dynamical behaviors of the twelve-poles electro-magnetic suspension system were investigated utilizing the *PD*-control algorithm for the first time by El-Shourbagy et al. [13]. They reported that proportional control gain can play an important role in reshaping the system dynamics. In addition, they demonstrated that the twelve-poles system may lose its stability at a strong excitation force. Saeed et al. [14] explored the dynamical characteristics of the sixteen-poles system with constant stiffness coefficients utilizing the conventional *PD*-control algorithm. Zhang et al. [15–18] introduced extensive investigations for the sixteen-poles rotor system with time-varying stiffness coefficients. Due to the controllability and flexibility of the rotor electro-magnetic suspension system, it was used as an active actuator to control the dynamical behaviors of some rotating machines [19–23].

The positive position feedback (*PPF*) control algorithm has been applied extensively to eliminate the resonant vibrations of many dynamical systems [24–28]. Saeed et al. [28] utilized the *PPF*-control strategy with a *PD* controller to mitigate the undesired vibrations of the eight-poles rotor system for the first time. They concluded that the *PPF* controller can eliminate the system's lateral vibration at the perfect resonance condition. However, the main drawback of this control strategy was that the controller may add excessive

vibratory motion to the rotor system if the tuning condition was lost. In addition, the integral resonance controller (*IRC*) was one of the feasible control methods that was applied to mitigate the undesired vibrations and eliminate the nonlinear bifurcations of different dynamical systems [29–36]. Recently, Saeed et al. [36] introduced the *IRC*-control algorithm for the first time to mitigate the unwanted vibrations of the eight-poles rotor system. They reported that the *IRC* controller can reduce the system's vibrations and suppress the corresponding catastrophic bifurcations. However, the main drawback of this control method was that the *IRC*-controller could not eliminate the rotor vibrations at a resonance condition close to zero.

In the present work, a new control strategy is introduced to eliminate the nonlinear lateral vibrations of the twelve-poles rotor system. The proposed controller is a combination of the three control algorithms: *PD*, *IRC*, and *PPF*. Accordingly, the whole-system mathematical model is derived as a four-degree-of-freedom dynamical system that is coupled to two first-order differential equations. Then, the system dynamical model is analyzed, and the corresponding slow-flow modulation equations are extracted. Based on the obtained slow-flow modulation equation, the performance of the suggested control technique is explored. The obtained analytical results showed that the *PD*, *IRC*, and *PD + IRC* controllers can mitigate the nonlinear oscillation of the system and force the rotor to respond as a linear system. but the main drawback of these types of controllers (i.e., *PD*, *IRC*, and *PD + IRC*) is that the controlled system may perform the maximum oscillation amplitude at the resonant condition. In addition, we found that the coupling of the *PD + PPF* controller to the system can eliminate the rotor's undesired oscillation at the perfect resonance, but the system may suffer from high oscillation amplitudes if the resonance condition is lost. Moreover, the acquired analytical and numerical investigations demonstrated that the *PD + IRC + PPF* controller has all the advantages of the individual control algorithms (i.e., *PD*, *PD + IRC*, and *IRC + PPF*), while avoiding their drawbacks.

## 2. Equations of Motion

The studied rotor system is assumed to be a rigid body with a two-degree-of-freedom system that has mass  $m$  and eccentricity  $e$  and rotates with angular velocity  $\psi$ , as shown in Figure 1. In addition, this rotor system is supported in its nominal position via the restoring forces  $f_x$  and  $f_y$  that are generated by twelve electro-magnetic poles. Therefore, the system equations of motion can be expressed as follows [37,38]:

$$m\ddot{x} - f_x = m\psi^2 \cos(\psi t) \quad (1)$$

$$m\ddot{y} - f_y = m\psi^2 \sin(\psi t) \quad (2)$$

where  $f_x$  and  $f_y$  represent the resultant restoring forces of the twelve poles in both the  $X$  and  $Y$  directions, respectively. In this study, the attractive forces  $f_j$  ( $j = 1, 2, \dots, 6$ ) are designed so that each adjacent pair of the poles generates a push-pull attractive force. Therefore,  $f_j$  ( $j = 1, 2, \dots, 6$ ) can be expressed according to the electro-magnetic theory, as follows [38]:

$$f_j = \Theta \left[ \frac{(I_0 - I_j)^2}{(c_0 - \delta_j)^2} - \frac{(I_0 + I_j)^2}{(c_0 + \delta_j)^2} \right], \quad j = 1, 2, \dots, 6 \quad (3)$$

where  $\Theta = \frac{1}{4}\mu_0 N^2 A \cos(\varphi)$  is constant,  $I_0$  is constant current defined as a bias current,  $I_j$  ( $j = 1, 2, \dots, 6$ ) is the control currents that will be defined later according to the purposed control algorithm,  $c_0$  is the nominal air-gap size between the rotor and the twelve poles, and  $\delta_j$  is the radial deviation of the rotor away from the geometric center  $O$  in the direction of the  $j^{\text{th}}$  pole.

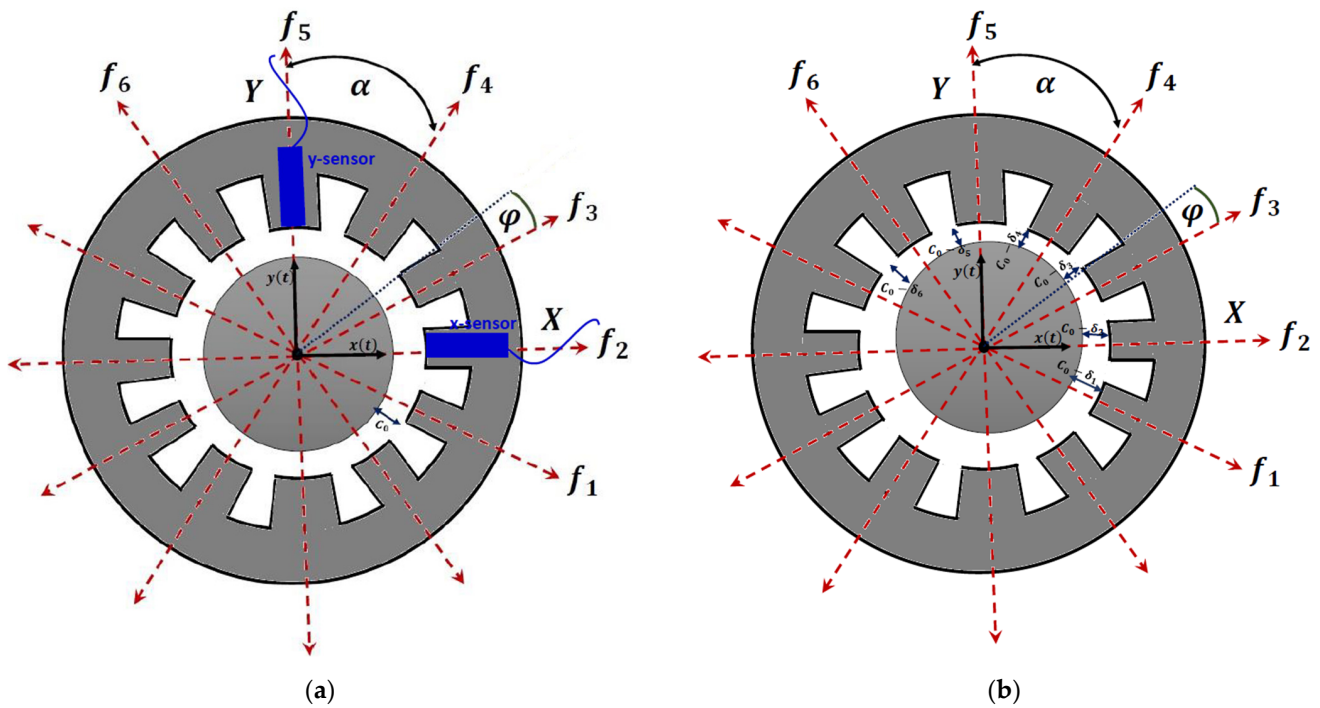


**Figure 1.** (a) twelve-poles rotor system at its nominal position, (b) twelve-poles rotor system with small displacements  $x(t)$  and  $y(t)$  in the horizontal and vertical directions, respectively.

Based on the system’s geometry as shown in Figure 1, for the small temporal Cartesian displacements  $x(t)$  and  $y(t)$  of the rotor in both the X and Y directions, one can express the radial displacements  $\delta_j$ , ( $j = 1, 2, \dots, 6$ ) of the rotor system as follows:

$$\left. \begin{aligned} \delta_1(x, y) &= x(t) \cos(\alpha) - y(t) \sin(\alpha), & \delta_2(x, y) &= x(t), \\ \delta_3(x, y) &= x(t) \cos(\alpha) + y(t) \sin(\alpha), & \delta_4(x, y) &= x(t) \sin(\alpha) + y(t) \cos(\alpha), \\ \delta_5(x, y) &= y(t), & \delta_6(x, y) &= -x(t) \sin(\alpha) + y(t) \cos(\alpha) \end{aligned} \right\} \quad (4)$$

where  $\alpha$  is the angle between every two consecutive poles (i.e.,  $\alpha = 360^\circ / 12 = 30^\circ$ ). In this work, the control currents were designed so that the control forces  $f_1$ ,  $f_2$ , and  $f_3$  depend on the horizontal displacement  $x(t)$ , while the forces  $f_4$ ,  $f_5$ , and  $f_6$  depend on the vertical displacement  $y(t)$ . Accordingly, the control currents  $I_j$  ( $j = 1, 2, \dots, 6$ ) are selected as follows:

$$I_X = I_1 = I_2 = I_3, \quad I_Y = I_4 = I_5 = I_6 \quad (5)$$

where  $I_X$  is the control current that is responsible for eliminating the nonlinear oscillations of the rotor system in the X direction, while  $I_Y$  is the control current that is responsible for eliminating the nonlinear oscillations of the rotor system in the Y direction. Accordingly, to eliminate the undesired vibrations of the system, an advanced control strategy was introduced. The suggested control method is a combination of three control algorithms: the PD controller, the IRC controller, and the PPF controller. Therefore, the control laws (i.e., control currents  $I_X$  and  $I_Y$ ) are designed as follows:

$$I_X = k_1x + k_2\dot{x} - k_3u_1 + k_4u_2, \quad I_Y = k_1y + k_2\dot{y} - k_5v_1 + k_6v_2 \quad (6)$$

where  $k_1$  and  $k_2$  are the control gains of the PD controller,  $k_3$  and  $k_5$  denote the control gains of the PPF controller, and  $k_4$  and  $k_6$  represent the control gains of the IRC controller. Accordingly,  $k_1x + k_2\dot{x}$  and  $k_1y + k_2\dot{y}$  are the components of the control currents ( $I_X$  and  $I_Y$ ) due to the PD controller in the X and Y directions, respectively,  $-k_3u_1$  and  $-k_5v_1$  are the components of the control currents due to the PPF controller in the X and Y directions, respectively, while  $+k_4u_2$  and  $+k_6v_2$  denote the control current components due to the IRC



controller in the X and Y directions, respectively. The equations of motion that describe the oscillatory behaviors of the PPF controllers are provided as follows [24–28]:

$$\ddot{u}_1 + c_1\dot{u}_1 + \lambda_1u_1 = L_1x \tag{7}$$

$$\ddot{v}_1 + c_2\dot{v}_1 + \lambda_2v_1 = L_2y \tag{8}$$

where  $c_1$  and  $c_2$  denote the damping coefficients of the PPF controllers,  $\lambda_1$  and  $\lambda_2$  represent the controller’s natural frequencies, and  $L_1$  and  $L_2$  are the feedback signals gains. In addition, the dynamical behaviors of the IRC controllers are governed by first-order differential equations that are provided as follows [29–36]:

$$\dot{u}_2 + \lambda_3u_2 = L_3x \tag{9}$$

$$\dot{v}_2 + \lambda_4v_2 = L_4y \tag{10}$$

where  $\lambda_3$  and  $\lambda_4$  denote the internal feedback gain of the IRC controller, and  $L_3$  and  $L_4$  represent the feedback signals gains. The interconnection between the twelve-poles system and the proposed control algorithm (i.e., the PD + IRC + PPF controllers) is illustrated schematically in Figure 2, where the temporal Cartesian oscillations (i.e.,  $x(t)$  and  $y(t)$ ) of the rotor in both the X and Y directions can be measured using two position sensors that may be fixed on the poles-housing in the +X and +Y directions, as shown in Figure 1a. Then, the measured signals,  $x(t)$  and  $y(t)$ , are fed into a digital computer on which the control algorithm (i.e., the PD+IRC+PPF controller) is implemented. According to the programmed algorithm, the controller computes the control currents  $I_X = k_1x + k_2\dot{x} - k_3u_1 + k_4u_2$  and  $I_Y = k_1y + k_2\dot{y} - k_5v_1 + k_6v_2$ , as shown in Figure 2. Finally, the computed control currents are applied to a power amplifiers network to energize the twelve-poles electrical coils in order to generate the electro-magnetic forces ( $f_1, f_2, \dots, f_6$ ), which in turn try to mitigate the lateral oscillations,  $x(t)$  and  $y(t)$ , of the rotor system.

Now, to investigate the performance of the proposed closed-loop system, the whole-system model should be obtained and then analyzed to report the optimum working conditions of this system. Therefore, by substituting Equations (4) to (6) into Equation (3), we have the following:

$$f_1 = \Theta\left(\frac{(I_0 - k_1x - k_2\dot{x} + k_3u_1 - k_4u_2)^2}{(c_0 - x \cos(\alpha) + y \sin(\alpha))^2} - \frac{(I_0 + k_1x + k_2\dot{x} - k_3u_1 + k_4u_2)^2}{(c_0 + x \cos(\alpha) - y \sin(\alpha))^2}\right) \tag{11}$$

$$f_2 = \Theta\left(\frac{(I_0 - k_1x - k_2\dot{x} + k_3u_1 - k_4u_2)^2}{(c_0 - x)^2} - \frac{(I_0 + k_1x + k_2\dot{x} - k_3u_1 + k_4u_2)^2}{(c_0 + x)^2}\right) \tag{12}$$

$$f_3 = \Theta\left(\frac{(I_0 - k_1x - k_2\dot{x} + k_3u_1 - k_4u_2)^2}{(c_0 - x \cos(\alpha) - y \sin(\alpha))^2} - \frac{(I_0 + k_1x + k_2\dot{x} - k_3u_1 + k_4u_2)^2}{(c_0 + x \cos(\alpha) + y \sin(\alpha))^2}\right) \tag{13}$$

$$f_4 = \Theta\left(\frac{(I_0 - k_1y - k_2\dot{y} + k_5v_1 - k_6v_2)^2}{(c_0 - x \sin(\alpha) - y \cos(\alpha))^2} - \frac{(I_0 + k_1y + k_2\dot{y} - k_5v_1 + k_6v_2)^2}{(c_0 + x \sin(\alpha) + y \cos(\alpha))^2}\right) \tag{14}$$

$$f_5 = \Theta\left(\frac{(I_0 - k_1y - k_2\dot{y} + k_5v_1 - k_6v_2)^2}{(c_0 - y)^2} - \frac{(I_0 + k_1y + k_2\dot{y} - k_5v_1 + k_6v_2)^2}{(c_0 + y)^2}\right) \tag{15}$$

$$f_6 = \Theta\left(\frac{(I_0 - k_1y - k_2\dot{y} + k_5v_1 - k_6v_2)^2}{(c_0 + x \sin(\alpha) - y \cos(\alpha))^2} - \frac{(I_0 + k_1y + k_2\dot{y} - k_5v_1 + k_6v_2)^2}{(c_0 - x \sin(\alpha) + y \cos(\alpha))^2}\right) \tag{16}$$

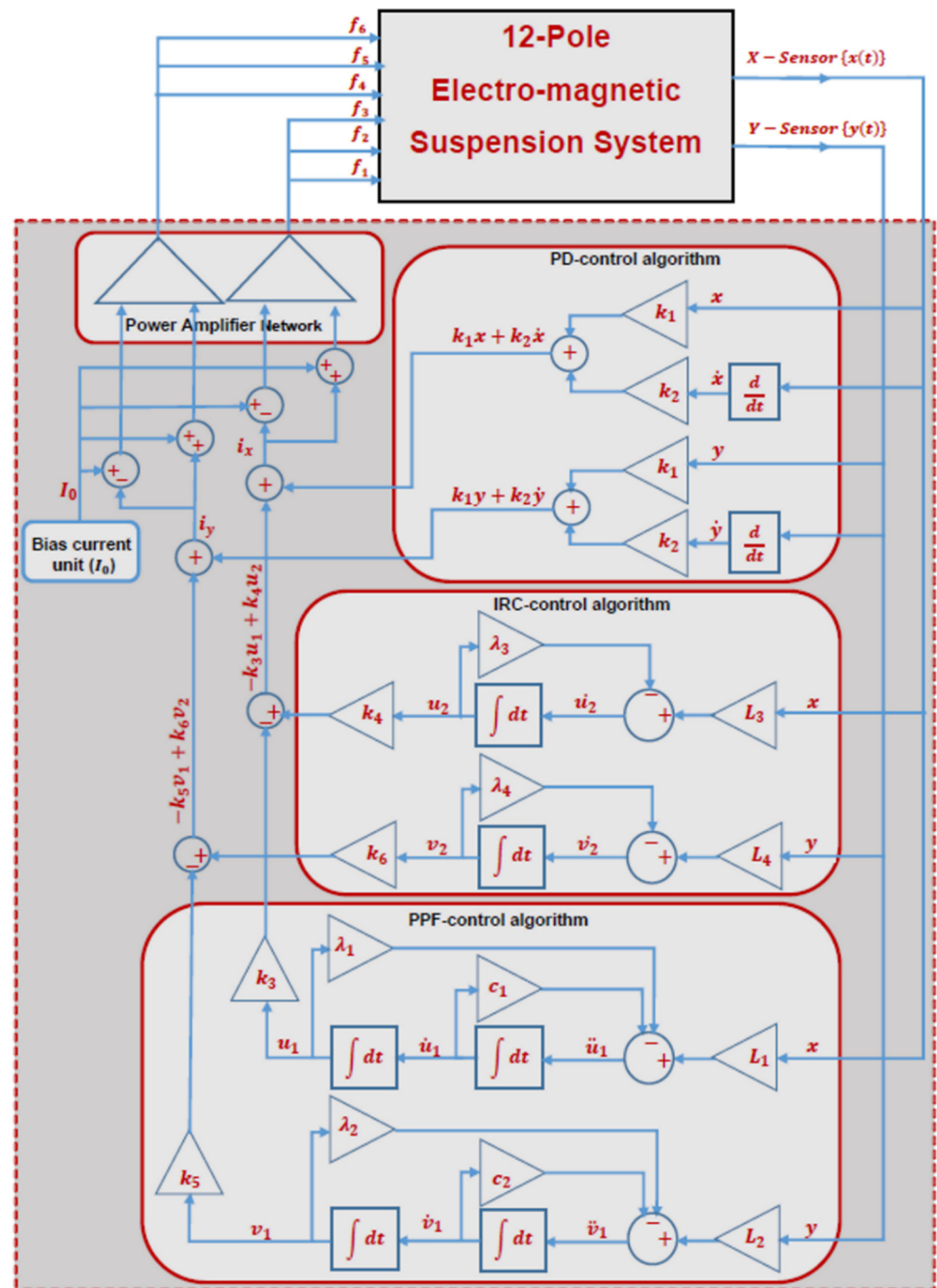


**Figure 2.** The engineering implementation of the combined control algorithm (i.e., PD + IRC + PPF controller).

Based on the system geometry, as shown in Figure 1, the resultant attractive forces  $f_x$  and  $f_y$  in the X and Y directions due to the forces  $f_1, f_2, \dots, f_6$  can be expressed as follows:

$$f_x = f_2 + (f_1 + f_3) \cos(\alpha) + (f_4 - f_6) \sin(\alpha) \tag{17}$$

$$f_y = f_5 + (f_4 + f_6) \cos(\alpha) + (f_3 - f_1) \sin(\alpha) \tag{18}$$

To simplify the rational form of the attractive forces  $f_1, f_2, \dots, f_6$ , Equations (11) to (16) were expanded, using the Maclaurin series, up to the third order approximation, as provided in Appendix A. Now, substituting the expanded Equations (A1) to (A6) that are

provided in Appendix A into Equations (17) and (18), then inserting the resulting equations into Equations (1) and (2) and introducing the dimensionless parameters:  $t^* = \vartheta t, z_1 = \frac{x}{c_0}, \dot{z}_1 = \frac{\dot{x}}{\vartheta c_0}, \ddot{z}_1 = \frac{\ddot{x}}{\vartheta^2 c_0}, z_2 = \frac{y}{c_0}, \dot{z}_2 = \frac{\dot{y}}{\vartheta c_0}, \ddot{z}_2 = \frac{\ddot{y}}{\vartheta^2 c_0}, z_3 = \frac{u_1}{c_0}, \dot{z}_3 = \frac{\dot{u}_1}{\vartheta c_0}, \ddot{z}_3 = \frac{\ddot{u}_1}{\vartheta^2 c_0}, z_4 = \frac{v_1}{c_0}, \dot{z}_4 = \frac{\dot{v}_1}{\vartheta c_0}, \ddot{z}_4 = \frac{\ddot{v}_1}{\vartheta^2 c_0}, z_5 = \frac{u_2}{c_0}, \dot{z}_5 = \frac{\dot{u}_2}{\vartheta c_0}, z_6 = \frac{v_2}{c_0}, \dot{z}_6 = \frac{\dot{v}_2}{\vartheta c_0}, \omega_1 = \sqrt{\frac{\lambda_1}{\vartheta^2}}, \omega_2 = \sqrt{\frac{\lambda_2}{\vartheta^2}}, \omega_3 = \frac{\lambda_3}{\vartheta}, \omega_4 = \frac{\lambda_4}{\vartheta}, \Omega = \frac{\psi}{\vartheta}, f = \frac{e}{c_0}, p = \frac{c_0}{I_0} k_1, d = \frac{c_0 \vartheta}{I_0} k_2, \mu_1 = \frac{c_1}{2\vartheta}, \mu_2 = \frac{c_2}{2\vartheta}, \eta_1 = \frac{(1+2\cos(\alpha))c_0}{I_0} k_3, \eta_2 = \frac{(1+2\cos(\alpha))c_0}{I_0} k_4, \eta_3 = \frac{(1+2\cos(\alpha))c_0}{I_0} k_5, \eta_4 = \frac{(1+2\cos(\alpha))c_0}{I_0} k_6, \eta_5 = \frac{L_1}{\vartheta^2}, \eta_6 = \frac{L_2}{\vartheta^2}, \eta_7 = \frac{L_3}{\vartheta}, \eta_8 = \frac{L_4}{\vartheta}, \vartheta = \sqrt{\Theta/mc_0^3}$ , one can obtain the following dimensionless equations of motion that govern the nonlinear dynamics of the proposed closed-loop system:

$$\begin{aligned} & \ddot{z}_1 + 2\mu\dot{z}_1 + \omega^2 z_1 - (\alpha_1 z_1^3 + \alpha_2 z_1 z_2^2 + \alpha_3 z_1^2 \dot{z}_1 + \alpha_4 \dot{z}_1 z_2^2 + \alpha_5 z_1 \dot{z}_2^2 + \alpha_6 z_1 \dot{z}_1^2 + \alpha_7 z_1 z_2 \dot{z}_2 \\ & + \beta_1 z_1^2 z_3 + \beta_2 z_1 \dot{z}_1 z_3 + \beta_3 z_1 z_3^2 + \beta_4 z_1 z_2 z_4 + \beta_5 z_1 z_4^2 + \beta_6 z_1 \dot{z}_2 z_4 + \beta_7 z_3 z_2^2 + \beta_8 z_1 z_3 z_5 \\ & + \beta_9 z_1 \dot{z}_1 z_5 + \beta_{10} z_1 z_4 z_6 + \beta_{11} z_1^2 z_5 + \beta_{12} z_1 z_6^2 + \beta_{13} z_1 z_2 z_6 + \beta_{14} z_1 \dot{z}_2 z_6 + \beta_{15} z_1 z_5^2 + \beta_{16} z_2^2 z_5) \\ & = \Omega^2 f \cos(\Omega t) + \eta_1 z_3 + \eta_2 z_5 \end{aligned} \tag{19}$$

$$\begin{aligned} & \ddot{z}_2 + 2\mu\dot{z}_2 + \omega^2 z_2 - (\alpha_1 z_2^3 + \alpha_2 z_2 z_1^2 + \alpha_3 z_2^2 \dot{z}_2 + \alpha_4 \dot{z}_2 z_1^2 + \alpha_5 z_2 \dot{z}_1^2 + \alpha_6 z_2 \dot{z}_2^2 + \alpha_7 z_2 z_1 \dot{z}_1 \\ & + \gamma_1 z_2^2 z_4 + \gamma_2 z_2 \dot{z}_2 z_4 + \gamma_3 z_2 z_4^2 + \gamma_4 z_2 z_1 z_3 + \gamma_5 z_2 z_3^2 + \gamma_6 z_2 \dot{z}_1 z_3 + \gamma_7 z_4 z_1^2 + \gamma_8 z_2 z_4 z_6 \\ & + \gamma_9 z_2 \dot{z}_2 z_6 + \gamma_{10} z_2 z_3 z_5 + \gamma_{11} z_2^2 z_6 + \gamma_{12} z_2 z_5^2 + \gamma_{13} z_2 z_1 z_5 + \gamma_{14} z_2 \dot{z}_1 z_5 + \gamma_{15} z_2 z_6^2 + \gamma_{16} z_1^2 z_6) \\ & = \Omega^2 f \sin(\Omega t) + \eta_3 z_4 + \eta_4 z_6 \end{aligned} \tag{20}$$

$$\ddot{z}_3 + 2\mu_1 \dot{z}_3 + \omega_1^2 z_3 = \eta_5 z_1 \tag{21}$$

$$\ddot{z}_4 + 2\mu_2 \dot{z}_4 + \omega_2^2 z_4 = \eta_6 z_2 \tag{22}$$

$$\dot{z}_5 + \omega_3 z_5 = \eta_7 z_1 \tag{23}$$

$$\dot{z}_6 + \omega_4 z_6 = \eta_8 z_2 \tag{24}$$

Equations (19) and (20) represent the dimensionless equations of motion of the controlled twelve-poles system, while Equations (21) and (22) are the dimensionless equations of motion of the PPF controller. In addition, Equations (23) and (24) are the dimensionless equations of motion of the IRC controller. Accordingly, the suggested closed-loop system is governed by six-coupled nonlinear ordinary differential equations, four of which are of the second order and the other two of which are of the first order, where the coefficients of the above six equations are provided in Appendix B.

### 3. Analytical Investigations

Many analytical methods have been introduced in the literature to investigate both the linear and nonlinear vibration problems [39–41]. Accordingly, to explore the efficiency of the introduced closed-loop system, we sought an approximate solution for the system equations of motions (i.e., Equations (19) to (24)) within this section, in the form of a first-order perturbation series as follows [39,40]:

$$z_1(t, \varepsilon) = z_{10}(T_0, T_1) + \varepsilon z_{11}(T_0, T_1) \tag{25}$$

$$z_2(t, \varepsilon) = z_{20}(T_0, T_1) + \varepsilon z_{21}(T_0, T_1) \tag{26}$$

$$z_3(t, \varepsilon) = z_{30}(T_0, T_1) + \varepsilon z_{31}(T_0, T_1) \tag{27}$$

$$z_4(t, \varepsilon) = z_{40}(T_0, T_1) + \varepsilon z_{41}(T_0, T_1) \tag{28}$$

$$z_5(t, \varepsilon) = \varepsilon z_{50}(T_0, T_1) + \varepsilon^2 z_{51}(T_0, T_1) \tag{29}$$

$$z_6(t, \varepsilon) = \varepsilon z_{60}(T_0, T_1) + \varepsilon^2 z_{61}(T_0, T_1) \tag{30}$$

where  $T_0 = t, T_1 = \epsilon t$ , and  $\epsilon$  is the perturbation parameter that was used as a bookkeeping coefficient during this analysis [40]. According to the introduced two-time scales (i.e.,  $T_0, T_1$ ), the ordinary derivatives  $\frac{d}{dt}$  and  $\frac{d^2}{dt^2}$  should be re-written as follows:

$$\frac{d}{dt} = D_0 + \epsilon D_1, \quad \frac{d^2}{dt^2} = D_0^2 + 2\epsilon D_0 D_1, \quad \text{and } D_j = \frac{\partial}{\partial T_j}, \quad j = 0, 1 \tag{31}$$

In addition, to perform the perturbation analysis using  $\epsilon$  as a bookkeeping coefficient, the parameters of Equations (19) to (24) should be re-scaled as follows:

$$f = \epsilon \tilde{f}, \quad \mu = \epsilon \tilde{\mu}, \quad \mu_1 = \epsilon \tilde{\mu}_1, \quad \mu_2 = \epsilon \tilde{\mu}_2, \quad \alpha_j = \epsilon \tilde{\alpha}_j, \quad \beta_j = \epsilon \tilde{\beta}_j, \quad \gamma_j = \epsilon \tilde{\gamma}_j, \quad \eta_k = \epsilon \tilde{\eta}_k; \tag{32}$$

$j = 1, \dots, 7, \quad k = 1, 3, 5, 6, 7, 8$

Then, by substituting Equations (25) to (32) into Equations (19) to (24), we have  $O(\epsilon^0)$ :

$$(D_0^2 + \omega^2)z_{10} = 0 \tag{33}$$

$$(D_0^2 + \omega^2)z_{20} = 0 \tag{34}$$

$$(D_0^2 + \omega_1^2)z_{30} = 0 \tag{35}$$

$$(D_0^2 + \omega_2^2)z_{40} = 0 \tag{36}$$

$O(\epsilon^1)$ :

$$\begin{aligned} (D_0^2 + \omega^2)z_{11} = & -2D_0 D_1 z_{10} - 2\tilde{\mu} D_0 z_{10} + \tilde{\alpha}_1 z_{10}^3 + \tilde{\alpha}_2 z_{10} z_{20}^2 + \tilde{\alpha}_3 z_{10}^2 D_0 z_{10} + \tilde{\alpha}_4 z_{20}^2 D_0 z_{10} \\ & + \tilde{\alpha}_5 z_{10} (D_0 z_{20})^2 + \tilde{\alpha}_6 z_{10} (D_0 z_{10})^2 + \tilde{\alpha}_7 z_{10} z_{20} D_0 z_{20} + \tilde{\beta}_1 z_{10}^2 z_{30} + \tilde{\beta}_2 z_{10} D_0 z_{10} z_{30} \\ & + \tilde{\beta}_3 z_{10} z_{30}^2 + \tilde{\beta}_4 z_{10} z_{20} z_{40} + \tilde{\beta}_5 z_{10} z_{40}^2 + \tilde{\beta}_6 z_{10} D_0 z_{20} z_{40} + \tilde{\beta}_7 z_{20}^2 z_{30} + \tilde{\beta}_8 z_{10} z_{30} z_{50} \\ & + \tilde{\beta}_9 z_{10} D_0 z_{10} z_{50} + \tilde{\beta}_{10} z_{10} z_{40} z_{60} + \tilde{\beta}_{11} z_{10}^2 z_{50} + \tilde{\beta}_{12} z_{10} z_{60}^2 + \tilde{\beta}_{13} z_{10} z_{20} z_{60} \\ & + \tilde{\beta}_{14} z_{10} D_0 z_{20} z_{60} + \tilde{\beta}_{15} z_{10} z_{50}^2 + \tilde{\beta}_{16} z_{20}^2 z_{50} + \Omega^2 \tilde{f} \cos(\Omega t) + \tilde{\eta}_1 z_{30} + \eta_2 z_{50} \end{aligned} \tag{37}$$

$$\begin{aligned} (D_0^2 + \omega^2)z_{21} = & -2D_0 D_1 z_{20} - 2\tilde{\mu} D_0 z_{20} + \tilde{\alpha}_1 z_{20}^3 + \tilde{\alpha}_2 z_{20} z_{10}^2 + \tilde{\alpha}_3 z_{20}^2 D_0 z_{20} + \tilde{\alpha}_4 z_{10}^2 D_0 z_{20} \\ & + \tilde{\alpha}_5 z_{20} (D_0 z_{10})^2 + \tilde{\alpha}_6 z_{20} (D_0 z_{20})^2 + \tilde{\alpha}_7 z_{20} z_{10} D_0 z_{10} + \tilde{\gamma}_1 z_{20}^2 z_{40} + \tilde{\gamma}_2 z_{20} D_0 z_{20} z_{40} \\ & + \tilde{\gamma}_3 z_{20} z_{40}^2 + \tilde{\gamma}_4 z_{20} z_{10} z_{30} + \tilde{\gamma}_5 z_{20} z_{30}^2 + \tilde{\gamma}_6 z_{20} D_0 z_{10} z_{30} + \tilde{\gamma}_7 z_{10}^2 z_{40} + \tilde{\gamma}_8 z_{20} z_{40} z_{60} \\ & + \tilde{\gamma}_9 z_{20} D_0 z_{20} z_{60} + \tilde{\gamma}_{10} z_{20} z_{30} z_{60} + \tilde{\gamma}_{11} z_{20}^2 z_{60} + \tilde{\gamma}_{12} z_{20} z_{50}^2 + \tilde{\gamma}_{13} z_{20} z_{10} z_{50} \\ & + \tilde{\gamma}_{14} z_{20} D_0 z_{10} z_{50} + \tilde{\gamma}_{15} z_{20} z_{60}^2 + \tilde{\gamma}_{16} z_{10}^2 z_{60} + \Omega^2 \tilde{f} \sin(\Omega t) + \tilde{\eta}_3 z_{40} + \eta_4 z_{60} \end{aligned} \tag{38}$$

$$(D_0^2 + \omega_1^2)z_{31} = -2D_0 D_1 z_{30} - 2\epsilon \tilde{\mu}_1 D_0 z_{30} + \tilde{\eta}_5 z_{10} \tag{39}$$

$$(D_0^2 + \omega_2^2)z_{41} = -2D_0 D_1 z_{40} - 2\tilde{\mu}_2 D_0 z_{40} + \tilde{\eta}_6 z_{20} \tag{40}$$

$$(D_0 + \omega_3)z_{50} = \tilde{\eta}_7 z_{10} \tag{41}$$

$$(D_0 + \omega_4)z_{60} = \tilde{\eta}_8 z_{20} \tag{42}$$

The steady-state periodic solutions of Equations (33) to (36), (41), and (42) can be written as follows:

$$z_{10}(T_0, T_1) = A_1(T_1)e^{i\omega T_0} + \bar{A}_1(T_1)e^{-i\omega T_0} \tag{43}$$

$$z_{20}(T_0, T_1) = A_2(T_1)e^{i\omega T_0} + \bar{A}_2(T_1)e^{-i\omega T_0} \tag{44}$$

$$z_{30}(T_0, T_1) = B_1(T_1)e^{i\omega_1 T_0} + \bar{B}_1(T_1)e^{-i\omega_1 T_0} \tag{45}$$

$$z_{40}(T_0, T_1) = B_2(T_1)e^{i\omega_2 T_0} + \bar{B}_2(T_1)e^{-i\omega_2 T_0} \tag{46}$$

$$z_{50}(T_0, T_1) = \rho_1 A_1(T_1)e^{i\omega T_0} + \bar{\rho}_1 \bar{A}_1(T_1)e^{-i\omega T_0} \tag{47}$$

$$z_{60}(T_0, T_1) = \rho_2 A_2(T_1)e^{i\omega T_0} + \bar{\rho}_2 \bar{A}_2(T_1)e^{-i\omega T_0} \tag{48}$$

where  $i = \sqrt{-1}, \rho_1 = \frac{\omega_3 - i\omega}{\omega_3^2 + \omega^2} \tilde{\eta}_7, \bar{\rho}_1 = \frac{\omega_3 + i\omega}{\omega_3^2 + \omega^2} \tilde{\eta}_7, \rho_2 = \frac{\omega_4 - i\omega}{\omega_4^2 + \omega^2} \tilde{\eta}_8, \bar{\rho}_2 = \frac{\omega_4 + i\omega}{\omega_4^2 + \omega^2} \tilde{\eta}_8$ .  $A_1(T_1), A_2(T_1), B_1(T_1)$  and  $B_2(T_1)$  are unknown that will be defined later.  $\bar{A}_1(T_1), \bar{A}_2(T_1), \bar{B}_1(T_1),$

and  $\bar{B}_2(T_1)$  are the complex conjugate forms of  $A_1(T_1)$ ,  $A_2(T_1)$ ,  $B_1(T_1)$ , and  $B_2(T_1)$ , respectively. Inserting Equations (43) to (48) into Equations (37) to (40), we have the following:

$$\begin{aligned}
 (D_0^2 + \omega^2)z_{11} = & (-2i\omega D_1 A_1 - 2i\tilde{\mu}\omega A_1 + 3\tilde{\alpha}_1 A_1^2 \bar{A}_1 + 2\tilde{\alpha}_2 A_1 A_2 \bar{A}_2 + \tilde{\alpha}_2 \bar{A}_1 A_2^2 + i\tilde{\alpha}_3 \omega A_1^2 \bar{A}_1 \\
 & + 2i\tilde{\alpha}_4 \omega A_1 A_2 \bar{A}_2 - i\tilde{\alpha}_4 \omega \bar{A}_1 A_2^2 + 2\tilde{\alpha}_5 \omega^2 A_1 A_2 \bar{A}_2 - \tilde{\alpha}_5 \omega^2 \bar{A}_1 A_2^2 + \tilde{\alpha}_6 \omega^2 A_1^2 \bar{A}_1 \\
 & + i\tilde{\alpha}_7 \omega \bar{A}_1 A_2^2 + 2\tilde{\beta}_3 A_1 B_1 \bar{B}_1 + 2\tilde{\beta}_5 A_1 B_2 \bar{B}_2 + 2\beta_{11} \rho_1 A_1^2 \bar{A}_1 + \beta_{12} \rho_2^2 \bar{A}_1 A_2^2 \\
 & + \beta_{13} \rho_2 A_1 A_2 \bar{A}_2 + \beta_{13} \rho_2 \bar{A}_1 A_2^2 - i\beta_{14} \omega \rho_2 A_1 A_2 \bar{A}_2 + i\beta_{14} \omega \rho_2 \bar{A}_1 A_2^2 \\
 & + \beta_{15} \rho_1^2 A_1^2 \bar{A}_1 + 2\beta_{16} \rho_1 A_1 A_2 \bar{A}_2 + \tilde{\eta}_2 \rho_1 A_1) e^{i\omega T_0} + \tilde{\eta}_1 B_1 e^{i\omega_1 T_0} + (\tilde{\alpha}_1 A_1^3 \\
 & + \tilde{\alpha}_2 A_1 A_2^2 + i\tilde{\alpha}_3 \omega A_1^3 + i\tilde{\alpha}_4 \omega A_1 A_2^2 - \tilde{\alpha}_5 \omega^2 A_1 A_2^2 - \tilde{\alpha}_6 \omega^2 A_1^3 + i\tilde{\alpha}_7 \omega A_1 A_2^2 \\
 & + i\beta_9 \omega \rho_1 A_1^3 + \beta_{11} \rho_1 A_1^3 + \beta_{12} \rho_2^2 A_1 A_2^2 + \beta_{13} \rho_2 A_1 A_2^2 + i\beta_{14} \omega \rho_2 A_1 A_2^2 \\
 & + \beta_{15} \rho_1^2 A_1^3 + \beta_{16} \rho_1 A_1 A_2^2) e^{3i\omega T_0} + (\tilde{\beta}_1 A_1^2 \bar{B}_1 + i\tilde{\beta}_2 \omega A_1^2 \bar{B}_1 + \tilde{\beta}_7 A_2^2 \bar{B}_1 \\
 & + \beta_8 \rho_1 A_1^2 \bar{B}_1) e^{i(2\omega + \omega_1) T_0} + (\tilde{\beta}_1 A_1^2 \bar{B}_1 + i\tilde{\beta}_2 \omega A_1^2 \bar{B}_1 + \tilde{\beta}_7 A_2^2 \bar{B}_1 + \beta_8 \rho_1 A_1^2 \bar{B}_1) e^{i(2\omega - \omega_1) T_0} \\
 & + (2\tilde{\beta}_1 A_1 \bar{A}_1 B_1 + 2\tilde{\beta}_7 A_2 \bar{A}_2 B_1 + \beta_8 \rho_1 A_1 \bar{A}_1 B_1) e^{i\omega_1 T_0} + \tilde{\beta}_3 A_1 B_1^2 e^{i(\omega + 2\omega_1) T_0} \\
 & + \tilde{\beta}_3 \bar{A}_1 B_1^2 e^{i(2\omega_1 - \omega) T_0} + (\tilde{\beta}_4 A_1 A_2 B_2 + i\tilde{\beta}_6 \omega A_1 A_2 B_2 + \beta_{10} \rho_2 A_1 A_2 B_2) e^{i(2\omega + \omega_2) T_0} \\
 & + (\tilde{\beta}_4 A_1 A_2 \bar{B}_2 + i\tilde{\beta}_6 \omega A_1 A_2 \bar{B}_2 + \beta_{10} \rho_2 A_1 A_2 \bar{B}_2) e^{i(2\omega - \omega_2) T_0} + (\tilde{\beta}_4 A_1 \bar{A}_2 B_2 \\
 & + \tilde{\beta}_4 \bar{A}_1 A_2 B_2 - i\tilde{\beta}_6 \omega A_1 \bar{A}_2 B_2 + i\tilde{\beta}_6 \omega \bar{A}_1 A_2 B_2 + \beta_{10} \rho_2 \bar{A}_1 A_2 B_2) e^{i\omega_2 T_0} \\
 & + \tilde{\beta}_5 A_1 B_2^2 e^{i(\omega + 2\omega_2) T_0} + \tilde{\beta}_5 \bar{A}_1 B_2^2 e^{i(2\omega_2 - \omega) T_0} + \frac{1}{2} \Omega^2 \tilde{f} e^{i\Omega T_0} + cc
 \end{aligned} \tag{49}$$

$$\begin{aligned}
 (D_0^2 + \omega^2)z_{21} = & (-2i\omega D_1 A_2 - 2i\tilde{\mu}\omega A_2 + 3\tilde{\alpha}_1 A_2^2 \bar{A}_2 + 2\tilde{\alpha}_2 A_2 A_1 \bar{A}_1 + \tilde{\alpha}_2 \bar{A}_2 A_1^2 + i\tilde{\alpha}_3 \omega A_2^2 \bar{A}_2 \\
 & + 2i\tilde{\alpha}_4 \omega A_2 A_1 \bar{A}_1 - i\tilde{\alpha}_4 \omega \bar{A}_2 A_1^2 + 2\tilde{\alpha}_5 \omega^2 A_2 A_1 \bar{A}_1 - \tilde{\alpha}_5 \omega^2 \bar{A}_2 A_1^2 + \tilde{\alpha}_6 \omega^2 A_2^2 \bar{A}_2 \\
 & + i\tilde{\alpha}_7 \omega \bar{A}_2 A_1^2 + 2\tilde{\gamma}_3 A_2 B_2 \bar{B}_2 + 2\tilde{\gamma}_5 A_2 B_1 \bar{B}_1 + 2\gamma_{11} \rho_2 A_2^2 \bar{A}_2 + \gamma_{12} \rho_1^2 \bar{A}_2 A_1^2 \\
 & + \gamma_{13} \rho_1 A_2 A_1 \bar{A}_1 + \gamma_{13} \rho_1 \bar{A}_2 A_1^2 - i\gamma_{14} \omega \rho_1 A_2 A_1 \bar{A}_1 + i\gamma_{14} \omega \rho_1 \bar{A}_2 A_1^2 + \gamma_{15} \rho_2^2 A_2^2 \bar{A}_2 \\
 & + 2\gamma_{16} \rho_2 A_2 A_1 \bar{A}_1 + \tilde{\eta}_4 \rho_2 A_2) e^{i\omega T_0} + \tilde{\eta}_3 B_2 e^{i\omega_2 T_0} + (\tilde{\alpha}_1 A_2^3 + \tilde{\alpha}_2 A_2 A_1^2 + i\tilde{\alpha}_3 \omega A_2^3 \\
 & + i\tilde{\alpha}_4 \omega A_2 A_1^2 - \tilde{\alpha}_5 \omega^2 A_2 A_1^2 - \tilde{\alpha}_6 \omega^2 A_2^3 + i\tilde{\alpha}_7 \omega A_2 A_1^2 + i\gamma_9 \omega \rho_2 A_2^3 + \gamma_{11} \rho_2 A_2^3 \\
 & + \gamma_{12} \rho_1^2 A_2 A_1^2 + \gamma_{13} \rho_1 A_2 A_1^2 + i\gamma_{14} \omega \rho_1 A_2 A_1^2 + \gamma_{15} \rho_2^2 A_2^3 + \gamma_{16} \rho_2 A_2 A_1^2) e^{3i\omega T_0} \\
 & + (\tilde{\gamma}_1 A_2^2 \bar{B}_2 + i\tilde{\gamma}_2 \omega A_2^2 \bar{B}_2 + \tilde{\gamma}_7 A_1^2 \bar{B}_2 + \gamma_8 \rho_2 A_2^2 \bar{B}_2) e^{i(2\omega + \omega_2) T_0} + (\tilde{\gamma}_1 A_2^2 \bar{B}_2 \\
 & + i\tilde{\gamma}_2 \omega A_2^2 \bar{B}_2 + \tilde{\gamma}_7 A_1^2 \bar{B}_2 + \gamma_8 \rho_2 A_2^2 \bar{B}_2) e^{i(2\omega - \omega_2) T_0} + (2\tilde{\gamma}_1 A_2 \bar{A}_2 B_2 + 2\tilde{\gamma}_7 A_1 \bar{A}_1 B_2 \\
 & + \gamma_8 \rho_2 A_2 \bar{A}_2 B_2) e^{i\omega_2 T_0} + \tilde{\gamma}_3 A_2 B_2^2 e^{i(\omega + 2\omega_2) T_0} + \tilde{\gamma}_3 \bar{A}_2 B_2^2 e^{i(2\omega_2 - \omega) T_0} + (\tilde{\gamma}_4 A_2 A_1 B_1 \\
 & + i\tilde{\gamma}_6 \omega A_2 A_1 B_1 + \gamma_{10} \rho_1 A_2 A_1 B_1) e^{i(2\omega + \omega_1) T_0} + (\tilde{\gamma}_4 A_2 A_1 \bar{B}_1 + i\tilde{\gamma}_6 \omega A_2 A_1 \bar{B}_1 \\
 & + \gamma_{10} \rho_1 \bar{A}_2 A_1 \bar{B}_1) e^{i(2\omega - \omega_1) T_0} + (\tilde{\gamma}_4 A_2 \bar{A}_1 B_1 + \tilde{\gamma}_4 \bar{A}_2 A_1 B_1 - i\tilde{\gamma}_6 \omega A_2 \bar{A}_1 B_1 \\
 & + i\tilde{\gamma}_6 \omega \bar{A}_2 A_1 B_1 + \gamma_{10} \rho_1 A_2 A_1 B_1) e^{i\omega_1 T_0} + \tilde{\gamma}_5 A_2 B_1^2 e^{i(\omega + 2\omega_1) T_0} + \tilde{\gamma}_5 \bar{A}_2 B_1^2 e^{i(2\omega_1 - \omega) T_0} \\
 & - \frac{1}{2} i \Omega^2 \tilde{f} e^{i\Omega T_0} + cc
 \end{aligned} \tag{50}$$

$$(D_0^2 + \omega_1^2)z_{31} = -2i\omega_1 D_1 B_1 e^{i\omega_1 T_0} - 2i\tilde{\mu}_1 \omega_1 B_1 e^{i\omega_1 T_0} + \tilde{\eta}_5 A_1 e^{i\omega_1 T_0} + cc \tag{51}$$

$$(D_0^2 + \omega_2^2)z_{41} = -2i\omega_2 D_1 B_2 e^{i\omega_2 T_0} - 2i\tilde{\mu}_2 \omega_2 B_2 e^{i\omega_2 T_0} + \tilde{\eta}_6 A_2 e^{i\omega_2 T_0} + cc \tag{52}$$

where  $cc$  in Equations (49) to (52) denote the complex conjugate term. To obtain the periodic solutions of Equations (49) to (52), the resonance conditions should be eliminated. Therefore, let  $\sigma$ ,  $\sigma_1$ , and  $\sigma_2$  represent the closeness of the rotor angular speed ( $\Omega$ ) and the controller natural frequencies ( $\omega_1$  and  $\omega_2$ ) to the rotor system natural frequency ( $\omega$ ), as follows:

$$\Omega = \omega + \sigma, \quad \omega_1 = \omega + \sigma_1, \quad \omega_2 = \omega + \sigma_2 \tag{53}$$

Inserting Equation (53) into Equations (49) to (52), one can extract the following solvability conditions:

$$\begin{aligned}
 -2i\omega D_1 A_1 - 2i\tilde{\mu}\omega A_1 + 3\tilde{\alpha}_1 A_1^2 \bar{A}_1 + 2\tilde{\alpha}_2 A_1 A_2 \bar{A}_2 + \tilde{\alpha}_2 \bar{A}_1 A_2^2 + i\tilde{\alpha}_3 \omega A_1^2 \bar{A}_1 + 2i\tilde{\alpha}_4 \omega A_1 A_2 \bar{A}_2 \\
 - i\tilde{\alpha}_4 \omega \bar{A}_1 A_2^2 + 2\tilde{\alpha}_5 \omega^2 A_1 A_2 \bar{A}_2 - \tilde{\alpha}_5 \omega^2 \bar{A}_1 A_2^2 + \tilde{\alpha}_6 \omega^2 A_1^2 \bar{A}_1 + i\tilde{\alpha}_7 \omega \bar{A}_1 A_2^2 + 2\tilde{\beta}_3 A_1 B_1 \bar{B}_1 \\
 + 2\tilde{\beta}_5 A_1 B_2 \bar{B}_2 + 2\beta_{11} \rho_1 A_1^2 \bar{A}_1 + \beta_{12} \rho_2^2 \bar{A}_1 A_2^2 + \beta_{13} \rho_2 A_1 A_2 \bar{A}_2 + \beta_{13} \rho_2 \bar{A}_1 A_2^2 - i\beta_{14} \omega \rho_2 A_1 A_2 \bar{A}_2 \\
 + i\beta_{14} \omega \rho_2 \bar{A}_1 A_2^2 + \beta_{15} \rho_1^2 A_1^2 \bar{A}_1 + 2\beta_{16} \rho_1 A_1 A_2 \bar{A}_2 + \tilde{\eta}_1 B_1 e^{i\tilde{\sigma}_1 T_0} + \tilde{\eta}_2 \rho_1 A_1 + (\tilde{\beta}_1 A_1^2 \bar{B}_1 \\
 + i\tilde{\beta}_2 \omega A_1^2 \bar{B}_1 + \beta_8 \rho_1 A_1^2 \bar{B}_1) e^{-i\tilde{\sigma}_1 T_0} + (2\tilde{\beta}_1 A_1 \bar{A}_1 B_1 + 2\tilde{\beta}_7 A_2 \bar{A}_2 B_1 + \beta_8 \rho_1 A_1 \bar{A}_1 B_1) e^{i\tilde{\sigma}_1 T_0} \\
 + (\tilde{\beta}_4 A_1 A_2 \bar{B}_2 + i\tilde{\beta}_6 \omega A_1 A_2 \bar{B}_2 + \beta_{10} \rho_2 A_1 A_2 \bar{B}_2) e^{-i\tilde{\sigma}_2 T_0} + \tilde{\beta}_3 \bar{A}_1 B_1^2 e^{2i\tilde{\sigma}_1 T_0} + (\tilde{\beta}_4 A_1 \bar{A}_2 B_2 \\
 + \tilde{\beta}_4 \bar{A}_1 A_2 B_2 - i\tilde{\beta}_6 \omega A_1 \bar{A}_2 B_2 + i\tilde{\beta}_6 \omega \bar{A}_1 A_2 B_2 + \beta_{10} \rho_2 \bar{A}_1 A_2 B_2) e^{i\tilde{\sigma}_2 T_0} + \tilde{\beta}_5 \bar{A}_1 B_2^2 e^{2i\tilde{\sigma}_2 T_0} \\
 + \frac{1}{2} (\omega + \tilde{\sigma})^2 \tilde{f} e^{i\tilde{\sigma} T_0} = 0
 \end{aligned} \tag{54}$$



$$\begin{aligned}
 & -2i\omega D_1 A_2 - 2i\tilde{\mu}\omega A_2 + 3\tilde{\alpha}_1 A_2^2 \bar{A}_2 + 2\tilde{\alpha}_2 A_2 A_1 \bar{A}_1 + \tilde{\alpha}_2 \bar{A}_2 A_1^2 + i\tilde{\alpha}_3 \omega A_2^2 \bar{A}_2 + 2i\tilde{\alpha}_4 \omega A_2 A_1 \bar{A}_1 \\
 & - i\tilde{\alpha}_4 \omega \bar{A}_2 A_1^2 + 2\tilde{\alpha}_5 \omega^2 A_2 A_1 \bar{A}_1 - \tilde{\alpha}_5 \omega^2 \bar{A}_2 A_1^2 + \tilde{\alpha}_6 \omega^2 A_2^2 \bar{A}_2 + i\tilde{\alpha}_7 \omega \bar{A}_2 A_1^2 + 2\tilde{\gamma}_3 A_2 B_2 \bar{B}_2 \\
 & + 2\tilde{\gamma}_5 A_2 B_1 \bar{B}_1 + 2\gamma_{11} \rho_2 A_2^2 \bar{A}_2 + \gamma_{12} \rho_1^2 \bar{A}_2 A_1^2 + \gamma_{13} \rho_1 A_2 A_1 \bar{A}_1 + \gamma_{13} \rho_1 \bar{A}_2 A_1^2 - i\gamma_{14} \omega \rho_1 A_2 A_1 \bar{A}_1 \\
 & + i\gamma_{14} \omega \rho_1 \bar{A}_2 A_1^2 + \gamma_{15} \rho_2^2 A_2^2 \bar{A}_2 + 2\gamma_{16} \rho_2 A_2 A_1 \bar{A}_1 + \tilde{\eta}_3 B_2 e^{i\tilde{\sigma}_2 T_0} + \tilde{\eta}_4 \rho_2 A_2 + (\tilde{\gamma}_1 A_2^2 \bar{B}_2 \\
 & + i\tilde{\gamma}_2 \omega A_2^2 \bar{B}_2 + \tilde{\gamma}_7 A_1^2 \bar{B}_2 + \gamma_8 \rho_2 A_2^2 \bar{B}_2) e^{-i\tilde{\epsilon}\tilde{\sigma}_2 T_0} + (2\tilde{\gamma}_1 A_2 \bar{A}_2 B_2 + 2\tilde{\gamma}_7 A_1 \bar{A}_1 B_2 + \gamma_8 \rho_2 A_2 \bar{A}_2 B_2) e^{i\tilde{\epsilon}\tilde{\sigma}_2 T_0} \\
 & + (\tilde{\gamma}_4 A_2 A_1 \bar{B}_1 + i\tilde{\gamma}_6 \omega A_2 A_1 \bar{B}_1 + \gamma_{10} \rho_1 A_2 A_1 \bar{B}_1) e^{-i\tilde{\epsilon}\tilde{\sigma}_1 T_0} + \tilde{\gamma}_3 \bar{A}_2 B_2^2 e^{2i\tilde{\epsilon}\tilde{\sigma}_2 T_0} + (\tilde{\gamma}_4 A_2 \bar{A}_1 B_1 \\
 & + \tilde{\gamma}_4 \bar{A}_2 A_1 B_1 - i\tilde{\gamma}_6 \omega A_2 \bar{A}_1 B_1 + i\tilde{\gamma}_6 \omega \bar{A}_2 A_1 B_1 + \gamma_{10} \rho_1 \bar{A}_2 A_1 B_1) e^{i\tilde{\epsilon}\tilde{\sigma}_1 T_0} + \tilde{\gamma}_5 \bar{A}_2 B_1^2 e^{2i\tilde{\epsilon}\tilde{\sigma}_1 T_0} \\
 & - \frac{1}{2} i (\omega + \tilde{\epsilon}\tilde{\sigma})^2 \tilde{f} e^{i\tilde{\epsilon}\tilde{\sigma} T_0} = 0
 \end{aligned} \tag{55}$$

$$-2i(\omega + \tilde{\epsilon}\tilde{\sigma}_1) D_1 B_1 e^{i\tilde{\epsilon}\tilde{\sigma}_1 T_0} - 2i\tilde{\mu}_1 (\omega + \tilde{\epsilon}\tilde{\sigma}_1) B_1 e^{i\tilde{\epsilon}\tilde{\sigma}_1 T_0} + \tilde{\eta}_5 A_1 = 0 \tag{56}$$

$$-2i(\omega + \tilde{\epsilon}\tilde{\sigma}_2) D_1 B_2 e^{i\tilde{\epsilon}\tilde{\sigma}_2 T_0} - 2i\tilde{\mu}_2 (\omega + \tilde{\epsilon}\tilde{\sigma}_2) B_2 e^{i\tilde{\epsilon}\tilde{\sigma}_2 T_0} + \tilde{\eta}_6 A_2 = 0 \tag{57}$$

To obtain the autonomous dynamical system that describes the oscillatory behaviors of the considered closed-loop system, let us express the unknown functions  $A_1$ ,  $A_2$ ,  $B_1$ , and  $B_2$  in the polar form as follows:

$$\left. \begin{aligned}
 A_1(T_1) &= \frac{1}{2} a_1(T_1) e^{i\theta_1(T_1)}, & A_2(T_1) &= \frac{1}{2} a_2(T_1) e^{i\theta_2(T_1)} \\
 B_1(T_1) &= \frac{1}{2} b_1(T_1) e^{i\theta_3(T_1)}, & B_2(T_1) &= \frac{1}{2} b_2(T_1) e^{i\theta_4(T_1)}
 \end{aligned} \right\} \tag{58}$$

According to Equation (58), we have the following:

$$\left. \begin{aligned}
 D_1 A_1 &= \frac{d}{\tilde{\epsilon} dt} A_1 = \frac{1}{2\tilde{\epsilon}} (\dot{a}_1 e^{i\theta_1} + i a_1 \dot{\theta}_1 e^{i\theta_1}), & D_1 A_2 &= \frac{d}{\tilde{\epsilon} dt} A_2 = \frac{1}{2\tilde{\epsilon}} (\dot{a}_2 e^{i\theta_2} + i a_2 \dot{\theta}_2 e^{i\theta_2}) \\
 D_1 B_1 &= \frac{d}{\tilde{\epsilon} dt} B_1 = \frac{1}{2\tilde{\epsilon}} (\dot{b}_1 e^{i\theta_3} + i b_1 \dot{\theta}_3 e^{i\theta_3}), & D_1 B_2 &= \frac{d}{\tilde{\epsilon} dt} B_2 = \frac{1}{2\tilde{\epsilon}} (\dot{b}_2 e^{i\theta_4} + i b_2 \dot{\theta}_4 e^{i\theta_4})
 \end{aligned} \right\} \tag{59}$$

Substituting Equations (58) and (59) into Equations (54) to (57) and separating the real and imaginary part yields the following:

$$\begin{aligned}
 \dot{a}_1 &= F_1(a_1, a_2, b_1, b_2, \phi_1, \phi_2, \phi_3, \phi_4) = -\frac{1}{2} (2\mu + \frac{\eta_2 \eta_7}{\omega_3^2 + \omega^2}) a_1 + \frac{1}{8} (\alpha_3 - \frac{2\beta_{11} \eta_7}{\omega_3^2 + \omega^2} - \frac{2\omega_3 \beta_{15} \eta_7^2}{(\omega_3^2 + \omega^2)^2}) a_1^3 \\
 &+ \frac{1}{8} (2\alpha_4 - \frac{\beta_{13} \eta_8}{\omega_4^2 + \omega^2} - \frac{\omega_4 \beta_{14} \eta_8}{\omega_4^2 + \omega^2} - \frac{2\beta_{16} \eta_7}{\omega_3^2 + \omega^2}) a_1 a_2^2 + \frac{1}{8} (-\alpha_4 + \alpha_7 + \frac{2\omega_4 \beta_{12} \eta_8^2}{(\omega_4^2 + \omega^2)^2} - \frac{\beta_{13} \eta_8}{\omega_4^2 + \omega^2} \\
 &+ \frac{\omega_4 \beta_{14} \eta_8}{\omega_4^2 + \omega^2}) a_1 a_2^2 \cos(2\phi_1 - 2\phi_2) + \frac{1}{8} (\frac{\alpha_2}{\omega} - \alpha_5 \omega + \frac{(\omega_4^2 - \omega^2) \beta_{12} \eta_8^2}{\omega(\omega_4^2 + \omega^2)^2} + \frac{\omega_4 \beta_{13} \eta_8}{\omega(\omega_4^2 + \omega^2)} \\
 &- \frac{\omega \beta_{14} \eta_8}{\omega_4^2 + \omega^2}) a_1 a_2^2 \sin(2\phi_1 - 2\phi_2) + (-\frac{1}{2\omega} \eta_1 b_1 - \frac{1}{8\omega} \beta_1 a_1^2 b_1 - \frac{1}{4\omega} \beta_7 a_2^2 b_1) \sin(\phi_3) \\
 &- \frac{1}{8\omega} \beta_3 a_1 b_1^2 \sin(2\phi_3) + \frac{1}{8} (\beta_2 - \frac{2\beta_8 \eta_7}{\omega_3^2 + \omega^2}) a_1^2 b_1 \cos(\phi_3) - \frac{1}{8} (\frac{\beta_{10} \eta_8}{\omega_4^2 + \omega^2}) a_1 a_2 b_2 \cos(\phi_4) \\
 &+ \frac{1}{8\omega} (\frac{\omega_4 \beta_{10} \eta_8}{\omega_4^2 + \omega^2}) a_1 a_2 b_2 \sin(\phi_4) + \frac{1}{8\omega} \beta_7 a_2^2 b_1 \sin(2\phi_1 - 2\phi_2 + \phi_3) + \frac{1}{8\omega} (\beta_6 \omega \\
 &- \frac{\omega \beta_{10} \eta_8}{\omega_4^2 + \omega^2}) a_1 a_2 b_2 \cos(2\phi_1 - 2\phi_2 - \phi_4) + \frac{1}{8\omega} (\beta_4 + \frac{\omega_4 \beta_{10} \eta_8}{\omega_4^2 + \omega^2}) a_1 a_2 b_2 \sin(2\phi_1 - 2\phi_2 - \phi_4) \\
 &+ \frac{1}{8\omega} \beta_5 a_1 b_2^2 \sin(2\phi_1 - 2\phi_2 - 2\phi_4) + \frac{1}{2\omega} (\omega + \sigma)^2 f \sin(\phi_1)
 \end{aligned} \tag{60}$$

$$\begin{aligned}
 \dot{a}_2 &= F_2(a_1, a_2, b_1, b_2, \phi_1, \phi_2, \phi_3, \phi_4) = -\frac{1}{2} (2\mu + \frac{\eta_4 \eta_8}{\omega_4^2 + \omega^2}) a_2 + \frac{1}{8} (\alpha_3 - \frac{2\gamma_{11} \eta_8}{\omega_4^2 + \omega^2} - \frac{2\omega_4 \gamma_{15} \eta_8^2}{(\omega_4^2 + \omega^2)^2}) a_2^3 \\
 &+ \frac{1}{8} (2\alpha_4 - \frac{\gamma_{13} \eta_7}{\omega_3^2 + \omega^2} - \frac{\omega_3 \gamma_{14} \eta_7}{\omega_3^2 + \omega^2} - \frac{2\gamma_{16} \eta_8}{\omega_4^2 + \omega^2}) a_2 a_1^2 + \frac{1}{8} (-\alpha_4 + \alpha_7 - \frac{2\omega_3 \gamma_{12} \eta_7^2}{(\omega_3^2 + \omega^2)^2} - \frac{\gamma_{13} \eta_7}{\omega_3^2 + \omega^2} \\
 &+ \frac{\omega_3 \gamma_{14} \eta_7}{\omega_3^2 + \omega^2}) a_2 a_1^2 \cos(2\phi_2 - 2\phi_1) + \frac{1}{8} (\frac{\alpha_2}{\omega} - \alpha_5 \omega + \frac{(\omega_3^2 - \omega^2) \gamma_{12} \eta_7^2}{\omega(\omega_3^2 + \omega^2)^2} + \frac{\omega_3 \gamma_{13} \eta_7}{\omega(\omega_3^2 + \omega^2)} \\
 &+ \frac{\omega \gamma_{14} \eta_7}{\omega_3^2 + \omega^2}) a_2 a_1^2 \sin(2\phi_2 - 2\phi_1) + (-\frac{1}{2\omega} \eta_3 b_2 - \frac{1}{8\omega} \gamma_1 a_2^2 b_2 - \frac{1}{4\omega} \gamma_7 a_1^2 b_2) \sin(\phi_4) \\
 &- \frac{1}{8\omega} \gamma_3 a_2 b_2^2 \sin(2\phi_4) + \frac{1}{8\omega} (\gamma_2 \omega - \frac{2\omega \gamma_8 \eta_8}{\omega_4^2 + \omega^2}) a_2^2 b_2 \cos(\phi_4) - \frac{1}{8\omega} (\frac{\omega \gamma_{10} \eta_7}{\omega_3^2 + \omega^2}) a_2 a_1 b_1 \cos(\phi_3) \\
 &+ \frac{1}{8\omega} (\frac{\omega_3 \gamma_{10} \eta_7}{\omega_3^2 + \omega^2}) a_2 a_1 b_1 \sin(\phi_3) + \frac{1}{8\omega} \gamma_7 a_1^2 b_2 \sin(2\phi_2 - 2\phi_1 + \phi_4) + \frac{1}{8\omega} (\gamma_6 \omega \\
 &- \frac{\omega \gamma_{10} \eta_7}{\omega_3^2 + \omega^2}) a_2 a_1 b_1 \cos(2\phi_2 - 2\phi_1 - \phi_3) + \frac{1}{8\omega} (\gamma_4 + \frac{\omega_3 \gamma_{10} \eta_7}{\omega_3^2 + \omega^2}) a_2 a_1 b_1 \sin(2\phi_2 - 2\phi_1 - \phi_3) \\
 &+ \frac{1}{8\omega} \gamma_5 a_2 b_1^2 \sin(2\phi_2 - 2\phi_1 - 2\phi_3) - \frac{1}{2\omega} (\omega + \sigma)^2 f \cos(\phi_2)
 \end{aligned} \tag{61}$$

$$\dot{b}_1 = F_3(a_1, a_2, b_1, b_2, \phi_1, \phi_2, \phi_3, \phi_4) = -\mu_1 b_1 + \frac{1}{2(\omega + \sigma_1)} \eta_5 a_1 \sin(\phi_3) \tag{62}$$

$$\dot{b}_2 = F_4(a_1, a_2, b_1, b_2, \phi_1, \phi_2, \phi_3, \phi_4) = -\mu_2 b_2 + \frac{1}{2(\omega + \sigma_2)} \eta_6 a_2 \sin(\phi_4) \tag{63}$$

$$\begin{aligned} \dot{\phi}_1 = F_5(a_1, a_2, b_1, b_2, \phi_1, \phi_2, \phi_3, \phi_4) = & \sigma + \frac{1}{2\omega} \left( \frac{\omega_3 \eta_2 \eta_7}{\omega_3^2 + \omega^2} \right) + \frac{1}{8\omega} (3\alpha_1 + \alpha_6 \omega^2 + \frac{2\omega_3 \beta_{11} \eta_7}{\omega_3^2 + \omega^2} \\ & + \frac{(\omega_3^2 - \omega^2) \beta_{15} \eta_7^2}{(\omega_3^2 + \omega^2)^2}) a_1^2 + \frac{1}{8\omega} (2\alpha_2 + 2\alpha_5 \omega^2 + \frac{\omega_4 \beta_{13} \eta_8}{\omega_4^2 + \omega^2} - \frac{\omega^2 \beta_{14} \eta_8}{\omega_4^2 + \omega^2} + \frac{2\omega_3 \beta_{16} \eta_7}{\omega_3^2 + \omega^2}) a_2^2 + \frac{1}{4\omega} \beta_3 b_1^2 \\ & + \frac{1}{4\omega} \beta_5 b_2^2 + \frac{1}{8\omega} (\alpha_2 - \alpha_5 \omega^2 + \frac{(\omega_4^2 - \omega^2) \beta_{12} \eta_8^2}{(\omega_4^2 + \omega^2)^2} + \frac{\omega_4 \beta_{13} \eta_8}{\omega_4^2 + \omega^2} + \frac{\omega^2 \beta_{14} \eta_8}{\omega_4^2 + \omega^2}) a_2^2 \cos(2\phi_1 - 2\phi_2) \\ & + \frac{1}{8\omega} (\alpha_4 \omega - \alpha_7 \omega + \frac{2\omega_4 \omega \beta_{12} \eta_8^2}{(\omega_4^2 + \omega^2)^2} + \frac{\omega \beta_{13} \eta_8}{\omega_4^2 + \omega^2} - \frac{\omega_4 \omega \beta_{14} \eta_8}{\omega_4^2 + \omega^2}) a_2^2 \sin(2\phi_1 - 2\phi_2) + (\frac{1}{2} \eta_1 b_1 \\ & + \frac{3}{8} \beta_1 a_1^2 b_1 + \frac{1}{4} \beta_7 a_2^2 b_1 + \frac{1}{4} \frac{\omega_3 \beta_8 \eta_7}{\omega_3^2 + \omega^2} a_1^2 b_1) \frac{\cos(\phi_3)}{\omega a_1} + \frac{1}{8\omega} \beta_3 b_1^2 \cos(2\phi_3) \\ & - \frac{1}{8} \frac{\beta_8 \eta_7}{\omega_3^2 + \omega^2} a_1 b_1 \sin(\phi_3) - \frac{1}{8} \beta_2 a_1 b_1 \sin(\phi_3) + \frac{1}{8\omega} (2\beta_4 + \frac{\omega_4 \beta_{10} \eta_8}{\omega_4^2 + \omega^2}) a_2 b_2 \cos(\phi_4) + \frac{1}{8} (-2\beta_6 \\ & + \frac{\beta_{10} \eta_8}{\omega_4^2 + \omega^2}) a_2 b_2 \sin(\phi_4) + \frac{1}{8\omega a_1} \beta_7 a_2^2 b_1 \cos(2\phi_1 - 2\phi_2 + \phi_3) + \frac{1}{8\omega} (\beta_4 \\ & + \frac{\omega_4 \beta_{10} \eta_8}{\omega_4^2 + \omega^2}) a_2 b_2 \cos(2\phi_1 - 2\phi_2 - \phi_4) + \frac{1}{8\omega} (-\beta_6 \omega + \frac{\omega \beta_{10} \eta_8}{\omega_4^2 + \omega^2}) a_2 b_2 \sin(2\phi_1 - 2\phi_2 - \phi_4) \\ & + \frac{1}{8\omega} \beta_5 b_2^2 \cos(2\phi_1 - 2\phi_2 - 2\phi_4) + \frac{1}{2\omega a_1} (\omega + \sigma)^2 f \cos(\phi_1) \end{aligned} \tag{64}$$

$$\begin{aligned} \dot{\phi}_2 = F_6(a_1, a_2, b_1, b_2, \phi_1, \phi_2, \phi_3, \phi_4) = & \sigma + \frac{1}{2\omega} \left( \frac{\omega_4 \eta_4 \eta_8}{\omega_4^2 + \omega^2} \right) + \frac{1}{8\omega} (3\alpha_1 + \alpha_6 \omega^2 + \frac{2\omega_4 \gamma_{11} \eta_8}{\omega_4^2 + \omega^2} \\ & + \frac{(\omega_4^2 - \omega^2) \gamma_{15} \eta_8^2}{(\omega_4^2 + \omega^2)^2}) a_2^2 + \frac{1}{8\omega} (2\alpha_2 + 2\alpha_5 \omega^2 + \frac{\omega_3 \gamma_{13} \eta_7}{\omega_3^2 + \omega^2} - \frac{\omega^2 \gamma_{14} \eta_7}{\omega_3^2 + \omega^2} + \frac{2\omega_4 \gamma_{16} \eta_8}{\omega_4^2 + \omega^2}) a_1^2 + \frac{1}{4\omega} \gamma_3 b_2^2 \\ & + \frac{1}{4\omega} \gamma_5 b_1^2 + \frac{1}{8\omega} (\alpha_2 - \alpha_5 \omega^2 + \frac{(\omega_3^2 - \omega^2) \gamma_{12} \eta_7^2}{(\omega_3^2 + \omega^2)^2} + \frac{\omega_3 \gamma_{13} \eta_7}{\omega_3^2 + \omega^2} + \frac{\omega^2 \gamma_{14} \eta_7}{\omega_3^2 + \omega^2}) a_1^2 \cos(2\phi_2 - 2\phi_1) \\ & + \frac{1}{8\omega} (\alpha_4 \omega - \alpha_7 \omega + \frac{2\omega_3 \omega \gamma_{12} \eta_7^2}{(\omega_3^2 + \omega^2)^2} - \frac{\omega \gamma_{13} \eta_7}{\omega_3^2 + \omega^2} + \frac{\omega_3 \omega \gamma_{14} \eta_7}{\omega_3^2 + \omega^2}) a_1^2 \sin(2\phi_2 - 2\phi_1) + (\frac{1}{2} \eta_3 b_2 \\ & + \frac{3}{8} \gamma_1 a_2^2 b_2 + \frac{1}{4} \gamma_7 a_1^2 b_2 + \frac{1}{4} \frac{\omega_4 \gamma_8 \eta_8}{\omega_4^2 + \omega^2} a_2^2 b_2) \frac{\cos(\phi_4)}{\omega a_2} + \frac{1}{8\omega} \gamma_3 b_2^2 \cos(2\phi_4) \\ & - \frac{1}{8} \frac{\gamma_8 \eta_8}{\omega_4^2 + \omega^2} a_2 b_2 \sin(\phi_4) - \frac{1}{8} \gamma_2 a_2 b_2 \sin(\phi_4) + \frac{1}{8\omega} (2\gamma_4 + \frac{\omega_3 \gamma_{10} \eta_7}{\omega_3^2 + \omega^2}) a_1 b_1 \cos(\phi_3) + \frac{1}{8} (-2\gamma_6 \\ & + \frac{\gamma_{10} \eta_7}{\omega_3^2 + \omega^2}) a_1 b_1 \sin(\phi_3) + \frac{1}{8\omega a_2} \gamma_7 a_1^2 b_2 \cos(2\phi_2 - 2\phi_1 + \phi_4) + \frac{1}{8\omega} (\gamma_4 \\ & + \frac{\omega_3 \gamma_{10} \eta_7}{\omega_3^2 + \omega^2}) a_1 b_1 \cos(2\phi_2 - 2\phi_1 - \phi_3) + \frac{1}{8} (-\gamma_6 + \frac{\gamma_{10} \eta_7}{\omega_3^2 + \omega^2}) a_1 b_1 \sin(2\phi_2 - 2\phi_1 - \phi_3) \\ & + \frac{1}{8\omega} \gamma_5 b_1^2 \cos(2\phi_2 - 2\phi_1 - 2\phi_3) + \frac{1}{2\omega a_2} (\omega + \sigma)^2 f \sin(\phi_2) \end{aligned} \tag{65}$$

$$\begin{aligned} \dot{\phi}_3 = F_7(a_1, a_2, b_1, b_2, \phi_1, \phi_2, \phi_3, \phi_4) = & -\sigma_1 + \frac{1}{2(\omega + \sigma_1)} \eta_5 a_1 \cos(\phi_3) - \frac{1}{2\omega} \left( \frac{\omega_3 \eta_2 \eta_7}{\omega_3^2 + \omega^2} \right) \\ & - \frac{1}{8\omega} (3\alpha_1 + \alpha_6 \omega^2 + \frac{2\omega_3 \beta_{11} \eta_7}{\omega_3^2 + \omega^2} + \frac{(\omega_3^2 - \omega^2) \beta_{15} \eta_7^2}{(\omega_3^2 + \omega^2)^2}) a_1^2 - \frac{1}{8\omega} (2\alpha_2 + 2\alpha_5 \omega^2 + \frac{\omega_4 \beta_{13} \eta_8}{\omega_4^2 + \omega^2} \\ & - \frac{\omega^2 \beta_{14} \eta_8}{\omega_4^2 + \omega^2} + \frac{2\omega_3 \beta_{16} \eta_7}{\omega_3^2 + \omega^2}) a_2^2 - \frac{1}{4\omega} \beta_3 b_1^2 - \frac{1}{4\omega} \beta_5 b_2^2 - \frac{1}{8\omega} (\alpha_2 - \alpha_5 \omega^2 + \frac{(\omega_4^2 - \omega^2) \beta_{12} \eta_8^2}{(\omega_4^2 + \omega^2)^2} \\ & + \frac{\omega_4 \beta_{13} \eta_8}{\omega_4^2 + \omega^2} + \frac{\omega^2 \beta_{14} \eta_8}{\omega_4^2 + \omega^2}) a_2^2 \cos(2\phi_1 - 2\phi_2) - \frac{1}{8\omega} (\alpha_4 \omega - \alpha_7 \omega + \frac{2\omega_4 \omega \beta_{12} \eta_8^2}{(\omega_4^2 + \omega^2)^2} + \frac{\omega \beta_{13} \eta_8}{\omega_4^2 + \omega^2} \\ & - \frac{\omega_4 \omega \beta_{14} \eta_8}{\omega_4^2 + \omega^2}) a_2^2 \sin(2\phi_1 - 2\phi_2) - (\frac{1}{2} \eta_1 b_1 + \frac{3}{8} \beta_1 a_1^2 b_1 + \frac{1}{4} \beta_7 a_2^2 b_1 + \frac{1}{4} \frac{\omega_3 \beta_8 \eta_7}{\omega_3^2 + \omega^2} a_1^2 b_1) \frac{\cos(\phi_3)}{\omega a_1} \\ & - \frac{1}{8\omega} \beta_3 b_1^2 \cos(2\phi_3) + \frac{1}{8} \frac{\beta_8 \eta_7}{\omega_3^2 + \omega^2} a_1 b_1 \sin(\phi_3) - \frac{1}{8} \beta_2 a_1 b_1 \sin(\phi_3) - \frac{1}{8\omega} (2\beta_4 \\ & + \frac{\omega_4 \beta_{10} \eta_8}{\omega_4^2 + \omega^2}) a_2 b_2 \cos(\phi_4) - \frac{1}{8} (-2\beta_6 + \frac{\beta_{10} \eta_8}{\omega_4^2 + \omega^2}) a_2 b_2 \sin(\phi_4) - \frac{1}{8\omega a_1} \beta_7 a_2^2 b_1 \cos(2\phi_1 - 2\phi_2 + \phi_3) \\ & - \frac{1}{8\omega} (\beta_4 + \frac{\omega_4 \beta_{10} \eta_8}{\omega_4^2 + \omega^2}) a_2 b_2 \cos(2\phi_1 - 2\phi_2 - \phi_4) - \frac{1}{8\omega} (-\beta_6 \omega + \frac{\omega \beta_{10} \eta_8}{\omega_4^2 + \omega^2}) a_2 b_2 \sin(2\phi_1 - 2\phi_2 - \phi_4) \\ & - \frac{1}{8\omega} \beta_5 b_2^2 \cos(2\phi_1 - 2\phi_2 - 2\phi_4) - \frac{1}{2\omega a_1} (\omega + \sigma)^2 f \cos(\phi_1) \end{aligned} \tag{66}$$

$$\begin{aligned}
 \dot{\phi}_4 = F_8(a_1, a_2, b_1, b_2, \phi_1, \phi_2, \phi_3, \phi_4) = & -\sigma_2 + \frac{1}{2(\omega + \sigma_2)b_2} \eta_6 a_2 \cos(\phi_4) - \frac{1}{2\omega} \left( \frac{\omega_4 \eta_4 \eta_8}{\omega_4^2 + \omega^2} \right) \\
 & - \frac{1}{8\omega} \left( 3\alpha_1 + \alpha_6 \omega^2 + \frac{2\omega_4 \gamma_{11} \eta_8}{\omega_4^2 + \omega^2} + \frac{(\omega_4^2 - \omega^2) \gamma_{15} \eta_8^2}{(\omega_4^2 + \omega^2)^2} \right) a_2^2 - \frac{1}{8\omega} \left( 2\alpha_2 + 2\alpha_5 \omega^2 + \frac{\omega_3 \gamma_{13} \eta_7}{\omega_3^2 + \omega^2} \right. \\
 & - \frac{\omega^2 \gamma_{14} \eta_7}{\omega_3^2 + \omega^2} + \frac{2\omega_4 \gamma_{16} \eta_8}{\omega_4^2 + \omega^2} \left. \right) a_1^2 - \frac{1}{4\omega} \gamma_3 b_2^2 - \frac{1}{4\omega} \gamma_5 b_1^2 - \frac{1}{8\omega} \left( \alpha_2 - \alpha_5 \omega^2 + \frac{(\omega_3^2 - \omega^2) \gamma_{12} \eta_7^2}{(\omega_3^2 + \omega^2)^2} \right. \\
 & + \frac{\omega_3 \gamma_{13} \eta_7}{\omega_3^2 + \omega^2} + \frac{\omega^2 \gamma_{14} \eta_7}{\omega_3^2 + \omega^2} \left. \right) a_1^2 \cos(2\phi_2 - 2\phi_1) - \frac{1}{8\omega} \left( \alpha_4 \omega - \alpha_7 \omega + \frac{2\omega_3 \omega \gamma_{12} \eta_7^2}{(\omega_3^2 + \omega^2)^2} - \frac{\omega \gamma_{13} \eta_7}{\omega_3^2 + \omega^2} \right. \\
 & + \frac{\omega_3 \omega \gamma_{14} \eta_7}{\omega_3^2 + \omega^2} \left. \right) a_1^2 \sin(2\phi_2 - 2\phi_1) - \left( \frac{1}{2} \eta_3 b_2 + \frac{3}{8} \gamma_1 a_2^2 b_2 + \frac{1}{4} \gamma_7 a_1^2 b_2 + \frac{1}{4} \frac{\omega_4 \gamma_8 \eta_8}{\omega_4^2 + \omega^2} a_2^2 b_2 \right) \frac{\cos(\phi_4)}{\omega a_2} \\
 & - \frac{1}{8\omega} \gamma_3 b_2^2 \cos(2\phi_4) + \frac{1}{8} \frac{\gamma_8 \eta_8}{\omega_4^2 + \omega^2} a_2 b_2 \sin(\phi_4) + \frac{1}{8} \gamma_2 a_2 b_2 \sin(\phi_4) - \frac{1}{8\omega} (2\gamma_4 \\
 & + \frac{\omega_3 \gamma_{10} \eta_7}{\omega_3^2 + \omega^2}) a_1 b_1 \cos(\phi_3) - \frac{1}{8} \left( -2\gamma_6 + \frac{\gamma_{10} \eta_7}{\omega_3^2 + \omega^2} \right) a_1 b_1 \sin(\phi_3) - \frac{1}{8\omega a_2} \gamma_7 a_1^2 b_2 \cos(2\phi_2 - 2\phi_1 + \phi_4) \\
 & - \frac{1}{8\omega} \left( \gamma_4 + \frac{\omega_3 \gamma_{10} \eta_7}{\omega_3^2 + \omega^2} \right) a_1 b_1 \cos(2\phi_2 - 2\phi_1 - \phi_3) - \frac{1}{8} \left( -\gamma_6 + \frac{\gamma_{10} \eta_7}{\omega_3^2 + \omega^2} \right) a_1 b_1 \sin(2\phi_2 - 2\phi_1 - \phi_3) \\
 & - \frac{1}{8\omega} \gamma_5 b_1^2 \cos(2\phi_2 - 2\phi_1 - 2\phi_3) - \frac{1}{2\omega a_2} (\omega + \sigma)^2 f \sin(\phi_2)
 \end{aligned} \tag{67}$$

where  $\phi_1 = \sigma t - \theta_1$ ,  $\phi_2 = \sigma t - \theta_2$ ,  $\phi_3 = \theta_1 - \theta_3 - \sigma_1 t$ , and  $\phi_4 = \theta_2 - \theta_4 - \sigma_2 t$ . By inserting Equations (43) to (48) and (58) into Equations (25) to (30), one can extract an approximate solution for the closed-loop system given by Equations (19) to (24), as follows:

$$z_1(t) = a_1(t) \cos(\Omega t - \phi_1(t)) \tag{68}$$

$$z_2(t) = a_2(t) \cos(\Omega t - \phi_2(t)) \tag{69}$$

$$z_3(t) = b_1(t) \cos(\Omega t - (\phi_1(t) + \phi_3(t))) \tag{70}$$

$$z_4(t) = b_2(t) \cos(\Omega t - (\phi_2(t) + \phi_4(t))) \tag{71}$$

$$z_5(t) = \frac{\eta_7 a_1}{\omega_3^2 + \omega^2} (\omega_3 \cos(\Omega t - \phi_1(t)) + \omega \sin(\Omega t - \phi_1(t))) \tag{72}$$

$$z_6(t) = \frac{\eta_8 a_2}{\omega_4^2 + \omega^2} (\omega_4 \cos(\Omega t - \phi_2(t)) + \omega \sin(\Omega t - \phi_2(t))) \tag{73}$$

It is clear from Equations (68) to (71) that  $a_1(t)$  and  $a_2(t)$  are the steady-state oscillation amplitudes of the twelve-poles rotor system, while  $\phi_1(t)$  and  $\phi_2(t)$  represent the phase angles of the controlled rotor. In addition,  $b_1(t)$  and  $b_2(t)$  represent the oscillation amplitudes of the PPF controllers and  $\phi_1(t) + \phi_3(t)$ ,  $\phi_2(t) + \phi_4(t)$  are the corresponding phase angles. In addition, Equations (72) and (73) show that the dynamical characteristics of the IRC controller depend on the dynamics of the rotor system (i.e.,  $z_5(t)$  depends on  $a_1(t)$ ,  $\phi_1(t)$  and  $z_6(t)$  depends on  $a_2(t)$ ,  $\phi_2(t)$ ). Moreover, the derived nonlinear autonomous system that is provided by Equations (60) to (67) governs the evolution of the oscillation amplitudes ( $a_1, a_2, b_1, b_2$ ) and the corresponding phase angles ( $\phi_1, \phi_2, \phi_3, \phi_4$ ) of the closed-loop system as a function of the different system parameters (i.e.,  $f, \sigma, \sigma_1, \sigma_2, p, d, \eta_1, \eta_2, \eta_3, \eta_4, \eta_5, \eta_6, \eta_7, \eta_8, \dots$ , etc.). Accordingly, the dynamical characteristics of the closed-loop system can be explored by investigating the nonlinear dynamical system provided by Equations (60) to (67). Therefore, one can explore the steady-state dynamics of the closed-loop system by inserting  $\dot{a}_1 = \dot{a}_2 = \dot{b}_1 = \dot{b}_2 = \dot{\phi}_1 = \dot{\phi}_2 = \dot{\phi}_3 = \dot{\phi}_4 = 0$  into Equations (60) to (67), which results in the following nonlinear algebraic system:

$$F_j(a_1, a_2, b_1, b_2, \phi_1, \phi_2, \phi_3, \phi_4) = 0; \quad j = 1, 2, \dots, 8 \tag{74}$$

Solving Equation (74), utilizing  $\sigma$  as a bifurcation parameter at the different values of the system and control parameters ( $f, \sigma_1, \sigma_2, p, d, \eta_1, \eta_2, \eta_3, \eta_4, \eta_5, \eta_6, \eta_7, \eta_8, \dots$ , etc.), we can explore the efficiency of the introduced control technique (i.e., PD + IRC + PPF controller). In addition, to investigate the stability of the solution of Equation (74), one can check the eigenvalues of the Jacobian matrix of the dynamical system given by Equations (60) to (67), which can be obtained via letting ( $a_{10}, a_{20}, b_{10}, b_{20}, \phi_{10}, \phi_{20}, \phi_{30}, \phi_{40}$ )

be the solution of Equation (74) and  $(a_{11}, a_{21}, b_{10}, b_{20}, \phi_{11}, \phi_{21}, \phi_{31}, \phi_{41})$  be a small deviation about this solution. Therefore, one can write

$$\begin{aligned} a_j &= a_{j0} + a_{j1}, & b_j &= b_{j0} + b_{j1}, & \phi_k &= \phi_{k0} + \phi_{k1}, & \dot{a}_j &= \dot{a}_{j1}, \\ \dot{b}_j &= \dot{b}_{j1}, & \dot{\phi}_k &= \dot{\phi}_{k1}; & j &= 1, 2; & k &= 1, 2, \dots, 4. \end{aligned} \tag{75}$$

Inserting Equation (75) into Equations (60) to (67) and expanding for the small deviations  $(a_{11}, a_{21}, b_{10}, b_{20}, \phi_{11}, \phi_{21}, \phi_{31}, \phi_{41})$ , retaining the linear terms only, one can derive the following linearized dynamical system:

$$\begin{pmatrix} \dot{a}_{11} \\ \dot{a}_{21} \\ \dot{b}_{11} \\ \dot{b}_{21} \\ \dot{\phi}_{11} \\ \dot{\phi}_{21} \\ \dot{\phi}_{31} \\ \dot{\phi}_{41} \end{pmatrix} = \begin{pmatrix} J_{11} & J_{12} & J_{13} & J_{14} & J_{15} & J_{16} & J_{17} & J_{18} \\ J_{21} & J_{22} & J_{23} & J_{24} & J_{25} & J_{26} & J_{27} & J_{28} \\ J_{31} & J_{32} & J_{33} & J_{34} & J_{35} & J_{36} & J_{37} & J_{38} \\ J_{41} & J_{42} & J_{43} & J_{44} & J_{45} & J_{46} & J_{47} & J_{48} \\ J_{51} & J_{52} & J_{53} & J_{54} & J_{55} & J_{56} & J_{57} & J_{58} \\ J_{61} & J_{62} & J_{63} & J_{64} & J_{65} & J_{66} & J_{67} & J_{68} \\ J_{71} & J_{72} & J_{73} & J_{74} & J_{75} & J_{76} & J_{77} & J_{78} \\ J_{81} & J_{82} & J_{83} & J_{84} & J_{85} & J_{86} & J_{87} & J_{88} \end{pmatrix} \begin{pmatrix} a_{11} \\ a_{21} \\ b_{11} \\ b_{21} \\ \phi_{11} \\ \phi_{21} \\ \phi_{31} \\ \phi_{41} \end{pmatrix} \tag{76}$$

where  $J_{mn}$  ( $m = 1, 2, \dots, 8, n = 1, 2, \dots, 8$ ) are provided in Appendix C. Accordingly, the stability of the dynamical system provided by Equations (60) to (67) has been studied by examining the eigenvalues of the linearized system provided by Equation (76) (see [42]), where the stable solution was illustrated as a solid-line, while the unstable solution was plotted as a dotted-line, as shown in the different bifurcation diagrams in Section 4.

#### 4. Steady-State Oscillation and Bifurcation Analysis

Based on both the derived mathematical model of the closed-loop system provided by Equations (19) to (24) and the nonlinear algebraic Equation (74), one can investigate the efficiency of the proposed control technique (i.e.,  $PD + IRC + PPF$  controller) in improving the oscillatory characteristics and eliminating the catastrophic bifurcation behaviors of the studied twelve-pole system. As Equation (74) governs the steady-state vibration amplitudes  $(a_1, a_2, b_1, b_2)$  and the corresponding phase angles (i.e.,  $\phi_1, \phi_2, \phi_3, \phi_4$ ), we can investigate the steady-state oscillatory behaviors of both the rotor system and the connected controller via solving Equation (74) numerically using the Newton–Raphson predictor–corrector algorithm (see [43]), utilizing  $\sigma$  as the bifurcation parameter, where the stable solution is plotted as a solid-line and the unstable solution is shown as a dotted-line. In addition, to validate the accuracy of the derived analytical solution (i.e., Equation (74)), as well as to investigate the full system response (i.e., steady-state and transient response) of the closed-loop system, one can simulate the system’s temporal equations of motion (i.e., Equations (19) to (24)) numerically using the Rung–Kutta method of fourth order. Accordingly, the following values of the parameters have been used to simulate the system dynamics [29,36]:  $f = 0.013, p = 1.5, d = 0.005, \eta_1 = \eta_2 = \eta_3 = \eta_4 = \eta_5 = \eta_6 = 0.2, \eta_7 = \eta_8 = 1, \mu_1 = \mu_2 = 0.01, \sigma = \sigma_1 = \sigma_2 = 0, \Omega = \omega + \sigma, \omega_1 = \omega + \sigma_1, \omega_2 = \omega + \sigma_2, \omega_3 = \omega_4 = 1, \alpha = 30^\circ$ , where the other system parameters  $\mu, \omega, \alpha_j, \beta_k, \gamma_k, (j = 1, 2, \dots, 7; k = 1, 2, \dots, 16)$  are defined below Equation (24). Before proceeding further, let us go back first to the normalized equations of motion (Equations (19) to (24)), where the rotor normalized temporal displacements in the X and Y directions are defined such that  $z_1(t) = \frac{x(t)}{c_0}$  and  $z_2(t) = \frac{y(t)}{c_0}$ , where  $c_0$  is the nominal air-gap size between the rotor and the poles-housing and  $x(t), y(t)$  are the actual temporal displacement of the rotor in the X and Y directions, respectively. Accordingly, for safe working conditions for the rotor system without the occurrence of rub and/or impact forces between the rotor and the pole housing,  $x(t)$  and  $y(t)$  should be smaller than the air-gap size  $c_0$  (i.e.,  $\left| \frac{x(t)}{c_0} \right| = |z_1(t)| < 1$  and  $\left| \frac{y(t)}{c_0} \right| = |z_2(t)| < 1$ ). Therefore, for the safe operation of the rotor system without rub

and/or impact between the rotor and the stator,  $|z_1(t)| = |a_1(t) \cos(\Omega t - \phi_1(t))|$  and  $|z_2(t)| = |a_2(t) \cos(\Omega t - \phi_2(t))|$  should be smaller than unity, which implies that  $|a_1|$  and  $|a_2|$  must be lower than unity (i.e.,  $|a_1| < 1$  &  $|a_2| < 1$ ). In addition, the parameter  $\sigma$  is defined in Equation (53) such that  $\Omega = \omega + \sigma$ . Accordingly,  $\sigma$  is used in the whole article as a bifurcation control parameter to describe the rotor dynamics when the system angular speed ( $\Omega$ ) is close to or equal to the rotor's natural frequency ( $\omega$ ).

#### 4.1. System Dynamics in the Case of PD-Control Algorithm

The parameters  $P = \frac{c_0}{I_0} k_1$  and  $d = \frac{c_0 \theta}{I_0} k_2$  denote the normalized proportional gain and derivative gain of the PD-control algorithm, respectively. In addition, the parameters  $\eta_1 = \frac{(1+2 \cos(\alpha)) c_0}{I_0} k_3$  and  $\eta_3 = \frac{(1+2 \cos(\alpha)) c_0}{I_0} k_5$  are the normalized control gains the PPF-control algorithm that is connected to the rotor system, while  $\eta_2 = \frac{(1+2 \cos(\alpha)) c_0}{I_0} k_4$  and  $\eta_4 = \frac{(1+2 \cos(\alpha)) c_0}{I_0} k_6$  represent the normalized control gains of the IRC-control algorithm (see Equations (6), (19) and (20)). Moreover, the parameters  $\eta_5 = \frac{L_1}{\theta^2}$  and  $\eta_6 = \frac{L_2}{\theta^2}$  are the normalized feedback gains of the PPF-control algorithm, while  $\eta_7 = \frac{L_3}{\theta}$ ,  $\eta_8 = \frac{L_4}{\theta}$  denote the feedback gains of the IRC-control algorithm (see Equations (7)–(10) and (21)–(24)). Accordingly, one can investigate the influence of the PD controller only on the rotor dynamics via setting  $\eta_k = 0$  ( $k = 1, 2, \dots, 4$ ).

This section is dedicated to investigating the rotor dynamics in the case of the PD-control algorithm only, at different levels of the excitation force  $f$ , as shown in Figure 3. The figure was obtained by solving the nonlinear system provided by Equation (74) when  $\eta_k = 0$ , ( $k = 1, 2, \dots, 8$ ) at  $f = 0.004, 0.007, 0.01, \text{ and } 0.013$ . Figure 3a,b shows the rotor steady-state vibration amplitudes in both the X and Y directions at four different values of the excitation force  $f$ , while Figure 3c shows the evolution of the phase angles  $\phi_1$  and  $\phi_2$  versus  $\sigma$  when  $f = 0.004$ . In addition, Figure 3d illustrates the phase angles  $\phi_1$  and  $\phi_2$  at  $f = 0.013$ . It is clear from Figure 3a,b that the vibration amplitudes ( $a_1$  and  $a_2$ ) of the twelve-poles system is a monotonic increasing function of the excitation force, where the rotor system may be subjected to rub and/or impact force between the rotating disk and the pole-housing if  $f \geq 0.013$  (i.e., the rotor may exhibit vibration amplitudes  $a_1 > 1$  and/or  $a_2 > 1$  if  $f \geq 0.013$ ). Accordingly, one can conclude that the considered system can work properly without a catastrophic rub and/or impact between the rotor and stator, as long as the excitation force  $f$  is smaller than 0.013 when only the PD-control algorithm is applied. In addition, Figure 3c,d depicts that the phase angle  $\phi_2$  is always greater than  $\phi_1$ , which means that the rotor system performs a forward whirling motion only (according to Equations (68) and (69)) along the  $\sigma$  axis, regardless of the excitation force magnitude. By examining Figure 3, one can note that the rotor system has symmetric oscillation amplitudes in both the X and Y directions (i.e.,  $a_1 = a_2$ ) and the phase difference  $\phi_2 - \phi_1$  is always  $\frac{\pi}{2}$ , which demonstrates that the rotor system performs a circular forward whirling motion along the  $\sigma$  axis, regardless of the excitation force magnitude.

#### 4.2. System Dynamics in the Case of the PD + PPF-Control Algorithm

The rotor dynamics at four different magnitudes of the excitation force were investigated when both the PD- and PPF-control algorithms were applied simultaneously. Figure 4a–c shows the steady-state vibration amplitudes of both the rotor system ( $a_1$  and  $a_2$ ) and the PPF-control algorithm ( $b_1$  and  $b_2$ ) when  $p = 1.5, d = 0.005, \eta_1 = \eta_3 = 0.2$ , and  $\eta_2 = \eta_4 = 0.0$  at the four excitation force amplitudes  $f = 0.0025, 0.0075, 0.0125, \text{ and } 0.0175$ . In addition, Figure 4e,f illustrates the evolution of the rotor phase angles  $\phi_1$  and  $\phi_2$  at  $f = 0.0025$  and  $f = 0.0175$ , respectively. By comparing Figure 3a,b with Figure 4a,b, one can deduce that the integration of the PPF-control algorithm to the twelve-poles rotor has suppressed the system's vibrations at the perfect resonance condition (i.e., it has suppressed the system's vibrations at  $\sigma = 0.0$ ). However, two undesired resonant peaks appeared on both sides of  $\sigma = 0.0$ . In addition, Figure 4a,b demonstrates that the rotor system may work safely without rub and/or impact between the rotor and the poles-housing, as long



as the excitation force  $f < 0.0175$  (i.e.,  $a_1 < 1$  and  $a_2 < 1$  as long as  $f < 0.0175$ ). Moreover, Figure 4e,f shows that the phase difference ( $\phi_2 - \phi_1$ ) of the rotor lateral oscillations in the X and Y directions is always constant, so that  $\phi_2 - \phi_1 = \frac{\pi}{2}$ , which implies that the system exhibits only a forward circular whirling motion, regardless of both the angular speed and the excitation force magnitude. Generally, Figure 4 shows that the integration of the PPF-control algorithm to the system with the P-controller suppressed the rotor's undesired vibrations at the perfect resonance condition (i.e., when  $\Omega = \omega + \sigma, \sigma = 0.0$ ), regardless of the excitation force amplitude; however, the system may suffer from high oscillation, especially if  $\Omega > \omega$ . Accordingly, the PPF-control algorithm acts as a notch filter that eliminates the system's vibrations at a specific frequency band.

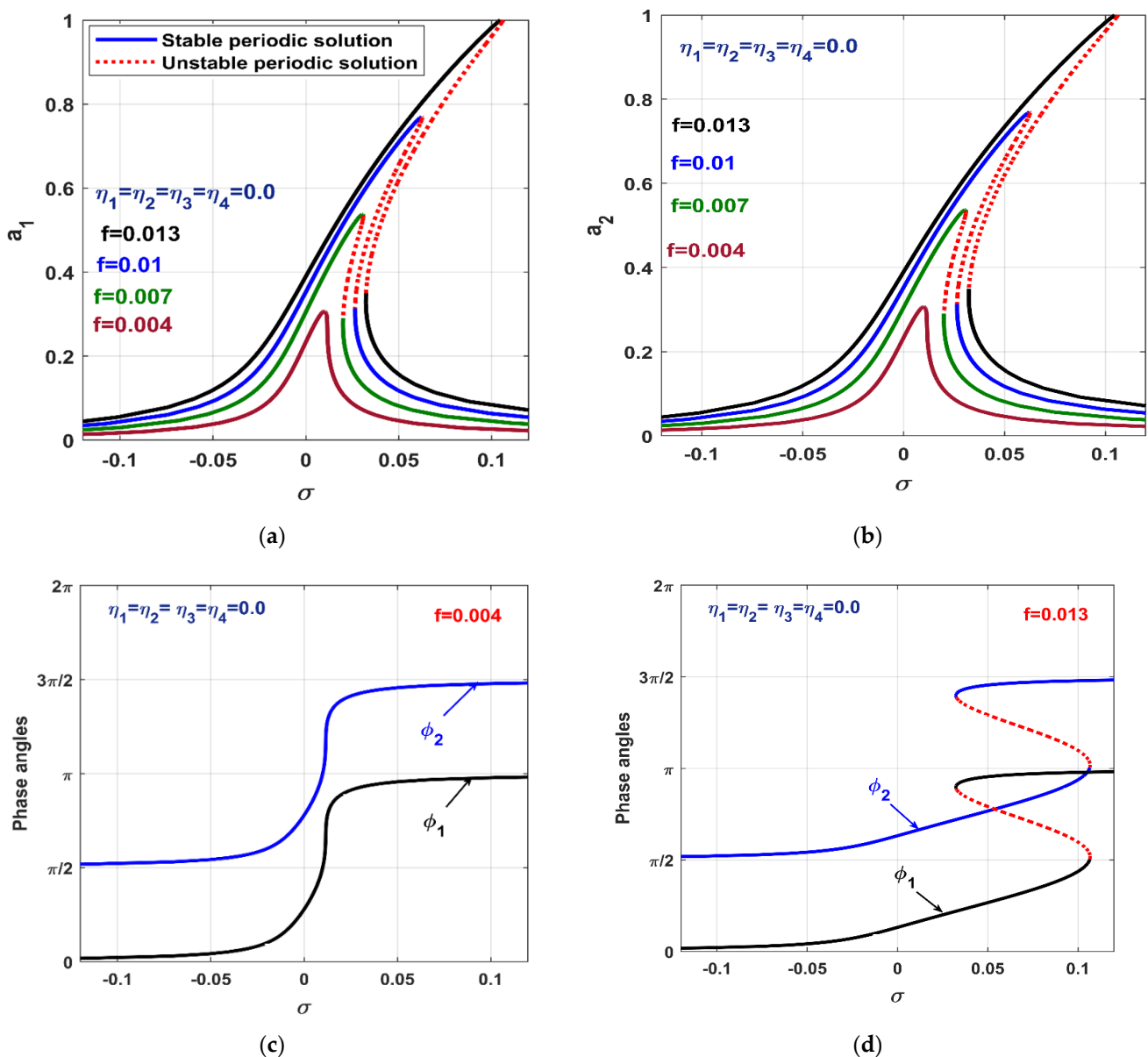


**Figure 3.** Vibration amplitudes and phase angles of the twelve-poles rotor in the case of the PD-control algorithm only: (a,b) vibration amplitudes ( $a_1, a_2$ ) when  $f = 0.004, 0.007, 0.01,$  and  $0.013,$  (c) phase angles ( $\phi_1, \phi_2$ ) when  $f = 0.004,$  (d) phase angles ( $\phi_1, \phi_2$ ) when  $f = 0.013.$

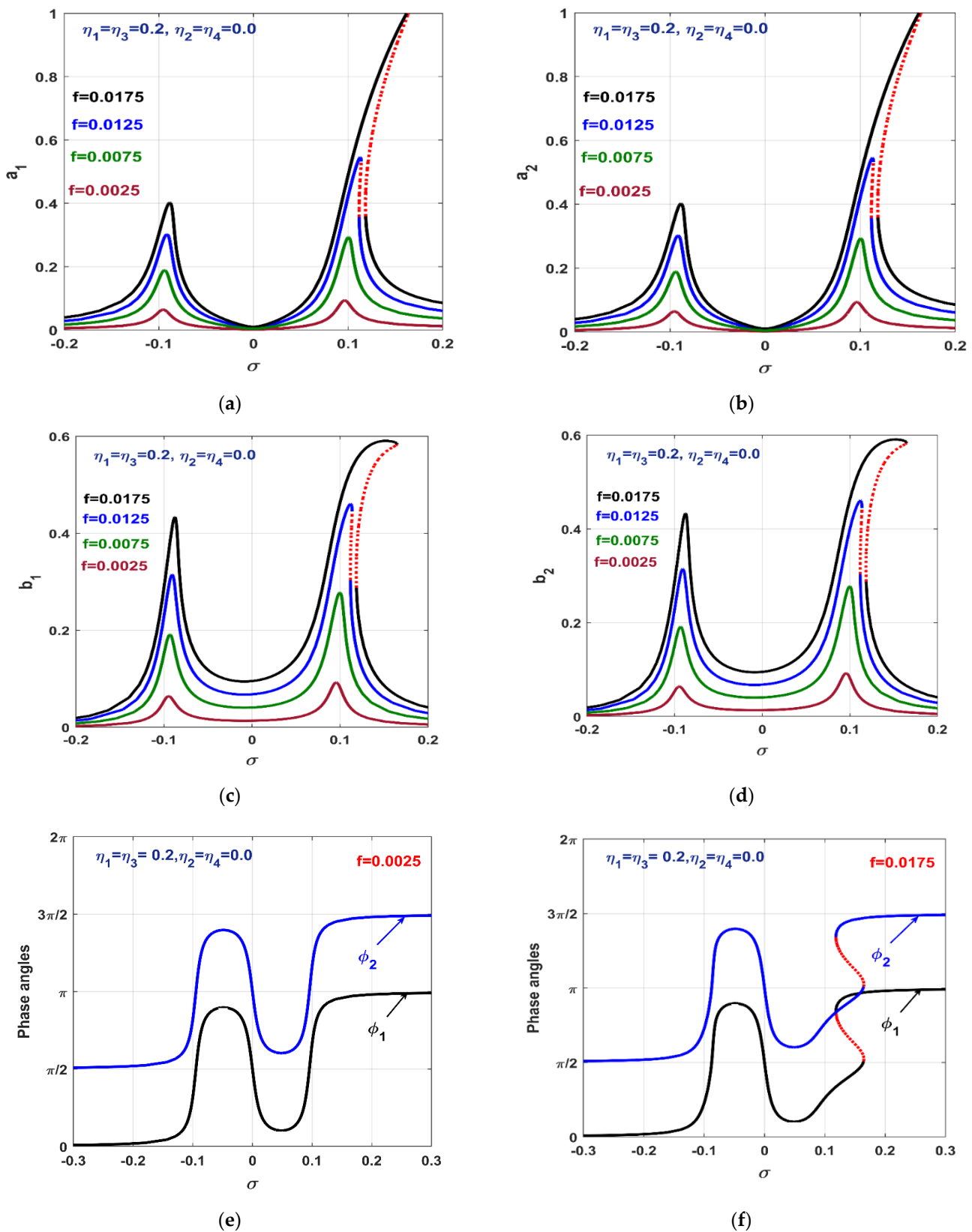


**Figure 4.** Vibration amplitudes of the twelve-poles rotor and the PPF controller in the case of the PD + PPF-control algorithm when  $f = 0.0025, 0.0075, 0.0125,$  and  $0.0175$ : (a,b) vibration amplitudes ( $a_1, a_2$ ) of the rotor, (c,d) vibration amplitudes ( $b_1, b_2$ ) of the PPF controller, (e) phase angles ( $\phi_1, \phi_2$ ) when  $f = 0.0025,$  and (f) phase angles ( $\phi_1, \phi_2$ ) when  $f = 0.0175.$

### 4.3. System Dynamics in the Case of the PD + IRC-Control Algorithm

The oscillatory behaviors of the system were explored when the IRC-control algorithm was coupled to the rotor system with the PD controller, while the PPF controller was turned off. Accordingly, Figure 5 shows the motion bifurcation of the rotor system when  $p = 1.5$ ,  $d = 0.005$ ,  $\eta_1 = \eta_3 = 0$ , and  $\eta_2 = \eta_4 = 0.2$  at four different magnitudes of the excitation force (i.e.,  $f = 0.02, 0.04, 0.06$  and  $0.08$ ). It is clear from Figure 5a,b that the IRC-control algorithm forced the twelve-poles system to respond like the linear system, even at the strong excitation forces. Moreover, Figure 5c,d demonstrates that the system can perform only a circular forward whirling motion along the  $\sigma$  axis, regardless of the excitation force magnitude, where  $\phi_2 - \phi_1 = \frac{\pi}{2}$  and  $a_1, a_2$  are symmetric on the interval  $-0.3 < \sigma < 0.3$ . By examining Figure 5, we can deduce that the system can rotate safely without rub and/or impact force between the rotor and the stator, even at the strong excitation forces (i.e.,  $f = 0.08$ ), compared with the case of the PD-control algorithm only, as shown in Figure 3. Therefore, coupling the IRC-control algorithm to the system increased the rotor linear damping coefficients, which ultimately decreased the lateral vibrations even at the large excitation forces. However, the IRC controller could not eliminate the system vibrations close to zero at the resonance condition (i.e., at  $\sigma = 0$ ), as in the case of the PPF-control technique, but the maximum vibration occurred at  $\sigma = 0$ . Therefore, utilizing the PPF- and IRC-control techniques as a one-control algorithm, along with the PD controller, may have the advantages of both the PPF and IRC controllers, as illustrated in the next subsection.

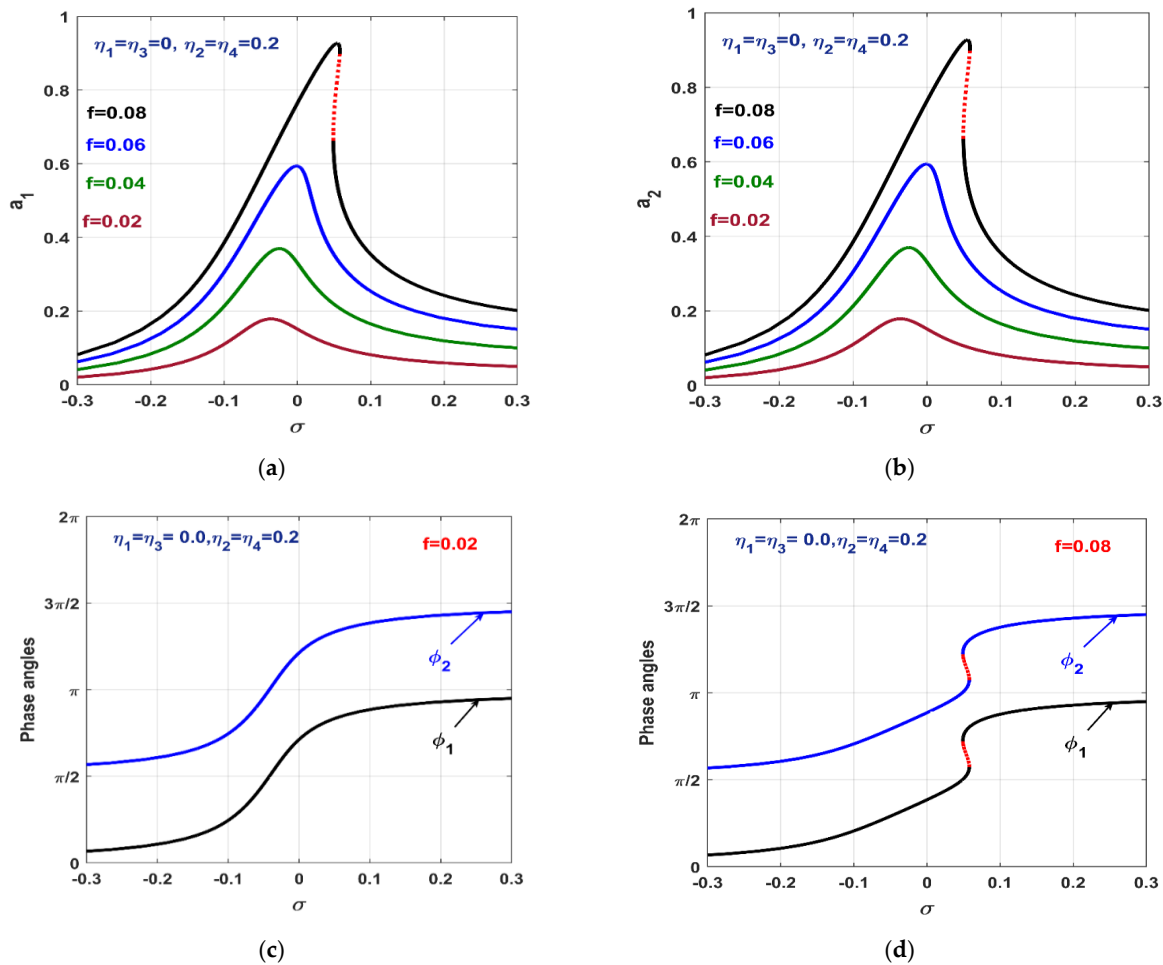


**Figure 5.** Vibration amplitudes of the twelve-poles rotor in the case of the PD + IRC-control algorithm when  $f = 0.02, 0.04, 0.06$ , and  $0.08$ : (a,b) vibration amplitudes ( $a_1, a_2$ ) of the rotor, (c) phase angles ( $\phi_1, \phi_2$ ) when  $f = 0.02$ , and (d) phase angles when  $f = 0.08$ .

4.4. System Dynamics in the Case of PD + IRC + PPF-Control Algorithm

The dynamical behaviors of the considered twelve-poles rotor system were explored when the three control algorithms (i.e., PD + IRC + PPF-control algorithms) were activated simultaneously. Figure 6 shows the nonlinear dynamics of the controlled rotor system when  $P = 1.5$ ,  $d = 0.005$ ,  $\eta_1 = \eta_2 = \eta_3 = \eta_4 = 0.2$  when the extinction force  $f = 0.025, 0.045, 0.065$ , and  $0.085$ . Figure 6a,b illustrates the evolution of the system's lateral vibrations ( $a_1, a_2$ ) against  $\sigma$ , while Figure 6c,d shows the vibration amplitudes of the PPF controller against the detuning parameter  $\sigma$ . In addition, Figure 6e,f illustrates the phase difference of the rotor's lateral vibrations in both the X and Y directions when  $f = 0.025$  and  $f = 0.085$ , respectively. It is clear from Figure 6a,b that the vibration amplitudes ( $a_1, a_2$ ) of the twelve-poles system was close to zero, regardless of the excitation force magnitude, as long as  $\sigma \cong 0$ , due to the effect of the PPF-control algorithm. In addition, the resonant peaks that appeared on both sides of  $\sigma = 0$  (as in Figure 4a,b) were mitigated, due to the effect of the IRC-control algorithm. Moreover, Figure 6a,b shows that the rotor system worked properly without impact occurrence between the rotor and stator, as long as  $f \leq 0.085$ . It was also clear from Figure 6e,f that the controlled rotor system performed a circular forward whirling motion, as long as  $-0.3 \leq \sigma \leq 0.3$ , where the phase difference was  $\phi_2 - \phi_1 = \pi/2$ . Based on Figure 3 to Figure 6, one can conclude that the integration of the PD-, IRC-, and PPF-control algorithms to act as a single controller can provide for the safe operation of the considered rotor system with small oscillation amplitudes at the resonant conditions (i.e., when  $\sigma = 0.0$ ), even if the excitation force is strong.

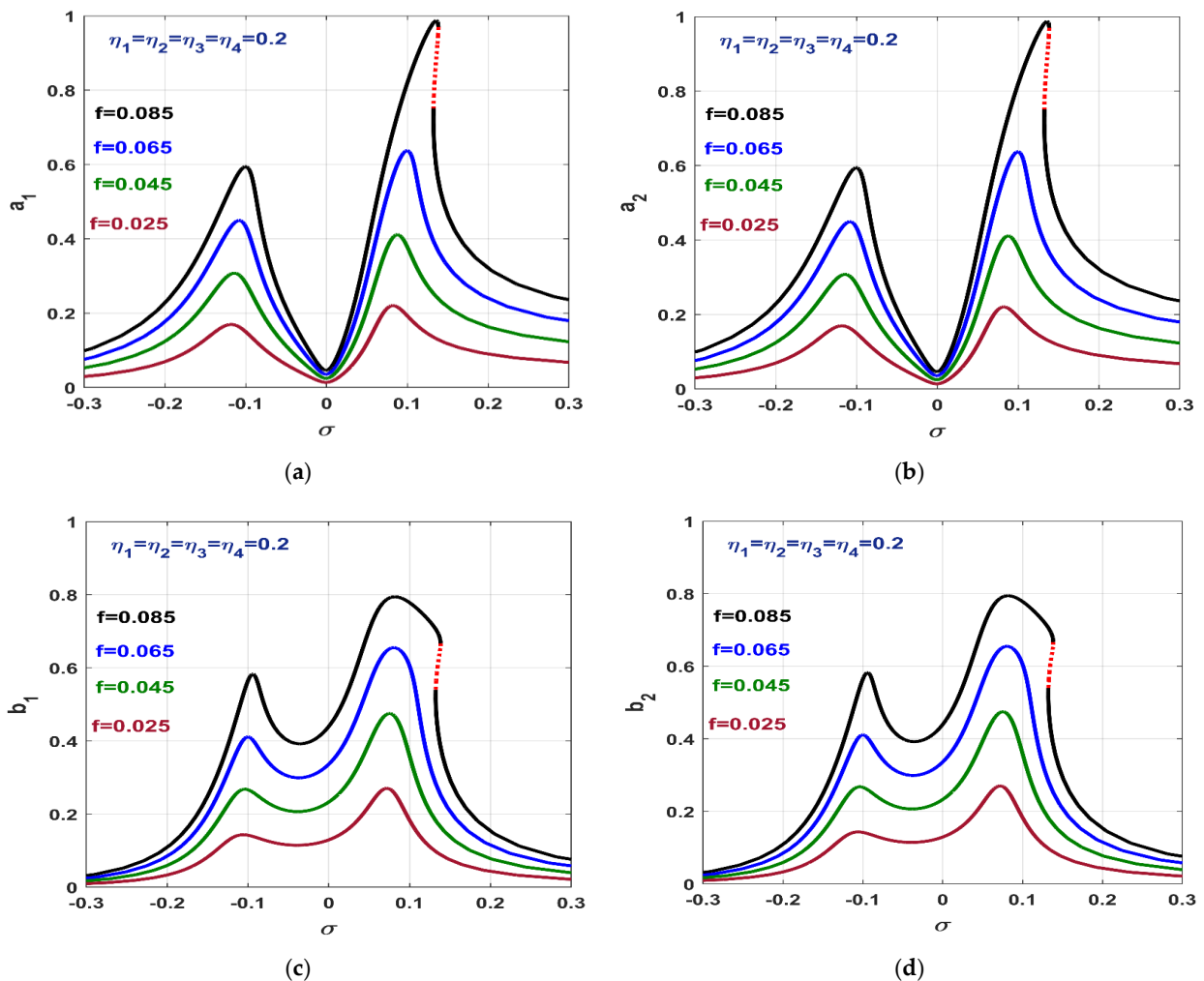
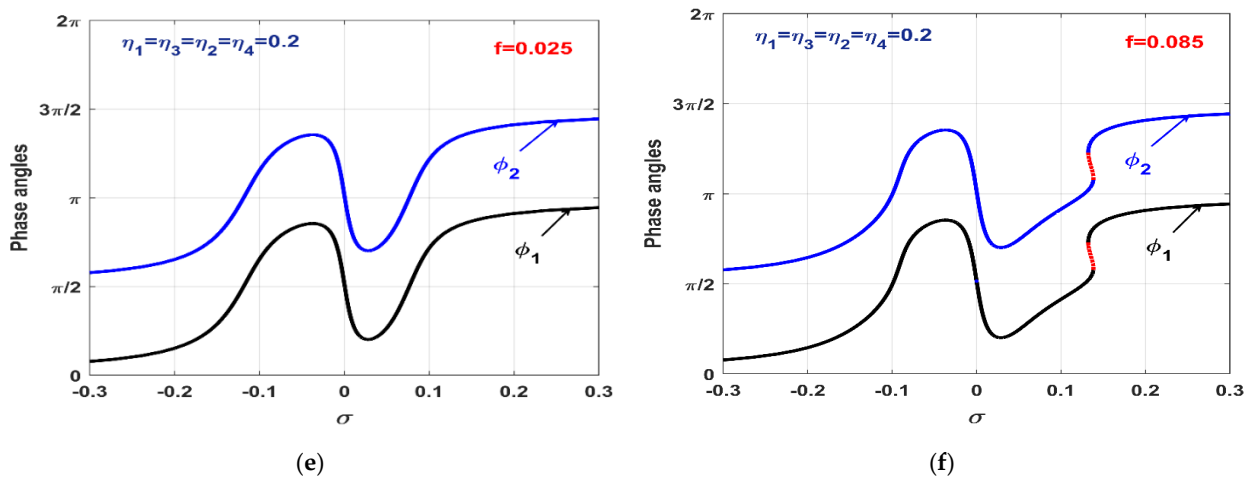


Figure 6. Cont.



**Figure 6.** Vibration amplitudes of the twelve-poles rotor in the case of the *PD + IRC + PPF*-control algorithm when  $f = 0.025, 0.045, 0.065,$  and  $0.085$ : (a,b) vibration amplitudes ( $a_1, a_2$ ) of the rotor, (c,d) vibration amplitudes ( $b_1, b_2$ ) of the *PPF* controller, (e) phase angles ( $\phi_1, \phi_2$ ) when  $f = 0.025,$  and (f) phase angles ( $\phi_1, \phi_2$ ) when  $f = 0.085$ .

4.5. Sensitivity Analysis of the *PD + IRC + PPF*-Control Algorithm

As the combined control algorithm (i.e., *PD + IRC + PPF*) has many advantages over the individual three control techniques, this subsection explores the sensitivity of this control method to the variation of different control gains. The effect of increasing the proportional gain ( $P$ ) on the vibration suppression efficiency of the control algorithm is illustrated in Figure 7. The figure shows that the increase in  $P$  increases the oscillation amplitudes ( $a_1, a_2$ ) of the twelve-poles system and degrades the control algorithm’s efficiency. Therefore, the  $P$  gain should be kept at the small possible value to guarantee the high performance of the proposed control technique. Based on the system parameters provided below Equation (24), the natural frequency of the rotor system  $\omega$  is defined as  $= \sqrt{2P \cos(\alpha) + P - 3}$ . Therefore, the minimum value of  $P$  should be selected in a way that guarantees that  $\omega > 0$ . On the other hand, the effect of the *PPF*-control gains (i.e.,  $\eta_1$  and  $\eta_3$ ) on the whole-system dynamics is depicted in Figure 8. The figure demonstrates that the increase of  $\eta_1$  and  $\eta_3$  (i.e.,  $\eta_1 = \eta_3 = 0.5$ ) enhanced the controller performance in eliminating the rotor oscillations at the perfect resonance condition (i.e., when  $\sigma = 0.0$ ), as well as widening the frequency band at which the system could work properly with small vibration amplitudes. In addition, Figure 9 demonstrates that the increase in the *IRC*-control gains (i.e.,  $\eta_2 = \eta_4 = 0.5$ ) decreased the resonant peaks that appeared on both sides of  $\sigma = 0.0$ , and improved the controller efficiency in suppressing the twelve-poles rotor vibrations along the  $\sigma$  axis (i.e., the controller was able to eliminate the rotor oscillations at any angular speed  $\Omega = \omega + \sigma, -0.3 \leq \sigma \leq 0.3$ ). Finally, the best tuning conditions between natural frequencies of both the rotor system ( $\omega$ ) and the suggested control technique ( $\omega_1$  and  $\omega_2$ ) are shown in Figure 10, where the rotor vibration amplitudes ( $a_1$  and  $a_2$ ) are plotted in 3D space against the variables  $\sigma$  and  $\sigma_1 = \sigma_2$ . By examining Figure 10a,b, we deduced that the smallest oscillation amplitudes of the rotor system (i.e.,  $a_1 = a_2 \cong 0$ ) occurred along the dashed line that had the equation  $\sigma = \sigma_1 = \sigma_2$ . Therefore, the best working condition of the introduced control algorithm occurred if  $\sigma = \sigma_1 = \sigma_2$ . Accordingly, one can conclude from Equation (53) that the optimum tuning conditions (i.e.,  $\sigma = \sigma_1 = \sigma_2$ ) occurred when adjusting the controller’s natural frequencies ( $\omega_1$  and  $\omega_2$ ) had the same value of rotor angular speed ( $\Omega$ ). Accordingly, the combined control algorithm eliminated the rotor vibrations close to zero, regardless of the excitation force amplitude and its angular speed, if the control gains and the tuning condition were applied, as discussed above.



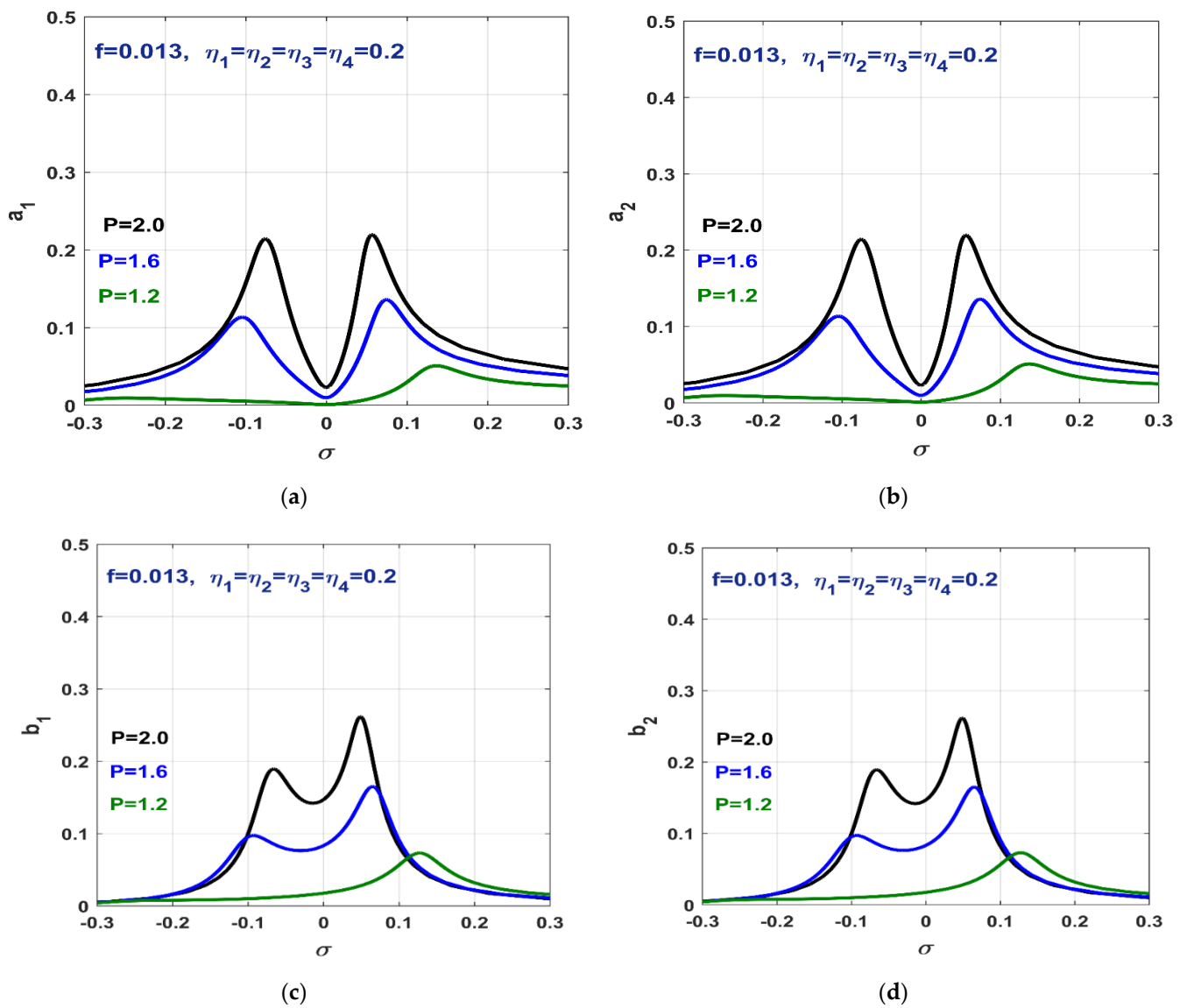


**Figure 7.** Vibration amplitudes of the twelve-poles rotor in the case of the PD + IRC + PPF-control algorithm at  $f = 0.013$ ,  $\eta_1 = \eta_2 = \eta_3 = \eta_4 = 0.2$  when  $p = 1.2, 1.6$ , and  $2.0$ : (a,b) vibration amplitudes ( $a_1, a_2$ ) of the rotor, and (c,d) vibration amplitudes ( $b_1, b_2$ ) of the PPF controller.

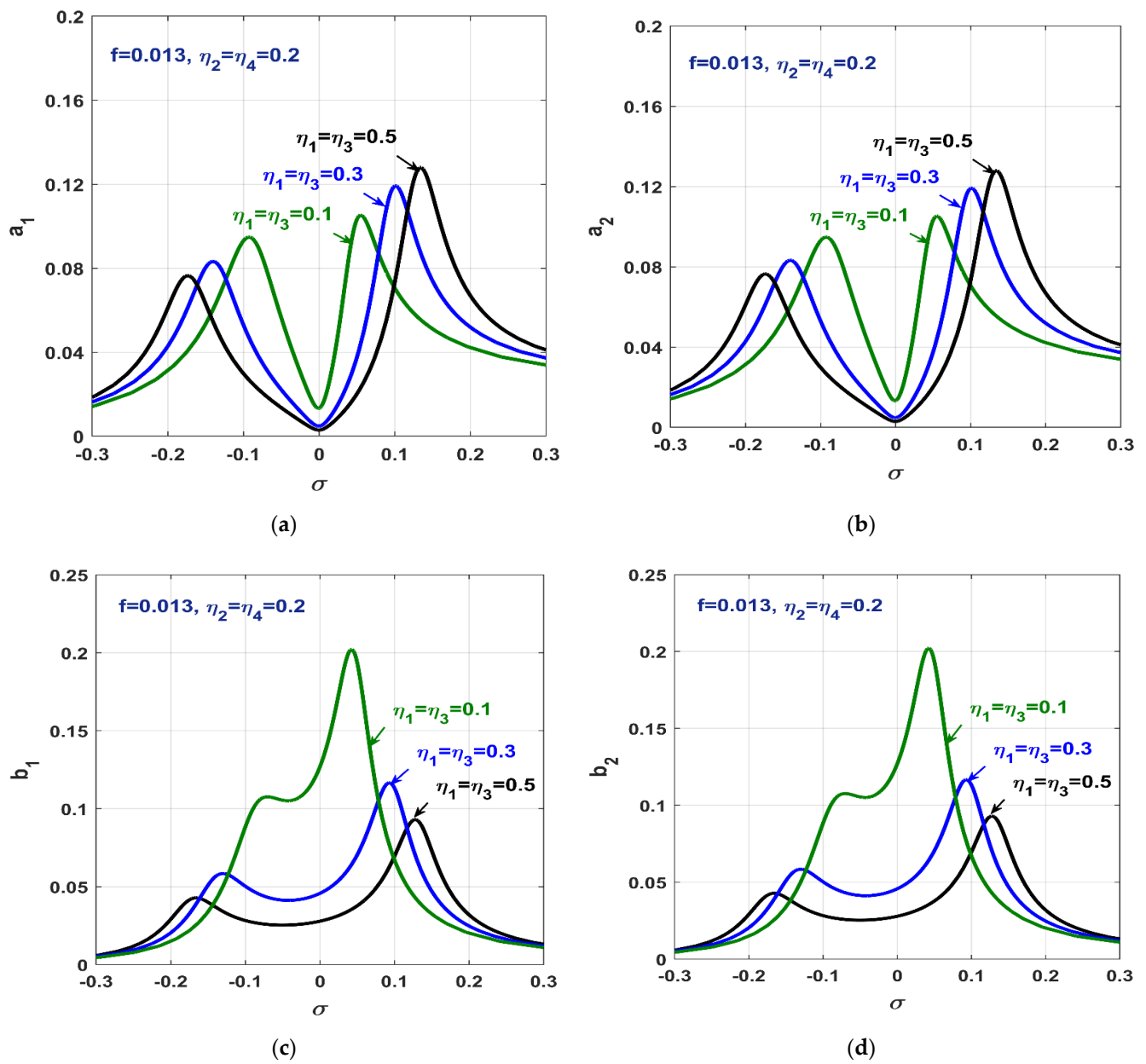


**Figure 8.** Vibration amplitudes of the twelve-poles rotor in the case of the *PD + IRC + PPF*-control algorithm at  $f = 0.013$ ,  $P = 1.5$ ,  $\eta_2 = \eta_4 = 0.2$  when  $\eta_1 = \eta_3 = 0.1, 0.3$ , and  $0.5$ : (a,b) vibration amplitudes ( $a_1, a_2$ ) of the rotor, and (c,d) vibration amplitudes ( $b_1, b_2$ ) of the PPF controller.

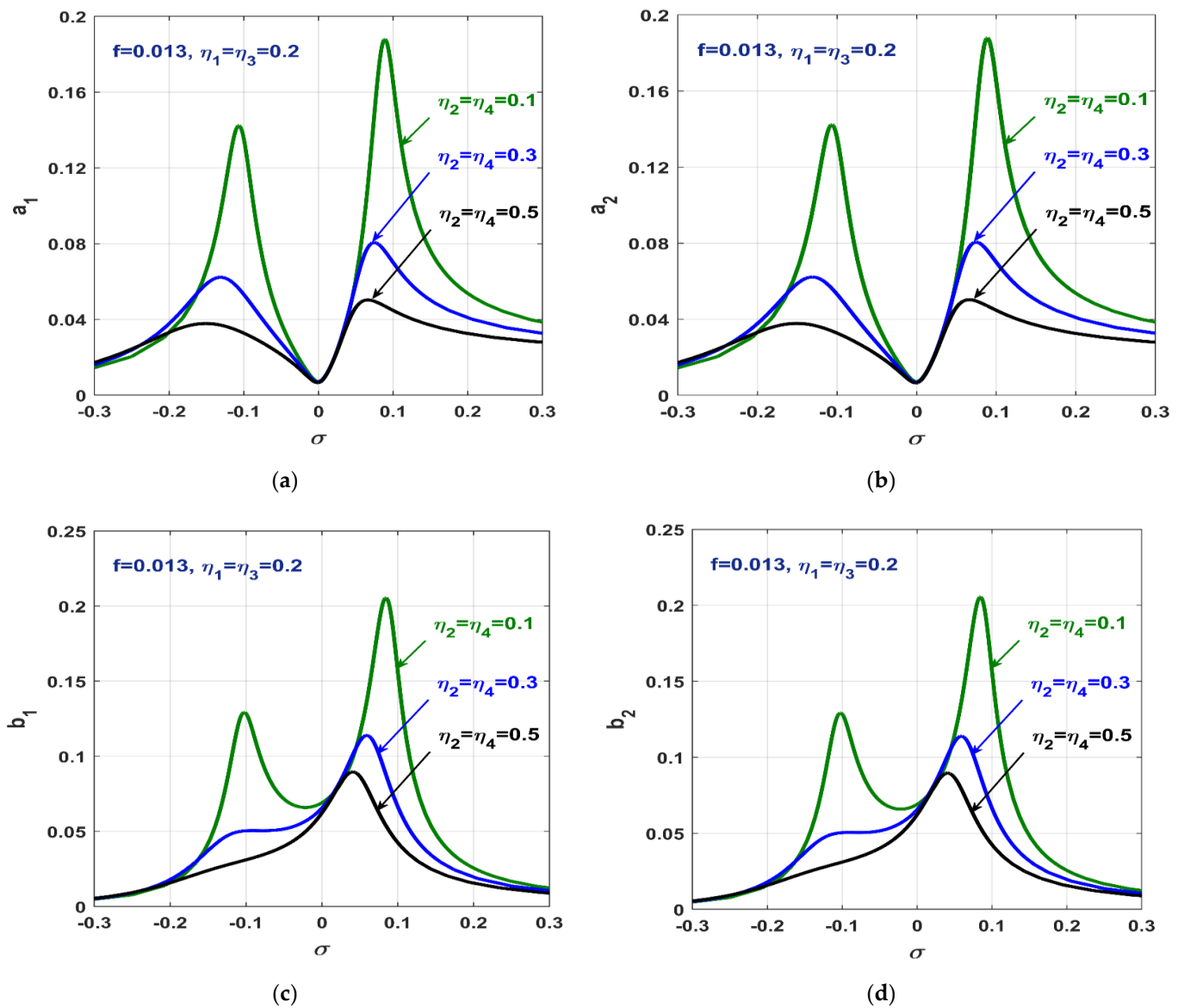


**Figure 9.** Vibration amplitudes of the twelve-poles rotor in the case of the *PD + IRC + PPF*-control algorithm at  $f = 0.013$ ,  $\eta_1 = \eta_3 = 0.2$ , when  $\eta_2 = \eta_4 = 0.1, 0.3$ , and  $0.5$ : (a,b) vibration amplitudes ( $a_1, a_2$ ) of the rotor, and (c,d) vibration amplitudes ( $b_1, b_2$ ) of the PPF controller.

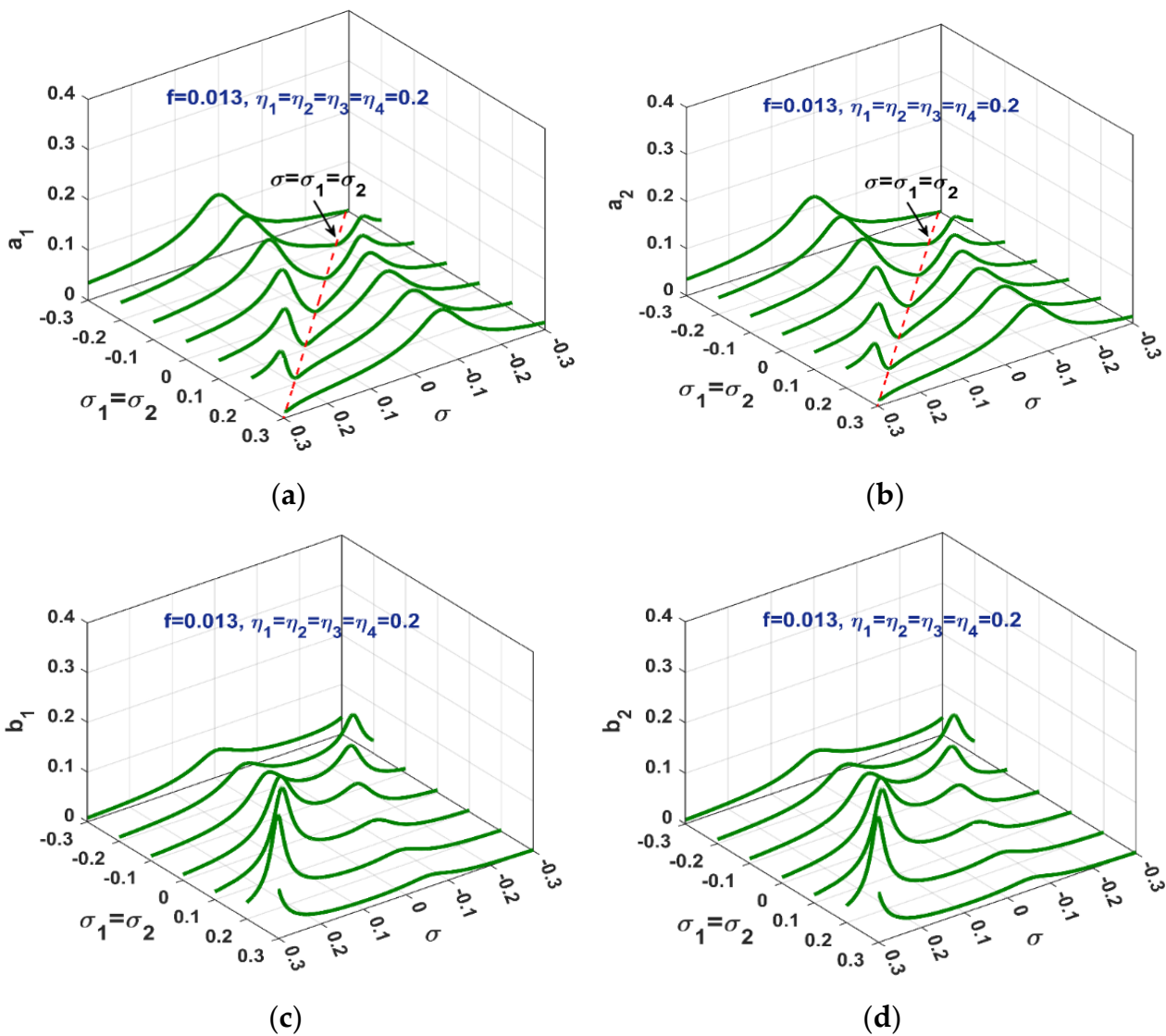


**Figure 10.** Vibration amplitudes of the twelve-poles s rotor in the case of the *PD + IRC + PPF*-control algorithm at  $f = 0.013$ , and  $\eta_1 = \eta_2 = \eta_3 = \eta_4 = 0.2$ : (a,b) vibration amplitudes ( $a_1, a_2$ ) of the rotor, and (c,d) vibration amplitudes ( $b_1, b_2$ ) of the *PPF* controller.

**5. Numerical Simulations and Comparative Study**

Numerical validations for all of the obtained results in Section 4 were validated numerically via solving the temporal equations of the closed-loop system (i.e., Equations (19) to (24)), using the Rung–Kutta method. In addition, the performances of the different control algorithms in eliminating the twelve-poles system vibrations were compared. It is worth mentioning that the small circles illustrated in Figure 11 represents the steady-state numerical solution of Equations (19) to (24). This numerical solution was obtained via solving Equations (19) to (24) numerically, using the ODE MATLAB solver for a long time-period until reaching the steady-state response at the different values of  $\sigma$  (notice that  $\Omega = \omega + \sigma$ ). Then, the maximum temporal vibration amplitudes at steady-state were captured as the steady-state vibration amplitudes (i.e.,  $a_1 = \max(z_1(t))$ ,  $a_2 = \max(z_2(t))$ ,  $a_3 = \max(z_3(t))$ ,  $a_4 = \max(z_4(t))$ ).

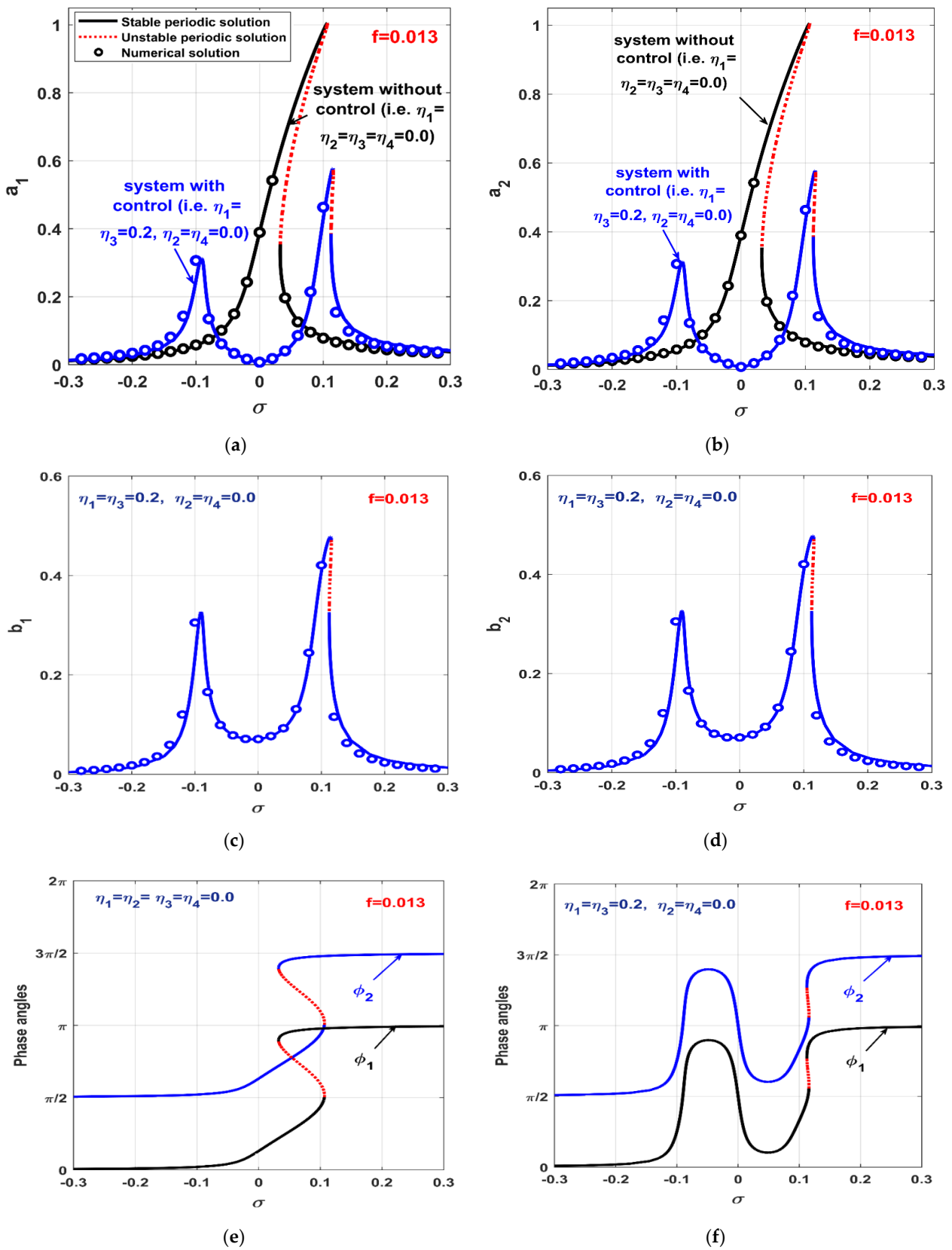


**Figure 11.** Vibration amplitudes and phase angles of the twelve-poles rotor in the case of both the PD-control only and the PD + PPF-control algorithms, when  $f = 0.013$ : (a,b) vibration amplitudes ( $a_1, a_2$ ) of the rotor, and (c,d) vibration amplitudes ( $b_1, b_2$ ) of the PPF-controller, (e) phase angles ( $\phi_1, \phi_2$ ) when  $\eta_1 = \eta_2 = \eta_3 = \eta_4 = 0.0$ , and (f) phase angles ( $\phi_1, \phi_2$ ) when  $\eta_1 = \eta_3 = 0.2, \eta_2 = \eta_4 = 0.0$ .

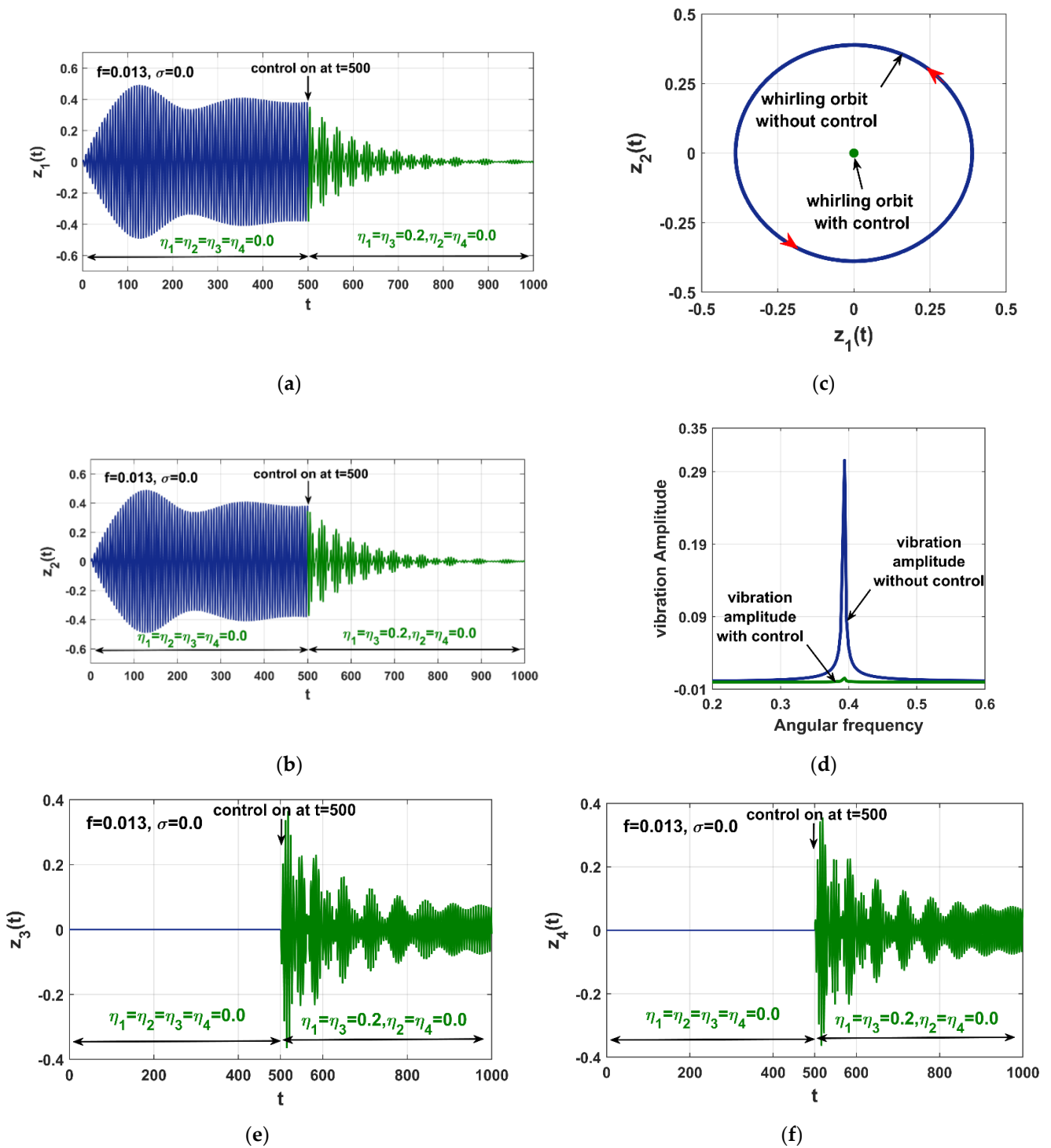


Figure 11 compares the rotor dynamics in the case of both the *PD*- and the *PD + PPF*-control algorithms, when the excitation force  $f = 0.013$ . The excellent correspondence between the numerical solutions (i.e., small circles) obtained by solving Equations (19)–(22) and the analytical solutions (i.e., solid and dotted lines) obtained by solving the algebraic system provided by Equation (74) is clear. In addition, the figure demonstrates that the coupling of the *PPF*-control algorithm with the *PD* controller eliminated the strong vibration amplitudes of the rotor at the resonance condition (i.e., when  $\sigma \rightarrow 0$ ); however, two resonant peaks appeared on both sides of  $\sigma = 0$ . Accordingly, we concluded that the *PD + PPF*-control algorithm had high efficiency in eliminating the rotor's undesired vibrations at the perfect resonance case (i.e., when  $\sigma = 0$  or, in other words, when the angular speed  $\Omega$  was equal to the system's natural frequency  $\omega$ ,  $\Omega = \omega + \sigma$ ). However, if the resonant condition was lost (i.e.,  $\Omega \neq \omega$ ), the controller may pump excessive vibratory energy to the rotor system, rather than suppress it (see, for example, Figure 11a,b at  $\sigma = 0.1$ ).

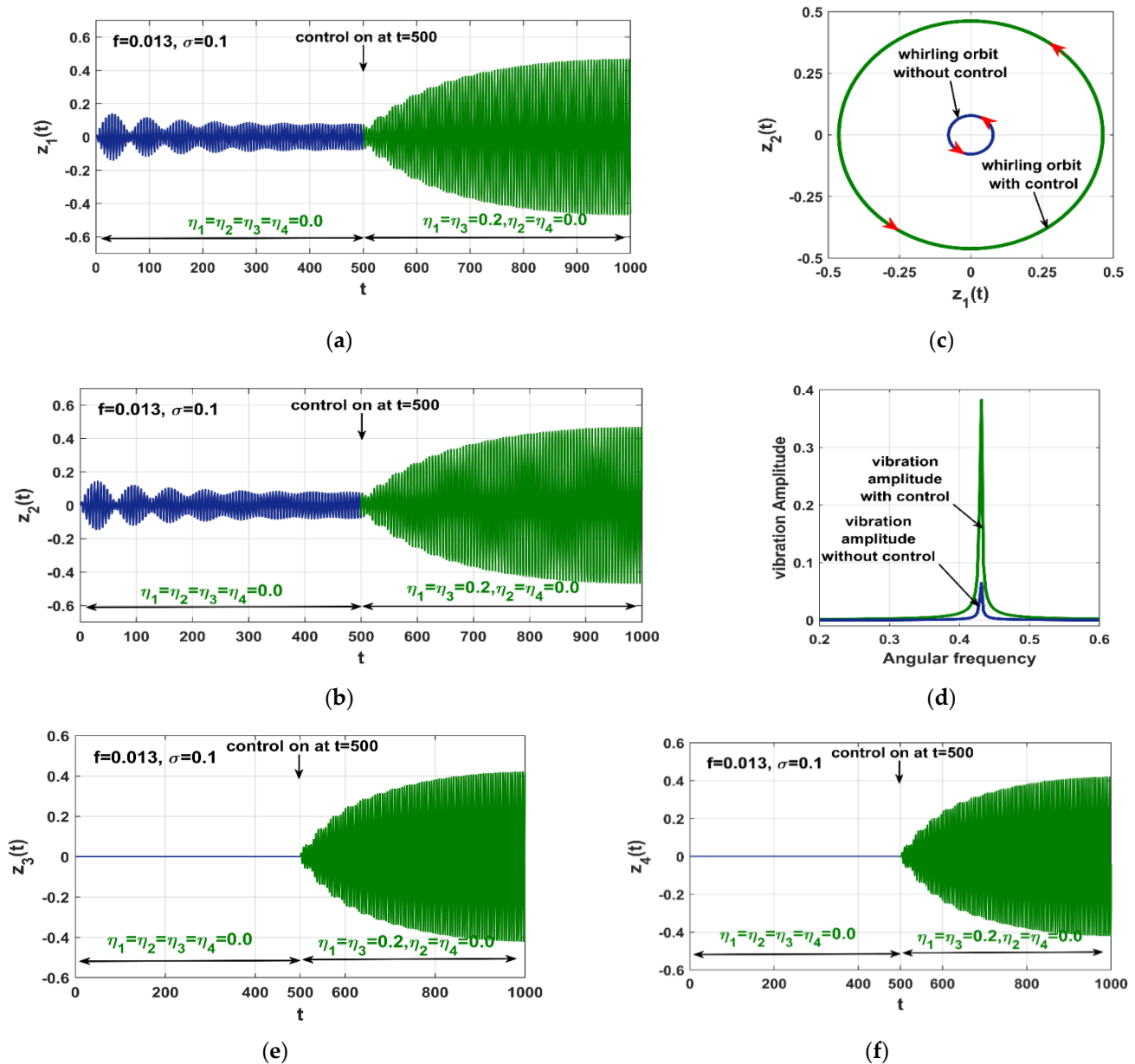
The instantaneous oscillations of the controlled twelve-poles system in the case of both the *PD*- and the *PD + PPF*-control algorithms are simulated in Figure 12, according to Figure 11, at  $\sigma = 0.0$ ,  $f = 0.013$ , and  $\Omega = \omega$ . The figure was obtained by solving Equations (19) to (22) numerically on the time interval  $0 \leq t < 500$  and turning off the *PPF*-control algorithm (i.e., with setting  $\eta_1 = \eta_3 = \eta_5 = \eta_6 = 0$ ); then, at the instant  $t = 500$ , the *PPF*-control algorithm was turned on via setting  $\eta_1 = \eta_3 = \eta_5 = \eta_6 = 0.2$  along the period  $500 \leq t \leq 1000$ . Figure 12a,b illustrates the instantaneous oscillations of the twelve-poles system in the case of both the *PD*-control algorithm on the time interval  $0 \leq t < 500$  and the *PD + PPF*-control algorithm on the time interval  $500 \leq t \leq 1000$ , while Figure 12c shows the rotor whirling orbit before and after turning on the *PPF*-control algorithm. Figure 12d compares the vibration amplitude of the rotor system in the case of both the *PD* and *PD + PPF*-control algorithms. In addition, Figure 12e,f illustrates the temporal oscillations of the *PPF* controller. It is clear from the figure that the high instantaneous oscillations of the rotor system (i.e.,  $z_1(t)$  and  $z_2(t)$ ) in the case of the *PD* controller only were suppressed close to zero when the *PPF*-control algorithm was activated at the time instant  $t = 500$ , where the rotor vibration energy was channeled to *PPF* controller.

Figure 13 illustrates the instantaneous oscillatory behaviors of the twelve-poles system in the case of both the *PD*-control algorithm only and the *PD + PPF*-control algorithm, according to Figure 11, when  $\sigma = 0.1$  (i.e., when the perfect resonance condition is lost,  $\Omega = \omega + 0.1$ ). Therefore, Figure 13 is a repetition of Figure 12, but  $\sigma = 0.1$ . It is clear from Figure 13a,b that the twelve-poles system exhibited small vibration amplitudes on the time interval  $0 \leq t < 500$ , as long as the *PD* controller only was activated. However, the figures demonstrate that the activation of the *PPF* controller along with *PD* controller on the time interval  $500 \leq t \leq 1000$  increased the rotor lateral vibration rather than suppressing it, which agrees with Figure 11 at  $\sigma = 0.1$ .

The steady-state oscillatory motion of the rotor system in the case of both the *PD*-control algorithm only and the *PD + IRC*-control algorithm is compared in Figure 14, when  $f = 0.013$ . It is clear from the figure that the high oscillation amplitudes that occurred at the resonance case (i.e., when  $\sigma \rightarrow 0$ ) in the case of the *PD*-control algorithm only was mitigated to small lateral oscillations when the combined *PD + IRC*-control algorithm was activated. However, while the *PD + IRC*-control algorithm can mitigate the rotor vibrations along the  $\sigma$  axis, it cannot eliminate the rotor vibration close to zero at the resonant condition, as in the case of the *PD + PPF*-control algorithm.



**Figure 12.** Time response of the rotor system according to Figure 11 when  $\sigma = 0$  (i.e., when  $\Omega = \omega$ ) in the case of the *PD*-control algorithm and the *PD + PPF*-control algorithm: (a,b) the temporal oscillations  $z_1(t)$  and  $z_2(t)$  of the rotor system, (c) the rotor whirling orbits, (d) the rotor frequency spectrum, and (e,f) the temporal oscillations  $z_3(t)$  and  $z_4(t)$  of the *PPF* controller.



**Figure 13.** Time response of the rotor system according to Figure 11 when  $\sigma = 0.1$  (i.e., when  $\Omega = \omega + 0.1$ ) in the case of the PD-control algorithm and the PD + PPF-control algorithm: (a,b) the temporal oscillations  $z_1(t)$  and  $z_2(t)$  of the rotor system, (c) the rotor whirling orbits, (d) the rotor frequency spectrum, and (e,f) the temporal oscillations  $z_3(t)$  and  $z_4(t)$  of the PPF controller.

Numerical simulations for the instantaneous lateral vibrations of the rotor system (i.e.,  $z_1(t)$  and  $z_2(t)$ ) and the IRC-control algorithm (i.e.,  $z_5(t)$  and  $z_6(t)$ ) are illustrated in Figures 15 and 16, according to Figure 14 when  $\sigma = 0.0$  and  $\sigma = 0.1$ , respectively. The two figures were obtained via solving Equations (19), (20), (23), and (24) using ODE45 MATLAB solver on the time interval  $0 \leq t < 700$  and deactivating the IRC-control algorithm (i.e., when  $\eta_2 = \eta_4 = \eta_7 = \eta_8 = 0$ ), while at  $t = 700$  the IRC controller was turned on by setting  $\eta_2 = \eta_4 = 0.2, \eta_7 = \eta_8 = 1$  on the interval  $700 \leq t \leq 1000$ . One can note from Figure 15 that the strong instantaneous vibrations of the system (i.e.,  $z_1(t)$  and  $z_2(t)$ ) in the case of the PD-control technique at  $\sigma = 0$  was reduced to small values (but not close to zero) when the IRC-control algorithm was turned on at  $t = 700$  and the rotor vibration energy was partially transferred to the IRC controller. On the other hand, Figure 16 shows that the IRC-control algorithm also reduced the rotor vibrations to a small value when  $\sigma = 0.1$  rather

than pumping more excess energy to the system, as in the case of the *PD + PPF*-control technique (see Figure 13).

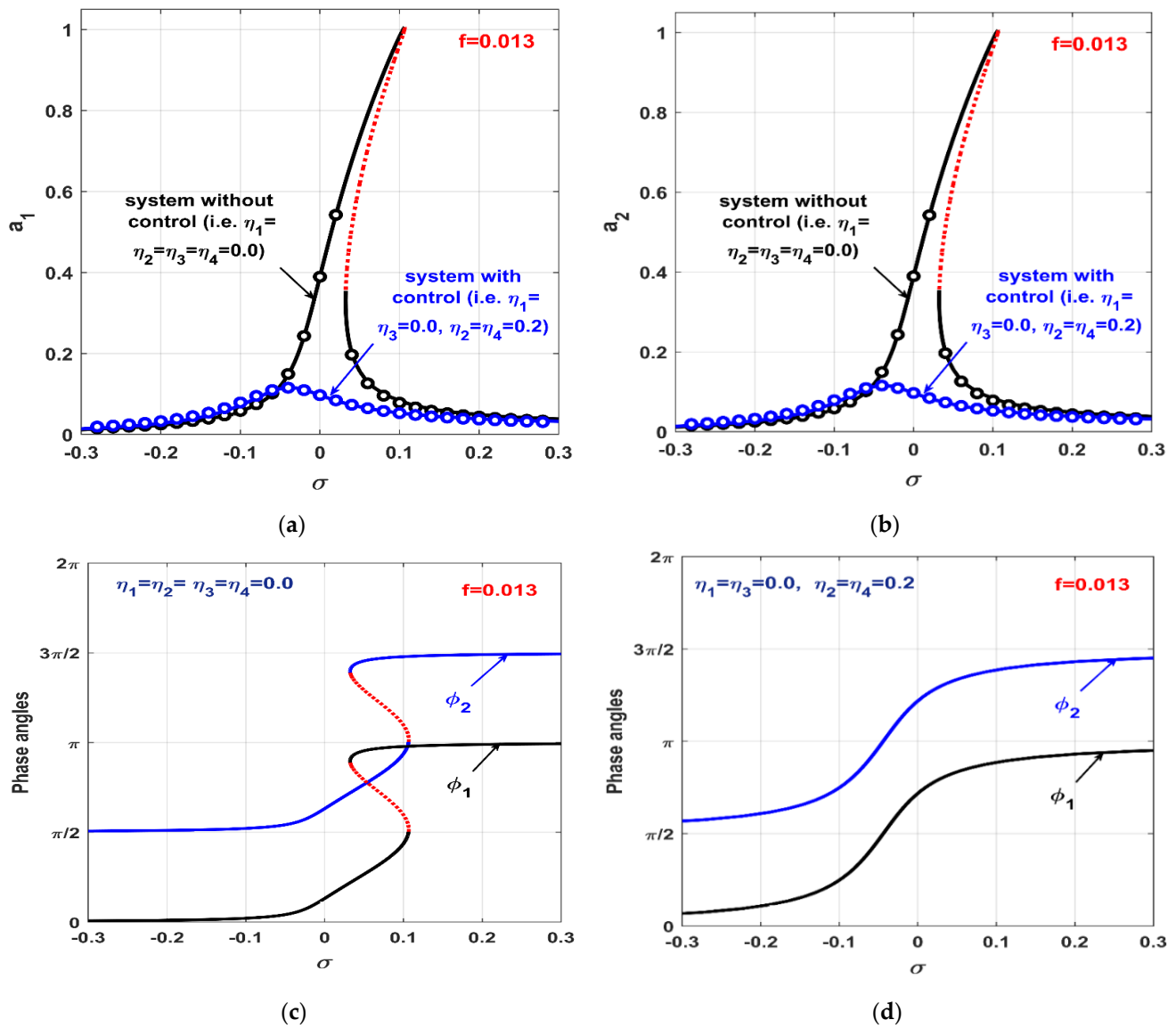


**Figure 14.** Vibration amplitudes and phase-angles of the twelve-poles rotor in the case of both the *PD*-control only and the *PD + IRC*-control algorithm when  $f = 0.013$ : (a,b) vibration amplitudes ( $a_1, a_2$ ) of the rotor, (c) phase angles ( $\phi_1, \phi_2$ ) when  $\eta_1 = \eta_2 = \eta_3 = \eta_4 = 0.0$ , and (d) phase angles ( $\phi_1, \phi_2$ ) when  $\eta_1 = \eta_3 = 0.0, \eta_2 = \eta_4 = 0.2$ .

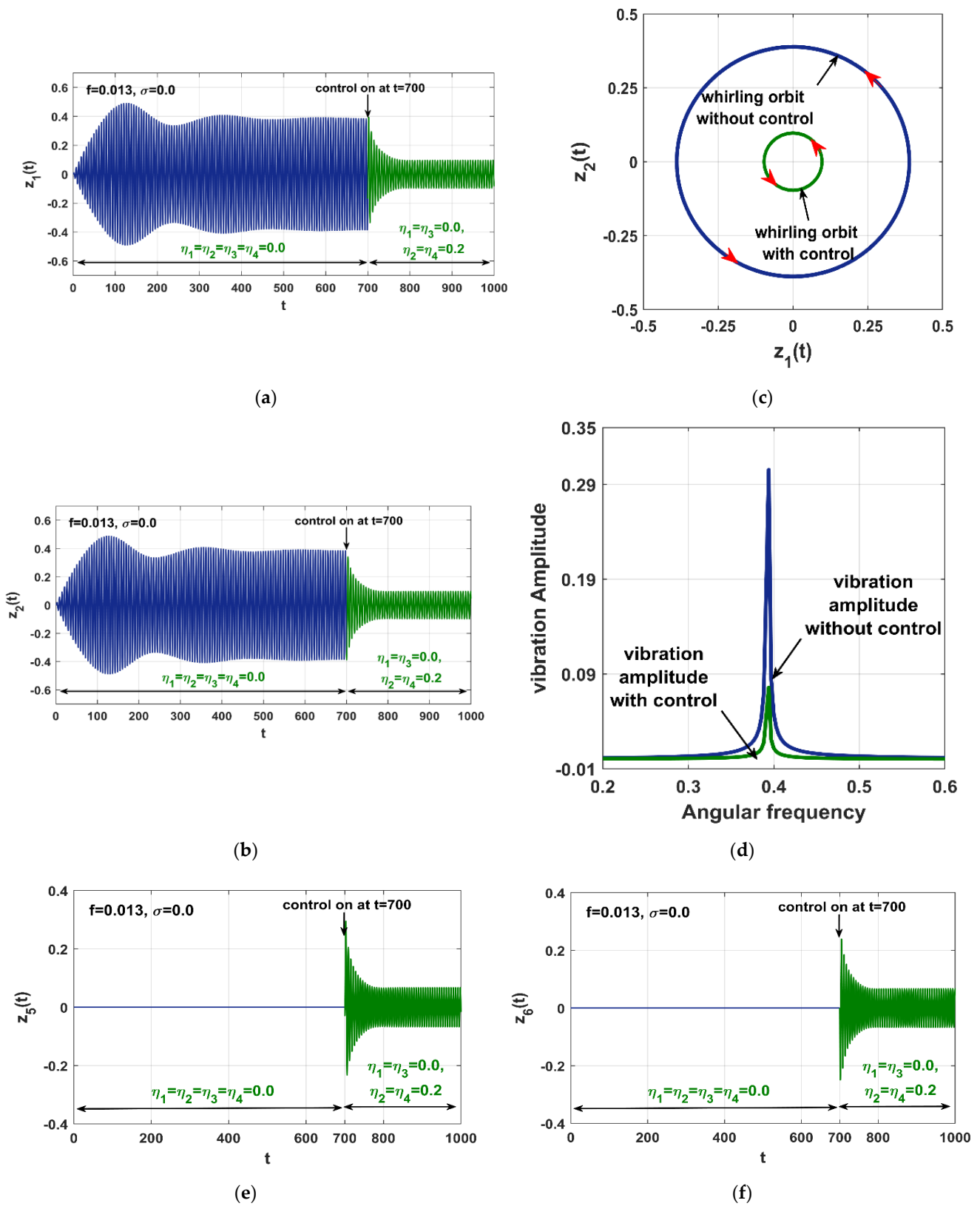


**Figure 15.** Time response of the rotor system according to Figure 14 when  $\sigma = 0.0$  (i.e., when  $\Omega = \omega$ ) in the case of the *PD*-control algorithm and the *PD + IRC*-control algorithm: (a,b) the temporal oscillations  $z_1(t)$  and  $z_2(t)$  of the rotor system, (c) the rotor whirling orbits, (d) the rotor frequency spectrum, and (e,f) the temporal oscillations  $z_5(t)$  and  $z_6(t)$  of the IRC controller.

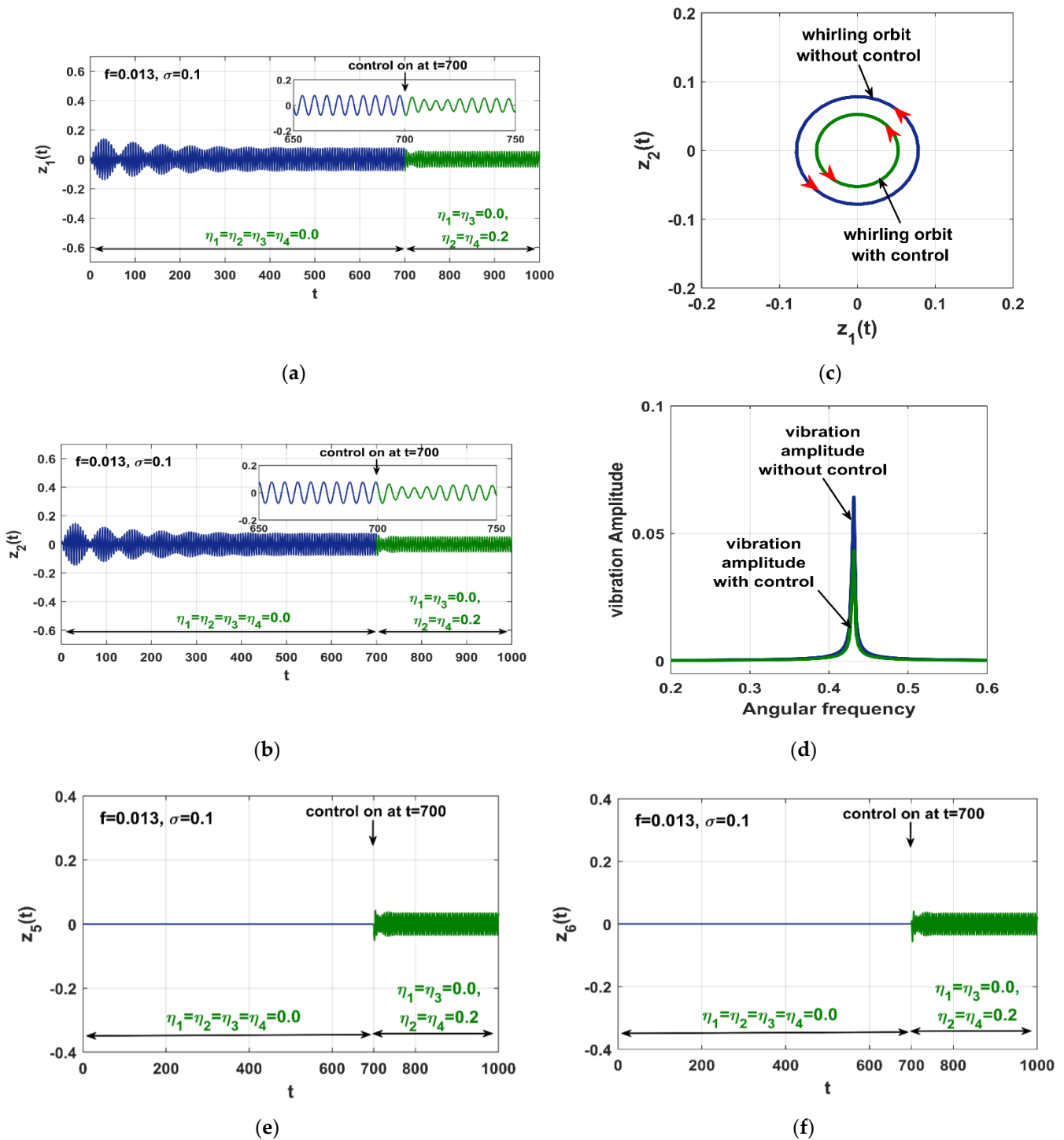


**Figure 16.** Time response of the rotor system according to Figure 14 when  $\sigma = 0.1$  (i.e., when  $\Omega = \omega + 0.1$ ) in the case of the *PD*-control algorithm and the *PD + IRC*-control algorithm: (a,b) the temporal oscillations  $z_1(t)$  and  $z_2(t)$  of the rotor system, (c) the rotor whirling orbits, (d) the rotor frequency spectrum, (e,f) the temporal oscillations  $z_5(t)$ , and  $z_6(t)$  of the IRC controller.

Finally, the rotor dynamics in the case of both the *PD*- and the *PD + IRC + PPF*-control algorithms are compared in Figure 17, when  $f = 0.013$ . It is clear from the figure that the high oscillation amplitudes of the rotor system in the vicinity of  $\sigma = 0$  in the case of the *PD*-control algorithm only have been eliminated close to zero, when the *PD + IRC + PPF*-control algorithm is considered. In addition, the resonant peaks that appeared in Figure 11 (i.e., in the case of *PD + PPF*-control) were also suppressed, as shown in Figure 17. In other

words, the *PD + IRC + PPF*-control algorithm had all the advantages of the individual control algorithms *PD*, *IRC*, and *PPF*, while avoiding their drawbacks.

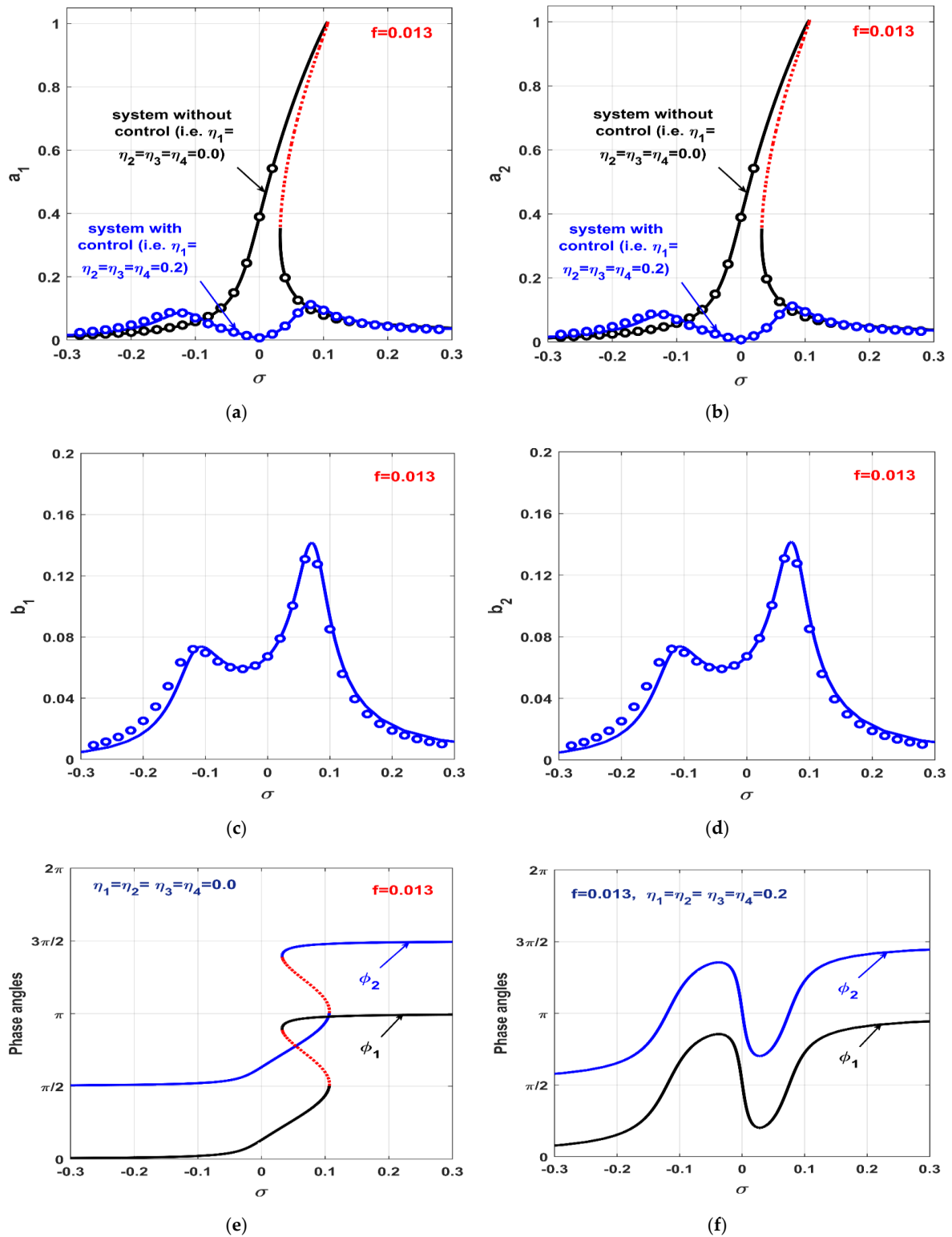


**Figure 17.** Vibration amplitudes and phase angles of the twelve-poles rotor in the case of both the *PD*-control algorithm only and the *PD + IRC + PPF*-control algorithm when  $f = 0.013$ : (a,b) vibration amplitudes ( $a_1$ ,  $a_2$ ) of the rotor, and (c,d) vibration amplitudes ( $b_1$ ,  $b_2$ ) of the *PPF* controller, (e) phase angles ( $\phi_1$ ,  $\phi_2$ ) when  $\eta_1 = \eta_2 = \eta_3 = \eta_4 = 0.0$ , and (f) phase angles ( $\phi_1$ ,  $\phi_2$ ) when  $\eta_1 = \eta_3 = \eta_2 = \eta_4 = 0.2$ .



Figures 18 and 19 compare the instantaneous oscillations of the rotor system in the care of both the *PD*- and the *PD + IRC + PPF*-control algorithms, according to Figure 17, when  $f = 0.013$  at  $\sigma = 0$  and  $\sigma = 0.1$ , respectively. Figure 18 was obtained by solving Equations (19) to (24) numerically, using the ODE45 solver along the time interval  $0 \leq t < 700$  and activating the *PD* controller only (i.e.,  $P = 1.5$ ,  $d = 0.005$ , and  $\eta_k = 0$ ,  $k = 1, 2, \dots, 4$ ); then, at the time instant  $t = 700$ , the *IRC + PPF*-control algorithm was turned on, along with the *PD* controller, via setting  $\eta_1 = \eta_2 = \eta_3 = \eta_4 = 0.2$  on the time interval  $700 \leq t \leq 1000$ . Figure 19 is a repetition of Figure 18, but when  $\sigma = 0.1$  rather than  $\sigma = 0.0$ . By examining Figure 18a–c, one can notice that the high oscillation amplitudes of the twelve-poles system were eliminated close to zero at a very small transient time as soon as the *PD + IRC + PPF* controller was turned on. In addition, Figure 19 demonstrates that the *PD + IRC + PPF*-control algorithm did not add excessive energy to the rotor system when the resonant condition was lost (i.e., when  $\sigma = 0.1$ ).

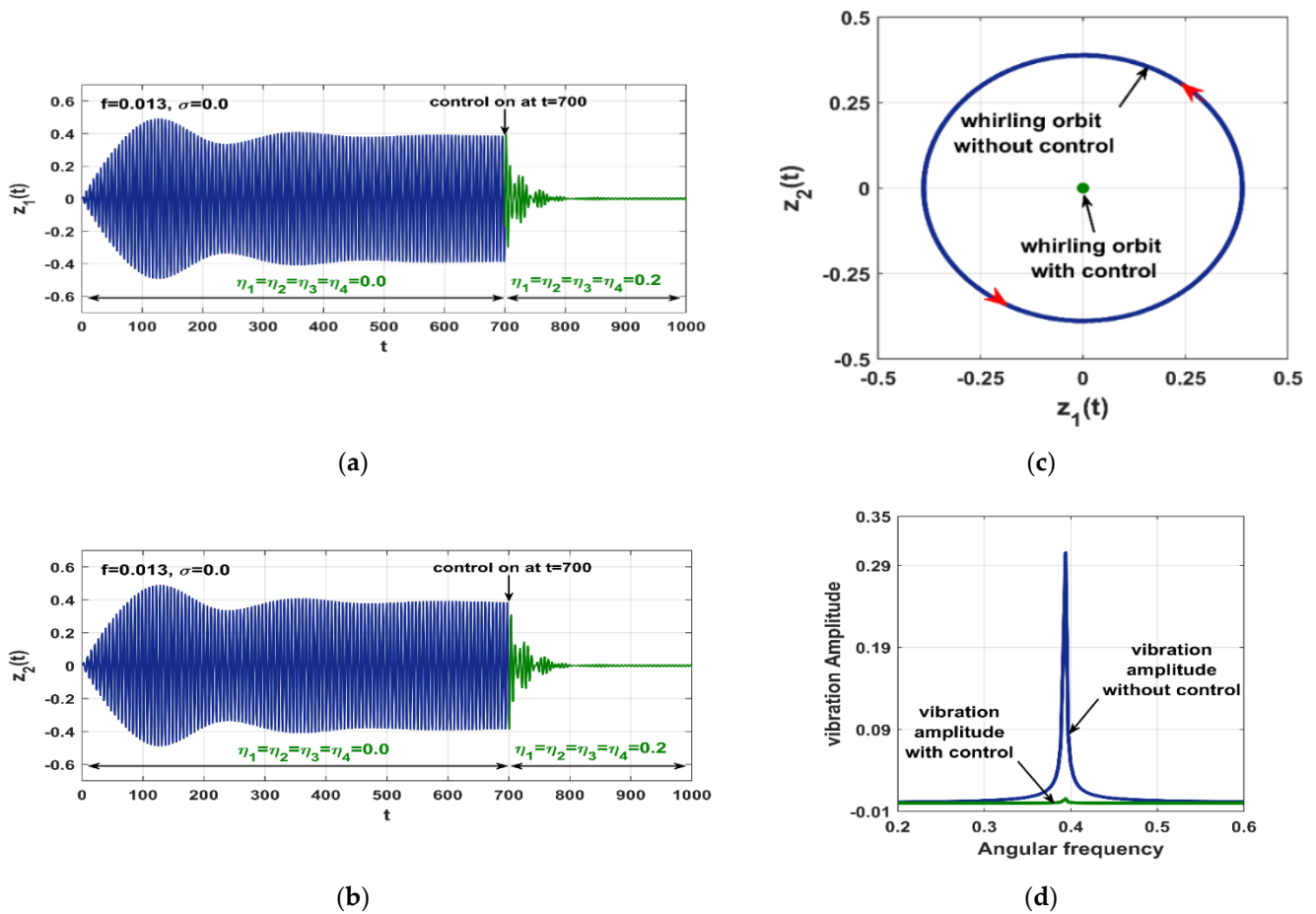
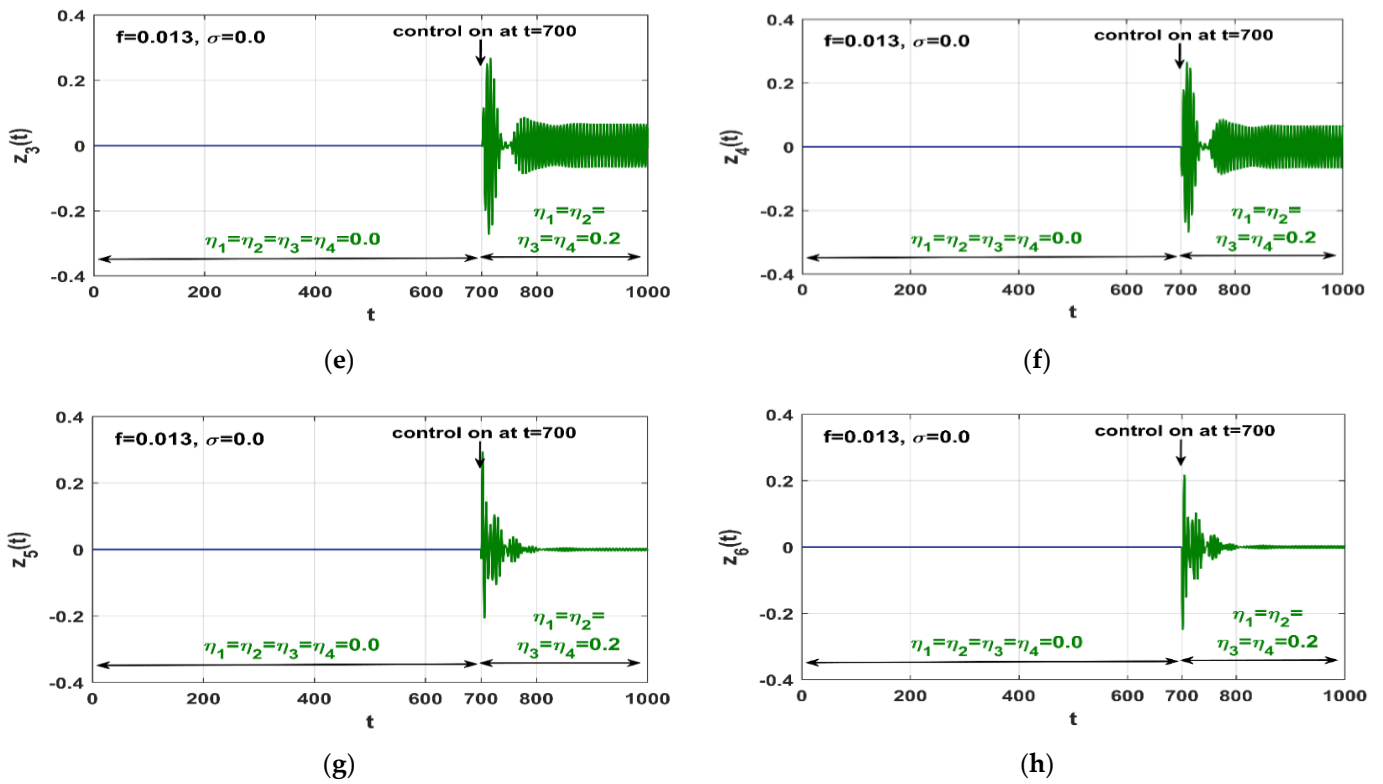
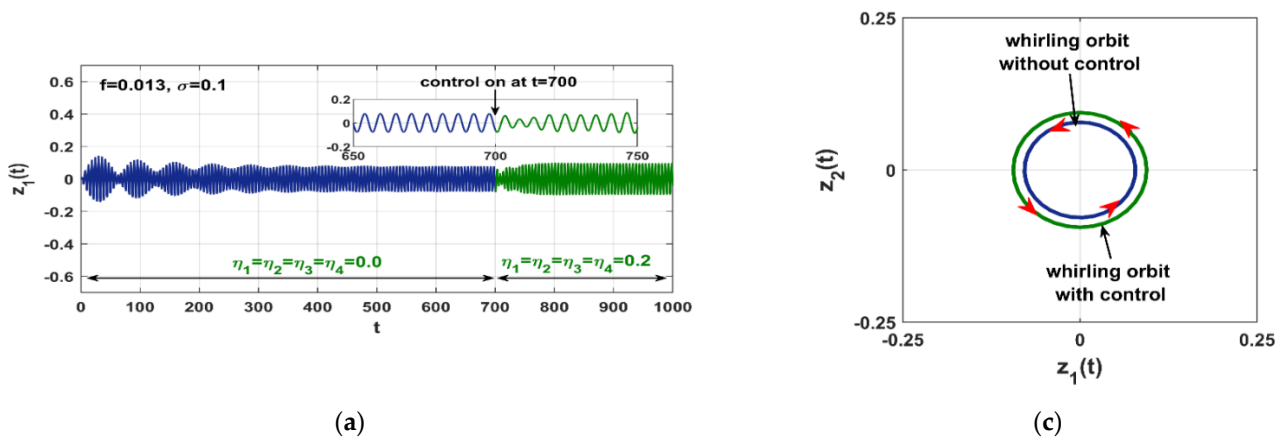


Figure 18. Cont.



**Figure 18.** Time response of the rotor system according to Figure 17 when  $\sigma = 0.0$  (i.e., when  $\Omega = \omega$ ) in the case of the *PD*-control algorithm and the *PD + IRC + PPF*-control algorithm: (a,b) the temporal oscillations  $z_1(t)$  and  $z_2(t)$  of the rotor system, (c) the rotor whirling orbits, (d) the rotor rotor frequency spectrum, (e,f) the temporal oscillations  $z_3(t)$  and  $z_4(t)$  of the *PPF* controller, and (g,h) the temporal oscillations  $z_5(t)$  and  $z_6(t)$  of the *IRC* controller.



**Figure 19.** Cont.

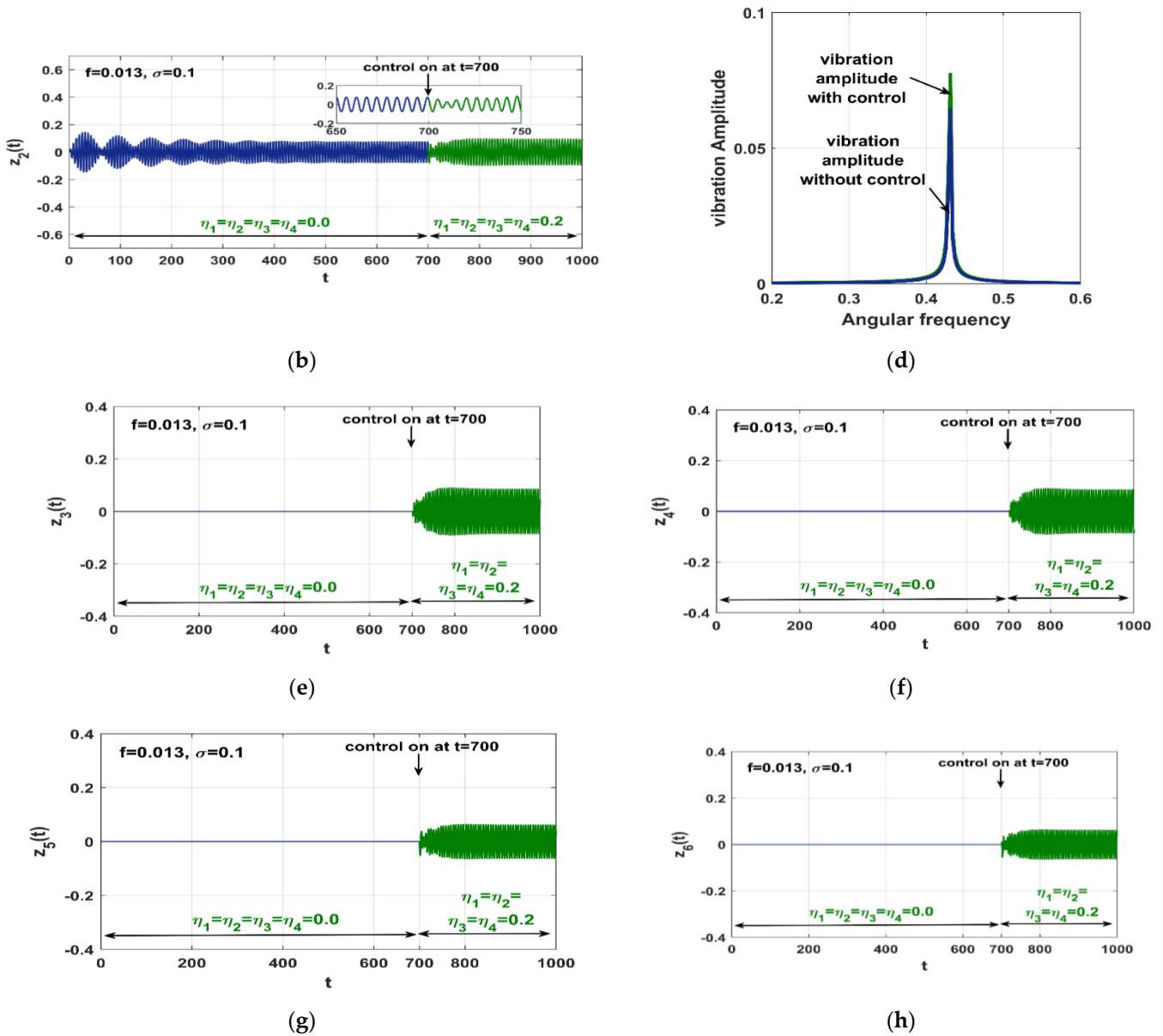


**Figure 19.** Time response of the rotor system according to Figure 17 when  $\sigma = 0.1$  (i.e., when  $\Omega = \omega + 0.1$ ) when the *PD*-control algorithm and the *PD + IRC + PPF*-control algorithm are applied: (a,b) the temporal oscillations  $z_1(t)$  and  $z_2(t)$  of the rotor system, (c) the rotor whirling orbits, (d) the rotor frequency spectrum, (e,f) the temporal oscillations  $z_3(t)$  and  $z_4(t)$  of the *PPF* controller, and (g,h) the temporal oscillations  $z_5(t)$  and  $z_6(t)$  of the *IRC* controller.

**6. Conclusions**

In this article, three different control techniques were introduced to eliminate the undesired vibrations of the twelve-poles electro-magnetic suspension system. The introduced control algorithms were the *PD*, *IRC*, and *PPF* controllers and their different combinations (i.e., *PD + IRC*, *PD + PPF*, *PD + IRC + PPF*). Relying on the classical mechanics’ principle, the dynamical model that governs the controlled twelve-poles rotor was established as a nonlinear four-degree-of-freedom system that is coupled to two first-order filters. Then, an approximate analytical solution for the controlled system mathematical model was obtained using the asymptotic analysis. Based on the derived analytical solution, the efficiency of the different control algorithms in suppressing the undesired vibrations and improving the bifurcation characteristics of the considered twelve-poles system was explored. In addition, numerical simulations were performed to confirm the accuracy of the

obtained analytical investigations, as well as to explore the transient oscillatory behaviors of the rotor system with the different control strategies. Based on our analysis and the discussions above, we reached the following conclusions:

1. The rotor system responds as a linear dynamical system with small vibration amplitudes in the case of the *PD*-control algorithm, as long as the excitation force  $f < 0.004$ .
2. When only the *PD*-control algorithm is activated, the twelve-poles rotor behaves like a hardening duffing oscillator, and the nonlinearities dominate its response when the rotor is exposed to a considerable excitation force amplitude (i.e.,  $f > 0.004$ ) at the resonance condition. In addition, the electro-magnetic suspension system may suffer from rub and/or impact force between the rotor and the stator if  $f > 0.013$  in the case of *PD*-control algorithm.
3. Integrating the *PPF*-control algorithm with *P*-controller can eliminate the rotor's undesired vibrations at the resonance condition (i.e., when  $\Omega \rightarrow \omega$ ,  $\sigma \rightarrow 0$ ) to negligible oscillation amplitudes, regardless of the excitation force magnitude, but two undesired resonant peaks appear on both sides of  $\sigma = 0.0$  that may result in high vibrations for the rotor system if the resonant condition is lost (i.e., if  $\Omega \neq \omega$ ).
4. The *IRC + PD*-control algorithm can mitigate the undesired vibrations and eliminate the nonlinear bifurcation behaviors of the twelve-poles system. However, the main drawback of this controller is that the rotor may perform high oscillation amplitude at the perfect resonance (i.e., when  $\Omega \rightarrow \omega$ ,  $\sigma \rightarrow 0$ ).
5. Utilizing the three control algorithms (i.e., *PD + IRC + PPF*) as one control strategy eliminated the high oscillation amplitudes of the rotor system close to zero at the perfect resonance conditions. In addition, the resonant peaks that appeared in the case of *PD + PPF* controller were also suppressed close to zero.
6. The *PD + IRC + PPF*-control algorithm has all the advantages of the individual control algorithms, *PD*, *PD + IRC* and *PD + PPF*, while avoiding their drawbacks.
7. Although both the *PD + PPF* and *PD + IRC + PPF*-control algorithms can eliminate the nonlinear vibrations of the twelve-poles system at the perfect resonance condition, the *PD + IRC + PPF* has the advantage of having the short transient time in suppressing this undesired motion.
8. Tuning the natural frequencies ( $\omega_1$  and  $\omega_2$ ) of the *PD + IRC + PPF*-control algorithm to be close to or equal to the rotor angular speed ( $\Omega$ ) guarantees the elimination of the system's lateral vibrations, regardless of the excitation force magnitude.

**Author Contributions:** Conceptualization, N.A.S., J.A. and K.A.G.; data curation, N.A.S.; formal analysis, S.M.E.-S. and J.A.; funding acquisition, J.A. and K.A.G.; investigation, N.A.S., S.M.E.-S., J.A. and K.A.G.; methodology, N.A.S., S.M.E.-S. and J.A.; project administration, M.K., K.R.R., J.A. and K.A.G.; resources, N.A.S., M.K. and J.A.; software, N.A.S., S.M.E.-S. and J.A.; supervision, N.A.S., M.K., K.R.R., J.A. and K.A.G.; validation, N.A.S., S.M.E.-S. and J.A.; visualization, N.A.S., S.M.E.-S. and J.A.; writing—original draft, N.A.S., S.M.E.-S. and J.A.; writing—review and editing, N.A.S., J.A. and K.A.G. All authors have read and agreed to the published version of the manuscript.

**Funding:** This research was funded by the Researchers Supporting Project, Taif University, Taif, Saudi Arabia, under grant number TURSP-2020/16. This work was also supported by the National Science Centre, Poland, under grant number OPUS 14 No. 2017/27/B/ST8/01330.

**Institutional Review Board Statement:** Not applicable.

**Informed Consent Statement:** Not applicable.

**Data Availability Statement:** Not applicable.

**Acknowledgments:** The authors thank to Taif University Researchers for Supporting Project number (TURSP-2020/16), Taif, Saudi Arabia.

**Conflicts of Interest:** The authors declared no potential conflict of interest with respect to the research, authorship, and/or publication of this article.

### Abbreviations

$z_1, \dot{z}_1, \ddot{z}_1$	Normalized displacement, velocity, and acceleration of the twelve-poles system in the X direction.
$z_2, \dot{z}_2, \ddot{z}_2$	Normalized displacement, velocity, and acceleration of the twelve-poles system in the Y direction.
$z_3, \dot{z}_3, \ddot{z}_3$	Normalized displacement, velocity, and acceleration of the PPF-control algorithm that connected to the twelve-poles system in the X direction.
$z_4, \dot{z}_4, \ddot{z}_4$	Normalized displacement, velocity, and acceleration of the PPF-control algorithm that connected to the twelve-poles system in the Y direction.
$z_5, \dot{z}_5$	Normalized displacement, and velocity of the IRC-control algorithm that connected to the twelve-poles system in the X direction.
$z_6, \dot{z}_6$	Normalized displacement, and velocity of the IRC-control algorithm that connected to the twelve-poles system in the Y direction.
$\mu$	Normalized damping parameter of the twelve-poles rotor system.
$\mu_1, \mu_2$	Normalized damping parameters of the PPF-control algorithms.
$\omega$	The normalized natural frequency of the twelve-poles rotor system.
$\omega_1, \omega_2$	Normalized natural frequencies of the PPF-control algorithms.
$\omega_3, \omega_4$	Normalized Internal-loop feedback gains of the IRC-control algorithms.
$\Omega$	The normalized angular speed of the twelve-poles rotor system.
$f$	Normalized excitation force of the twelve-poles rotor system.
$P, d$	Normalized proportional and derivative control gains of the PD-control algorithm, respectively.
$\eta_1, \eta_3$	Normalized control gains of the PPF-control algorithms.
$\eta_2, \eta_4$	Normalized control gains of the IRC-control algorithms.
$\eta_5, \eta_6$	Normalized feedback gains of the PPF-control algorithms.
$\eta_7, \eta_8$	Normalized feedback gains of the IRC-control algorithms.
$\alpha_j, j = 1, \dots, 7$	Normalized nonlinear coupling coefficients due to the PD-control algorithm.
$\beta_j, j = 1, \dots, 16$	Normalized nonlinear coupling coefficients due to both the IRC and PPF control algorithms in the X direction.
$\gamma_j, j = 1, \dots, 16$	Normalized nonlinear coupling coefficients due to both the IRC and PPF control algorithms in the Y direction.
$a_1, a_2$	Normalized vibration amplitudes of the twelve-poles rotor system in the X and Y directions, respectively.
$\phi_1, \phi_2$	Phase angles of the twelve-poles rotor system in the X and Y directions, respectively.
$a_3, a_4$	Normalized vibration amplitudes of the PPF-control algorithms in the X and Y directions, respectively.
$\phi_3, \phi_4$	Phase angles of the PPF-control algorithms in the X and Y directions, respectively.
$\sigma$	Difference between the angular speed ( $\Omega$ ) and the normalized natural frequency ( $\omega$ ): $\sigma = \Omega - \omega$ .

### Appendix A

Expanding Equations (11) to (16), using the Maclaurin series up to the third-order approximation, yields the following:

$$\begin{aligned}
 f_1 \simeq & \frac{4}{c_0^3} \mu_0 N^2 A \cos(\varphi) [(I_0^2 c_0^2 \sin(\alpha))y + (k_1 I_0 c_0^3 - I_0^2 c_0^2 \cos(\alpha))x + (-2I_0^2 \cos^3(\alpha) - k_1^2 c_0^2 \cos(\alpha) + 3k_1 I_0 c_0 \cos^2(\alpha))x^3 \\
 & + (2I_0^2 \sin(\alpha) - 2I_0^2 \sin(\alpha) \cos^2(\alpha))y^3 + (3k_1 I_0 c_0 - 3k_1 I_0 c_0 \cos^2(\alpha) - 6I_0^2 \cos(\alpha) + 6I_0^2 \cos^3(\alpha))xy^2 \\
 & + (6I_0^2 \cos^2(\alpha) \sin(\alpha) - 6k_1 I_0 c_0 \cos(\alpha) \sin(\alpha) + k_1^2 c_0^2 \sin(\alpha))x^2y + (3k_2 I_0 c_0 - 3k_2 I_0 c_0 \cos^2(\alpha))y^2\dot{x} \\
 & + (k_2^2 c_0^2 \sin(\alpha))y\dot{x}^2 + (-k_2^2 c_0^2 \cos(\alpha))x\dot{x}^2 + (k_2 I_0 c_0^3)\dot{x} + (3k_2 I_0 c_0 \cos^2(\alpha) - 2k_1 k_3 c_0^2 \cos(\alpha))x^2\dot{x} \\
 & + (-6k_2 I_0 c_0 \cos(\alpha) \sin(\alpha) + 2k_1 k_2 c_0^2 \sin(\alpha))x\dot{x}y + (-2k_2 k_3 c_0^2 \cos(\alpha) + 3k_3 I_0 c_0 \cos^2(\alpha))x^2u_1 \\
 & + (-2k_2 k_4 c_0^2 \cos(\alpha) + 3k_4 I_0 c_0 \cos^2(\alpha))x^2u_2 + (3k_3 I_0 c_0 - 3k_3 I_0 c_0 \cos^2(\alpha))y^2u_1 + (3k_4 I_0 c_0 - 3k_4 I_0 c_0 \cos^2(\alpha))y^2u_2 \\
 & + (2k_2 k_3 c_0^2 \sin^2(\alpha) - 6k_3 I_0 c_0 \sin(\alpha) \cos(\alpha))xyu_1 + (2k_2 k_4 c_0^2 \sin^2(\alpha) - 6k_4 I_0 c_0 \sin(\alpha) \cos(\alpha))xyu_2 \\
 & + (k_3^2 c_0^2 \cos(\alpha))xu_1^2 + (k_4^2 c_0^2 \cos(\alpha))xu_2^2 + (-k_3^2 c_0^2 \sin(\alpha))yu_1^2 + (-k_4^2 c_0^2 \sin(\alpha))yu_2^2 + (2k_3 k_4 c_0^2 \cos(\alpha))xu_1u_2 \\
 & + (-2k_3 k_4 c_0^2 \sin(\alpha))yu_1u_2 + (-2k_1 k_3 c_0^2 \cos(\alpha) - 2k_1 k_4 c_0^2 \cos(\alpha))x\dot{x}u_1 + (2k_1 k_3 c_0^2 \sin(\alpha) + 2k_1 k_4 c_0^2 \sin(\alpha))y\dot{x}u_1 \\
 & + (k_3 I_0 c_0^3)u_1 + (k_4 I_0 c_0^3)u_2]
 \end{aligned} \tag{A1}$$

$$\begin{aligned}
 f_2 \simeq & \frac{4}{c_0^3} \mu_0 N^2 A \cos(\varphi) [(-k_1 I_0 c_0^3 - I_0^2 c_0^2)x + (2I_0^2 + k_1^2 c_0^2 - 3k_1 I_0 c_0)x^3 + (k_2^2 c_0^2)x\dot{x}^2 + (-k_2 I_0 c_0^3)\dot{x} \\
 & + (-3k_2 I_0 c_0 + 2k_1 k_3 c_0^2)x^2\dot{x} + (-2k_2 k_3 c_0^2 + 3k_3 I_0 c_0)x^2u_1 + (-2k_2 k_4 c_0^2 + 3k_4 I_0 c_0)x^2u_2 + (k_3^2 c_0^2)xu_1^2 + (k_4^2 c_0^2)xu_2^2 \\
 & + (-2k_1 k_3 c_0^2)x\dot{x}u_1 + (-2k_1 k_4 c_0^2)x\dot{x}u_2 + (2k_3 k_4 c_0^2)xu_1u_2 + (k_3 I_0 c_0^3)u_1 + (k_4 I_0 c_0^3)u_2]
 \end{aligned} \tag{A2}$$

$$\begin{aligned}
f_3 = & \frac{4}{c_0^3} \mu_0 N^2 A \cos(\varphi) [(I_0^2 c_0^2 \sin(\alpha)) y + (-k_1 I_0 c_0^3 + I_0^2 c_0^2 \cos(\alpha)) x + (2I_0^2 \cos^3(\alpha) + k_1^2 c_0^2 \cos(\alpha) - 3k_1 I_0 c_0 \cos^2(\alpha)) x^3 \\
& + (2I_0^2 \sin(\alpha) - 2I_0^2 \sin(\alpha) \cos^2(\alpha)) y^3 + (-3k_1 I_0 c_0 + 3k_1 I_0 c_0 \cos^2(\alpha) + 6I_0^2 \cos(\alpha) - 6I_0^2 \cos^3(\alpha)) x y^2 \\
& + (6I_0^2 \cos^2(\alpha) \sin(\alpha) - 6k_1 I_0 c_0 \cos(\alpha) \sin(\alpha) + k_1^2 c_0^2 \sin(\alpha)) x^2 y + (-3k_2 I_0 c_0 + 3k_2 I_0 c_0 \cos^2(\alpha)) y^2 \dot{x} \\
& + (k_2^2 c_0^2 \sin(\alpha)) y \dot{x}^2 + (k_2^2 c_0^2 \cos(\alpha)) x \dot{x}^2 + (-k_2 I_0 c_0^3) \dot{x} + (-3k_2 I_0 c_0 \cos^2(\alpha) + 2k_1 k_3 c_0^2 \cos(\alpha)) x^2 \dot{x} \\
& + (-6k_2 I_0 c_0 \cos(\alpha) \sin(\alpha) + 2k_1 k_2 c_0^2 \sin(\alpha)) x \dot{x} y + (-2k_2 k_3 c_0^2 \cos(\alpha) + 3k_3 I_0 c_0 \cos^2(\alpha)) x^2 u_1 \\
& + (-2k_2 k_4 c_0^2 \cos(\alpha) + 3k_4 I_0 c_0 \cos^2(\alpha)) x^2 u_2 + (3k_3 I_0 c_0 - 3k_3 I_0 c_0 \cos^2(\alpha)) y^2 u_1 + (3k_4 I_0 c_0 - 3k_4 I_0 c_0 \cos^2(\alpha)) y^2 u_2 \\
& + (2k_2 k_3 c_0^2 \sin^2(\alpha) + 6k_3 I_0 c_0 \sin(\alpha) \cos(\alpha)) x y u_1 + (2k_2 k_4 c_0^2 \sin^2(\alpha) + 6k_4 I_0 c_0 \sin(\alpha) \cos(\alpha)) x y u_2 \\
& + (k_3^2 c_0^2 \cos(\alpha)) x u_1^2 + (k_4^2 c_0^2 \cos(\alpha)) x u_2^2 + (k_3^2 c_0^2 \sin(\alpha)) y u_1^2 + (k_4^2 c_0^2 \sin(\alpha)) y u_2^2 + (2k_3 k_4 c_0^2 \cos(\alpha)) x u_1 u_2 \\
& + (2k_3 k_4 c_0^2 \sin(\alpha)) y u_1 u_2 + (-2k_1 k_3 c_0^2 \cos(\alpha) - 2k_1 k_4 c_0^2 \cos(\alpha)) x \dot{x} u_1 + (-2k_1 k_3 c_0^2 \sin(\alpha) - 2k_1 k_4 c_0^2 \sin(\alpha)) y \dot{x} u_1 \\
& + (k_3 I_0 c_0^3) u_1 + (k_4 I_0 c_0^3) u_2] \tag{A3}
\end{aligned}$$

$$\begin{aligned}
f_4 = & \frac{4}{c_0^3} \mu_0 N^2 A \cos(\varphi) [(-I_0^2 c_0^2 \sin(\alpha)) x + (k_1 I_0 c_0^3 - I_0^2 c_0^2 \cos(\alpha)) y + (-2I_0^2 \cos^3(\alpha) - k_1^2 c_0^2 \cos(\alpha) + 3k_1 I_0 c_0 \cos^2(\alpha)) y^3 \\
& + (-2I_0^2 \sin(\alpha) + 2I_0^2 \sin(\alpha) \cos^2(\alpha)) x^3 + (3k_1 I_0 c_0 - 3k_1 I_0 c_0 \cos^2(\alpha) - 6I_0^2 \cos(\alpha) + 6I_0^2 \cos^3(\alpha)) y x^2 \\
& + (-6I_0^2 \cos^2(\alpha) \sin(\alpha) + 6k_1 I_0 c_0 \cos(\alpha) \sin(\alpha) - k_1^2 c_0^2 \sin(\alpha)) y^2 x + (3k_2 I_0 c_0 - 3k_2 I_0 c_0 \cos^2(\alpha)) x^2 \dot{y} \\
& + (-k_2^2 c_0^2 \sin(\alpha)) x \dot{y}^2 + (-k_2^2 c_0^2 \cos(\alpha)) y \dot{y}^2 + (k_2 I_0 c_0^3) \dot{y} + (3k_2 I_0 c_0 \cos^2(\alpha) - 2k_1 k_3 c_0^2 \cos(\alpha)) y^2 \dot{y} \\
& + (6k_2 I_0 c_0 \cos(\alpha) \sin(\alpha) - 2k_1 k_2 c_0^2 \sin(\alpha)) y \dot{y} x + (-2k_2 k_5 c_0^2 \cos(\alpha) + 3k_5 I_0 c_0 \cos^2(\alpha)) y^2 v_1 \\
& + (-2k_2 k_6 c_0^2 \cos(\alpha) + 3k_6 I_0 c_0 \cos^2(\alpha)) y^2 v_2 + (3k_5 I_0 c_0 - 3k_5 I_0 c_0 \cos^2(\alpha)) x^2 v_1 + (3k_6 I_0 c_0 - 3k_6 I_0 c_0 \cos^2(\alpha)) x^2 v_2 \\
& + (-2k_2 k_5 c_0^2 \sin^2(\alpha) + 6k_5 I_0 c_0 \sin(\alpha) \cos(\alpha)) x y v_1 + (-2k_2 k_6 c_0^2 \sin^2(\alpha) + 6k_6 I_0 c_0 \sin(\alpha) \cos(\alpha)) x y v_2 \\
& + (k_5^2 c_0^2 \cos(\alpha)) y v_1^2 + (k_6^2 c_0^2 \cos(\alpha)) y v_2^2 + (k_5^2 c_0^2 \sin(\alpha)) x v_1^2 + (k_6^2 c_0^2 \sin(\alpha)) x v_2^2 + (2k_5 k_6 c_0^2 \cos(\alpha)) y v_1 v_2 \\
& + (-2k_5 k_6 c_0^2 \sin(\alpha)) x v_1 v_2 + (-2k_1 k_6 c_0^2 \cos(\alpha) - 2k_1 k_5 c_0^2 \cos(\alpha)) y \dot{y} v_1 + (2k_1 k_6 c_0^2 \sin(\alpha) + 2k_1 k_5 c_0^2 \sin(\alpha)) x \dot{y} v_1 \\
& + (k_5 I_0 c_0^3) v_1 + (k_6 I_0 c_0^3) v_2] \tag{A4}
\end{aligned}$$

$$\begin{aligned}
f_5 = & \frac{4}{c_0^3} \mu_0 N^2 A \cos(\varphi) [(-k_1 I_0 c_0^3 - I_0^2 c_0^2) y + (2I_0^2 + k_1^2 c_0^2 - 3k_1 I_0 c_0) y^3 + (k_2^2 c_0^2) y \dot{y}^2 + (-k_2 I_0 c_0^3) \dot{y} \\
& + (-3k_2 I_0 c_0 + 2k_1 k_3 c_0^2) y^2 \dot{y} + (-2k_2 k_5 c_0^2 + 3k_5 I_0 c_0) y^2 v_1 + (-2k_2 k_6 c_0^2 + 3k_6 I_0 c_0) y^2 v_2 + (k_5^2 c_0^2) y v_1^2 + (k_6^2 c_0^2) y v_2^2 \\
& + (-2k_1 k_5 c_0^2) y \dot{y} v_1 + (-2k_1 k_6 c_0^2) y \dot{y} v_2 + (2k_5 k_6 c_0^2) y v_1 v_2 + (k_5 I_0 c_0^3) v_1 + (k_6 I_0 c_0^3) v_2 + (O)^3] \tag{A5}
\end{aligned}$$

$$\begin{aligned}
f_6 = & \frac{4}{c_0^3} \mu_0 N^2 A \cos(\varphi) [(-I_0^2 c_0^2 \sin(\alpha)) x + (-k_1 I_0 c_0^3 + I_0^2 c_0^2 \cos(\alpha)) y + (2I_0^2 \cos^3(\alpha) + k_1^2 c_0^2 \cos(\alpha) - 3k_1 I_0 c_0 \cos^2(\alpha)) y^3 \\
& + (-2I_0^2 \sin(\alpha) + 2I_0^2 \sin(\alpha) \cos^2(\alpha)) x^3 + (-3k_1 I_0 c_0 + 3k_1 I_0 c_0 \cos^2(\alpha) + 6I_0^2 \cos(\alpha) - 6I_0^2 \cos^3(\alpha)) y x^2 \\
& + (-6I_0^2 \cos^2(\alpha) \sin(\alpha) + 6k_1 I_0 c_0 \cos(\alpha) \sin(\alpha) - k_1^2 c_0^2 \sin(\alpha)) y^2 x + (-3k_2 I_0 c_0 + 3k_2 I_0 c_0 \cos^2(\alpha)) x^2 \dot{y} \\
& + (-k_2^2 c_0^2 \sin(\alpha)) x \dot{y}^2 + (k_2^2 c_0^2 \cos(\alpha)) y \dot{y}^2 + (-k_2 I_0 c_0^3) \dot{y} + (-3k_2 I_0 c_0 \cos^2(\alpha) + 2k_1 k_3 c_0^2 \cos(\alpha)) y^2 \dot{y} \\
& + (6k_2 I_0 c_0 \cos(\alpha) \sin(\alpha) - 2k_1 k_2 c_0^2 \sin(\alpha)) y \dot{y} x + (-2k_2 k_5 c_0^2 \cos(\alpha) + 3k_5 I_0 c_0 \cos^2(\alpha)) y^2 v_1 \\
& + (-2k_2 k_6 c_0^2 \cos(\alpha) + 3k_6 I_0 c_0 \cos^2(\alpha)) y^2 v_2 + (3k_5 I_0 c_0 - 3k_5 I_0 c_0 \cos^2(\alpha)) x^2 v_1 + (3k_6 I_0 c_0 - 3k_6 I_0 c_0 \cos^2(\alpha)) x^2 v_2 \\
& + (2k_2 k_5 c_0^2 \sin^2(\alpha) - 6k_5 I_0 c_0 \sin(\alpha) \cos(\alpha)) x y v_1 + (2k_2 k_6 c_0^2 \sin^2(\alpha) - 6k_6 I_0 c_0 \sin(\alpha) \cos(\alpha)) x y v_2 \\
& + (k_5^2 c_0^2 \cos(\alpha)) y v_1^2 + (k_6^2 c_0^2 \cos(\alpha)) y v_2^2 + (-k_5^2 c_0^2 \sin(\alpha)) x v_1^2 + (-k_6^2 c_0^2 \sin(\alpha)) x v_2^2 + (2k_5 k_6 c_0^2 \cos(\alpha)) y v_1 v_2 \\
& + (-2k_5 k_6 c_0^2 \sin(\alpha)) x v_1 v_2 + (-2k_1 k_6 c_0^2 \cos(\alpha) - 2k_1 k_5 c_0^2 \cos(\alpha)) y \dot{y} v_1 + (2k_1 k_6 c_0^2 \sin(\alpha) + 2k_1 k_5 c_0^2 \sin(\alpha)) x \dot{y} v_1 \\
& + (k_5 I_0 c_0^3) v_1 + (k_6 I_0 c_0^3) v_2] \tag{A6}
\end{aligned}$$

### Appendix B

$$\begin{aligned} \mu &= \frac{1}{2}(2d \cos(\alpha) + d), & \omega &= \sqrt{2p \cos(\alpha) + p - 3}, \\ \alpha_1 &= -6p \cos^3(\alpha) - 3p + 2p^2 \cos^2(\alpha) + 6 + p^2 + 8 \cos^4(\alpha) - 8 \cos^2(\alpha), & \alpha_4 &= 6d \cos^3(\alpha) - 6d \cos(\alpha), \\ \alpha_2 &= 2p^2 - 2p^2 \cos^2(\alpha) + 24 \cos^2(\alpha) - 24 \cos^4(\alpha) - 18p \cos(\alpha) + 18p \cos^3(\alpha), & \alpha_6 &= d^2(1 + 2 \cos^2(\alpha)), \\ \alpha_3 &= -3d + 2pd + 4pd \cos^2(\alpha) - 6d \cos^3(\alpha), & \beta_1 &= \frac{\eta_1}{1+2 \cos(\alpha)}(3 - 2p + 6 \cos^3(\alpha) - 4p \cos^2(\alpha)), \\ \alpha_5 &= 2d^2 \sin^2(\alpha), & \beta_2 &= \frac{\eta_1}{1+2 \cos(\alpha)}(-2d - 4d \cos^2(\alpha)), \\ \alpha_7 &= 4d(3 \cos^3(\alpha) - 3 \cos(\alpha) + p \sin^2(\alpha)), & \beta_3 &= \frac{\eta_1^2}{(1+2 \cos(\alpha))^2}(1 + 2 \cos^2(\alpha)), \\ \gamma_1 &= \frac{\eta_3}{1+2 \cos(\alpha)}(3 - 2p + 6 \cos^3(\alpha) - 4p \cos^2(\alpha)), & \beta_4 &= \frac{4\eta_3}{1+2 \cos(\alpha)}(-p \sin^2(\alpha) + 3 \cos(\alpha) \sin^2(\alpha)), \\ \gamma_2 &= \frac{\eta_3}{1+2 \cos(\alpha)}(-2d - 4d \cos^2(\alpha)), & \beta_5 &= \frac{2\eta_3^2 \sin^2(\alpha)}{(1+2 \cos(\alpha))^2}, \\ \gamma_3 &= \frac{\eta_3^2}{(1+2 \cos(\alpha))^2}(1 + 2 \cos^2(\alpha)), & \beta_6 &= \frac{-4d\eta_3 \sin^2(\alpha)}{1+2 \cos(\alpha)}, \\ \gamma_4 &= \frac{4\eta_1}{1+2 \cos(\alpha)}(-\sin^2(\alpha) + 3 \cos(\alpha) \sin^2(\alpha)), & \beta_7 &= \frac{6\eta_1 \cos(\alpha) \sin^2(\alpha)}{1+2 \cos(\alpha)}, \\ \gamma_5 &= \frac{2\eta_1^2 \sin^2(\alpha)}{(1+2 \cos(\alpha))^2}, & \beta_8 &= \frac{\eta_1 \eta_2}{(1+2 \cos(\alpha))^2}(-2 - 4 \cos^2(\alpha)), \\ \gamma_6 &= \frac{-4d\eta_1 \sin^2(\alpha)}{1+2 \cos(\alpha)}, & \beta_9 &= \frac{\eta_2}{1+2 \cos(\alpha)}(2d + 4d \cos^2(\alpha)), \\ \gamma_7 &= \frac{6\eta_3 \cos(\alpha) \sin^2(\alpha)}{1+2 \cos(\alpha)}, & \beta_{10} &= \frac{-4\eta_3 \eta_4 \sin^2(\alpha)}{(1+2 \cos(\alpha))^2}, \\ \gamma_8 &= \frac{\eta_3 \eta_4}{(1+2 \cos(\alpha))^2}(-2 - 4 \cos^2(\alpha)), & \beta_{11} &= \frac{\eta_2}{1+2 \cos(\alpha)}(-3 + 2p + 4p \cos^2(\alpha) - 6 \cos^3(\alpha)), \\ \gamma_9 &= \frac{\eta_3}{1+2 \cos(\alpha)}(2d + 4d \cos^2(\alpha)), & \beta_{12} &= \frac{-2\eta_4^2 \sin^2(\alpha)}{(1+2 \cos(\alpha))^2}, \\ \gamma_{10} &= \frac{-4\eta_1 \eta_2 \sin^2(\alpha)}{(1+2 \cos(\alpha))^2}, & \beta_{13} &= \frac{\eta_4}{1+2 \cos(\alpha)}(4p \sin^2(\alpha) - 12 \cos(\alpha) \sin^2(\alpha)), \\ \gamma_{11} &= \frac{\eta_4}{1+2 \cos(\alpha)}(-3 + 2p + 4p \cos^2(\alpha) - 6 \cos^3(\alpha)), & \beta_{14} &= \frac{4d\eta_4 \sin^2(\alpha)}{1+2 \cos(\alpha)}, \\ \gamma_{12} &= \frac{-2\eta_2^2 \sin^2(\alpha)}{(1+2 \cos(\alpha))^2}, & \beta_{15} &= \frac{-\eta_2^2}{(1+2 \cos(\alpha))^2}(1 + 2 \cos^2(\alpha)), \\ \gamma_{13} &= \frac{\eta_2}{1+2 \cos(\alpha)}(4p \sin^2(\alpha) - 12 \cos(\alpha) \sin^2(\alpha)), & \beta_{16} &= \frac{-6\eta_2 \cos(\alpha) \sin^2(\alpha)}{1+2 \cos(\alpha)}, \\ \gamma_{14} &= \frac{4d\eta_2 \sin^2(\alpha)}{1+2 \cos(\alpha)}, \\ \gamma_{15} &= \frac{-\eta_4^2}{(1+2 \cos(\alpha))^2}(1 + 2 \cos^2(\alpha)), \\ \gamma_{16} &= \frac{-6\eta_4 \cos(\alpha) \sin^2(\alpha)}{1+2 \cos(\alpha)}. \end{aligned}$$

### Appendix C

$$\begin{aligned} J_{11} &= \frac{\partial F_1}{\partial a_{11}} = -\frac{1}{2}(2\mu + \frac{\eta_2 \eta_7}{\omega_3^2 + \omega^2}) + \frac{3}{8}(\alpha_3 - \frac{2\beta_{11} \eta_7}{\omega_3^2 + \omega^2} - \frac{2\omega_3 \beta_{15} \eta_7^2}{(\omega_3^2 + \omega^2)^2})a_{10}^2 + \frac{1}{8}(2\alpha_4 - \frac{\beta_{13} \eta_8}{\omega_4^2 + \omega^2} - \frac{\omega_4 \beta_{14} \eta_8}{\omega_4^2 + \omega^2} \\ &\quad - \frac{2\beta_{16} \eta_7}{\omega_3^2 + \omega^2})a_{20}^2 + \frac{1}{8}(-\alpha_4 + \alpha_7 + \frac{2\omega_4 \beta_{12} \eta_8^2}{(\omega_4^2 + \omega^2)^2} - \frac{\beta_{13} \eta_8}{\omega_4^2 + \omega^2} + \frac{\omega_4 \beta_{14} \eta_8}{\omega_4^2 + \omega^2})a_{20}^2 \cos(2\phi_{10} - 2\phi_{20}) + \frac{1}{8}(\frac{\alpha_2}{\omega} \\ &\quad - \alpha_5 \omega + \frac{(\omega_4^2 - \omega^2) \beta_{12} \eta_8^2}{\omega(\omega_4^2 + \omega^2)^2} + \frac{\omega_4 \beta_{13} \eta_8}{\omega(\omega_4^2 + \omega^2)} - \frac{\omega \beta_{14} \eta_8}{\omega_4^2 + \omega^2})a_{20}^2 \sin(2\phi_{10} - 2\phi_{20}) - \frac{1}{4\omega} \beta_1 a_{10} b_{10} \sin(\phi_{30}) \\ &\quad - \frac{1}{8\omega} \beta_3 b_{10}^2 \sin(2\phi_{30}) + \frac{1}{4}(\beta_2 - \frac{2\beta_8 \eta_7}{\omega_3^2 + \omega^2})a_{10} b_{10} \cos(\phi_{30}) - \frac{1}{8}(\frac{\beta_{10} \eta_8}{\omega_4^2 + \omega^2})a_{20} b_{20} \cos(\phi_{40}) \\ &\quad + \frac{1}{8\omega}(\frac{\omega_4 \beta_{10} \eta_8}{\omega_4^2 + \omega^2})a_{20} b_{20} \sin(\phi_{40}) + \frac{1}{8\omega}(\beta_6 \omega - \frac{\omega \beta_{10} \eta_8}{\omega_4^2 + \omega^2})a_{20} b_{20} \cos(2\phi_{10} - 2\phi_{20} - \phi_{40}) \\ &\quad + \frac{1}{8\omega}(\beta_4 + \frac{\omega_4 \beta_{10} \eta_8}{\omega_4^2 + \omega^2})a_{20} b_{20} \sin(2\phi_{10} - 2\phi_{20} - \phi_{40}) + \frac{1}{8\omega} \beta_5 b_{20}^2 \sin(2\phi_{10} - 2\phi_{20} - 2\phi_{40}), \\ J_{12} &= \frac{\partial F_1}{\partial a_{21}} = \frac{1}{4}(2\alpha_4 - \frac{\beta_{13} \eta_8}{\omega_4^2 + \omega^2} - \frac{\omega_4 \beta_{14} \eta_8}{\omega_4^2 + \omega^2} - \frac{2\beta_{16} \eta_7}{\omega_3^2 + \omega^2})a_{10} a_{20} + \frac{1}{4}(-\alpha_4 + \alpha_7 + \frac{2\omega_4 \beta_{12} \eta_8^2}{(\omega_4^2 + \omega^2)^2} - \frac{\beta_{13} \eta_8}{\omega_4^2 + \omega^2} \\ &\quad + \frac{\omega_4 \beta_{14} \eta_8}{\omega_4^2 + \omega^2})a_{10} a_{20} \cos(2\phi_{10} - 2\phi_{20}) + \frac{1}{4}(\frac{\alpha_2}{\omega} - \alpha_5 \omega + \frac{(\omega_4^2 - \omega^2) \beta_{12} \eta_8^2}{\omega(\omega_4^2 + \omega^2)^2} + \frac{\omega_4 \beta_{13} \eta_8}{\omega(\omega_4^2 + \omega^2)} \\ &\quad - \frac{\omega \beta_{14} \eta_8}{\omega_4^2 + \omega^2})a_{10} a_{20} \sin(2\phi_{10} - 2\phi_{20}) - \frac{1}{2\omega} \beta_7 a_{20} b_{10} \sin(\phi_{30}) - \frac{1}{8}(\frac{\beta_{10} \eta_8}{\omega_4^2 + \omega^2})a_{10} b_{20} \cos(\phi_{40}) \\ &\quad + \frac{1}{8\omega}(\frac{\omega_4 \beta_{10} \eta_8}{\omega_4^2 + \omega^2})a_{10} b_{20} \sin(\phi_{40}) + \frac{1}{4\omega} \beta_7 a_{20} b_{10} \sin(2\phi_{10} - 2\phi_{20} + \phi_{30}) + \frac{1}{8\omega}(\beta_6 \omega \\ &\quad - \frac{\omega \beta_{10} \eta_8}{\omega_4^2 + \omega^2})a_{10} b_{20} \cos(2\phi_{10} - 2\phi_{20} - \phi_{40}) + \frac{1}{8\omega}(\beta_4 + \frac{\omega_4 \beta_{10} \eta_8}{\omega_4^2 + \omega^2})a_{10} b_{20} \sin(2\phi_{10} - 2\phi_{20} - \phi_{40}), \\ J_{13} &= \frac{\partial F_1}{\partial b_{11}} = (-\frac{1}{2\omega} \eta_1 - \frac{1}{8\omega} \beta_1 a_{10}^2 - \frac{1}{4\omega} \beta_7 a_{20}^2) \sin(\phi_{30}) - \frac{1}{4\omega} \beta_3 a_{10} b_{10} \sin(2\phi_{30}) \\ &\quad + \frac{1}{8}(\beta_2 - \frac{2\beta_8 \eta_7}{\omega_3^2 + \omega^2})a_{10}^2 \cos(\phi_{30}) + \frac{1}{8\omega} \beta_7 a_{20}^2 \sin(2\phi_{10} - 2\phi_{20} + \phi_{30}), \end{aligned}$$



$$J_{14} = \frac{\partial F_1}{\partial b_{21}} = -\frac{1}{8} \left( \frac{\beta_{10}\eta_8}{\omega_4^2 + \omega^2} \right) a_{10} a_{20} \cos(\phi_{40}) + \frac{1}{8\omega} \left( \frac{\omega_4 \beta_{10}\eta_8}{\omega_4^2 + \omega^2} \right) a_{10} a_{20} \sin(\phi_{40}) + \frac{1}{8\omega} (\beta_6 \omega - \frac{\omega \beta_{10}\eta_8}{\omega_4^2 + \omega^2}) a_{10} a_{20} \cos(2\phi_{10} - 2\phi_{20} - \phi_{40}) + \frac{1}{8\omega} (\beta_4 + \frac{\omega_4 \beta_{10}\eta_8}{\omega_4^2 + \omega^2}) a_{10} a_{20} \sin(2\phi_{10} - 2\phi_{20} - \phi_{40}) + \frac{1}{4\omega} \beta_5 a_{10} b_{20} \sin(2\phi_{10} - 2\phi_{20} - 2\phi_{40}),$$

$$J_{15} = \frac{\partial F_1}{\partial \phi_{11}} = -\frac{1}{4} (-\alpha_4 + \alpha_7 + \frac{2\omega_4 \beta_{12}\eta_8^2}{(\omega_4^2 + \omega^2)^2} - \frac{\beta_{13}\eta_8}{\omega_4^2 + \omega^2} + \frac{\omega_4 \beta_{14}\eta_8}{\omega_4^2 + \omega^2}) a_{10} a_{20}^2 \sin(2\phi_{10} - 2\phi_{20}) + \frac{1}{4} (\frac{\alpha_2}{\omega} - \alpha_5 \omega + \frac{(\omega_4^2 - \omega^2) \beta_{12}\eta_8^2}{\omega(\omega_4^2 + \omega^2)^2} + \frac{\omega_4 \beta_{13}\eta_8}{\omega(\omega_4^2 + \omega^2)} - \frac{\omega \beta_{14}\eta_8}{\omega_4^2 + \omega^2}) a_{10} a_{20}^2 \cos(2\phi_{10} - 2\phi_{20}) - \frac{1}{4\omega} \beta_7 a_{20}^2 b_{10} \sin(2\phi_{10} - 2\phi_{20} + \phi_{30}) + \frac{1}{8\omega} (\beta_6 \omega - \frac{\omega \beta_{10}\eta_8}{\omega_4^2 + \omega^2}) a_{10} a_{20} b_{20} \sin(2\phi_{10} - 2\phi_{20} - \phi_{40}) + \frac{1}{4\omega} (\beta_4 + \frac{\omega_4 \beta_{10}\eta_8}{\omega_4^2 + \omega^2}) a_{10} a_{20} b_{20} \cos(2\phi_{10} - 2\phi_{20} - \phi_{40}) + \frac{1}{4\omega} \beta_5 a_{10} b_{20}^2 \cos(2\phi_{10} - 2\phi_{20} - 2\phi_{40}) + \frac{1}{2\omega} (\omega + \sigma)^2 f \cos(\phi_{10}),$$

$$J_{16} = \frac{\partial F_1}{\partial \phi_{21}} = \frac{1}{4} (-\alpha_4 + \alpha_7 + \frac{2\omega_4 \beta_{12}\eta_8^2}{(\omega_4^2 + \omega^2)^2} - \frac{\beta_{13}\eta_8}{\omega_4^2 + \omega^2} + \frac{\omega_4 \beta_{14}\eta_8}{\omega_4^2 + \omega^2}) a_{10} a_{20}^2 \sin(2\phi_{10} - 2\phi_{20}) - \frac{1}{4} (\frac{\alpha_2}{\omega} - \alpha_5 \omega + \frac{(\omega_4^2 - \omega^2) \beta_{12}\eta_8^2}{\omega(\omega_4^2 + \omega^2)^2} + \frac{\omega_4 \beta_{13}\eta_8}{\omega(\omega_4^2 + \omega^2)} - \frac{\omega \beta_{14}\eta_8}{\omega_4^2 + \omega^2}) a_{10} a_{20}^2 \cos(2\phi_{10} - 2\phi_{20}) + \frac{1}{4\omega} \beta_7 a_{20}^2 b_{10} \sin(2\phi_{10} - 2\phi_{20} + \phi_{30}) + \frac{1}{8\omega} (\beta_6 \omega - \frac{\omega \beta_{10}\eta_8}{\omega_4^2 + \omega^2}) a_{10} a_{20} b_{20} \sin(2\phi_{10} - 2\phi_{20} - \phi_{40}) - \frac{1}{4\omega} (\beta_4 + \frac{\omega_4 \beta_{10}\eta_8}{\omega_4^2 + \omega^2}) a_{10} a_{20} b_{20} \cos(2\phi_{10} - 2\phi_{20} - \phi_{40}) - \frac{1}{4\omega} \beta_5 a_{10} b_{20}^2 \cos(2\phi_{10} - 2\phi_{20} - 2\phi_{40}),$$

$$J_{17} = \frac{\partial F_1}{\partial \phi_{31}} = (-\frac{1}{2\omega} \eta_1 b_{10} - \frac{1}{8\omega} \beta_1 a_{10}^2 b_{10} - \frac{1}{4\omega} \beta_7 a_{20}^2 b_{10}) \cos(\phi_{30}) - \frac{1}{4\omega} \beta_3 a_{10} b_{10}^2 \cos(2\phi_{30}) - \frac{1}{8} (\beta_2 - \frac{2\beta_8 \eta_7}{\omega_3^2 + \omega^2}) a_{10}^2 b_{10} \sin(\phi_{30}) + \frac{1}{8\omega} \beta_7 a_{20}^2 b_{10} \cos(2\phi_{10} - 2\phi_{20} + \phi_{30}),$$

$$J_{18} = \frac{\partial F_1}{\partial \phi_{41}} = \frac{1}{8} \left( \frac{\beta_{10}\eta_8}{\omega_4^2 + \omega^2} \right) a_{10} a_{20} b_{20} \sin(\phi_{40}) + \frac{1}{8\omega} \left( \frac{\omega_4 \beta_{10}\eta_8}{\omega_4^2 + \omega^2} \right) a_{10} a_{20} b_{20} \cos(\phi_{40}) + \frac{1}{8\omega} (\beta_6 \omega - \frac{\omega \beta_{10}\eta_8}{\omega_4^2 + \omega^2}) a_{10} a_{20} b_{20} \sin(2\phi_{10} - 2\phi_{20} - \phi_{40}) - \frac{1}{8\omega} (\beta_4 + \frac{\omega_4 \beta_{10}\eta_8}{\omega_4^2 + \omega^2}) a_{10} a_{20} b_{20} \cos(2\phi_{10} - 2\phi_{20} - \phi_{40}) - \frac{1}{4\omega} \beta_5 a_{10} b_{20}^2 \cos(2\phi_{10} - 2\phi_{20} - 2\phi_{40}),$$

$$J_{21} = \frac{\partial F_2}{\partial a_{11}} = \frac{1}{4} (2\alpha_4 - \frac{\gamma_{13}\eta_7}{\omega_3^2 + \omega^2} - \frac{\omega_3 \gamma_{14}\eta_7}{\omega_3^2 + \omega^2} - \frac{2\gamma_{16}\eta_8}{\omega_4^2 + \omega^2}) a_{20} a_{10} + \frac{1}{4} (-\alpha_4 + \alpha_7 - \frac{2\omega_3 \gamma_{12}\eta_7^2}{(\omega_3^2 + \omega^2)^2} - \frac{\gamma_{13}\eta_7}{\omega_3^2 + \omega^2} + \frac{\omega_3 \gamma_{14}\eta_7}{\omega_3^2 + \omega^2}) a_{20} a_{10} \cos(2\phi_{20} - 2\phi_{10}) + \frac{1}{4} (\frac{\alpha_2}{\omega} - \alpha_5 \omega + \frac{(\omega_3^2 - \omega^2) \gamma_{12}\eta_7^2}{\omega(\omega_3^2 + \omega^2)^2} + \frac{\omega_3 \gamma_{13}\eta_7}{\omega(\omega_3^2 + \omega^2)} + \frac{\omega \gamma_{14}\eta_7}{\omega_3^2 + \omega^2}) a_{20} a_{10} \sin(2\phi_{20} - 2\phi_{10}) - \frac{1}{2\omega} \gamma_7 a_{10} b_{20} \sin(\phi_{40}) - \frac{1}{8\omega} (\frac{\omega \gamma_{10}\eta_7}{\omega_3^2 + \omega^2}) a_{20} b_{10} \cos(\phi_{30}) + \frac{1}{8\omega} (\frac{\omega_3 \gamma_{10}\eta_7}{\omega_3^2 + \omega^2}) a_{20} b_{10} \sin(\phi_{30}) + \frac{1}{4\omega} \gamma_7 a_{10} b_{20} \sin(2\phi_{20} - 2\phi_{10} + \phi_{40}) + \frac{1}{8\omega} (\gamma_6 \omega - \frac{\omega \gamma_{10}\eta_7}{\omega_3^2 + \omega^2}) a_{20} b_{10} \cos(2\phi_{20} - 2\phi_{10} - \phi_{30}) + \frac{1}{8\omega} (\gamma_4 + \frac{\omega_3 \gamma_{10}\eta_7}{\omega_3^2 + \omega^2}) a_{20} b_{10} \sin(2\phi_{20} - 2\phi_{10} - \phi_{30}),$$

$$J_{22} = \frac{\partial F_2}{\partial a_{21}} = -\frac{1}{2} (2\mu + \frac{\eta_4 \eta_8}{\omega_4^2 + \omega^2}) + \frac{3}{8} (\alpha_3 - \frac{2\gamma_{11}\eta_8}{\omega_4^2 + \omega^2} - \frac{2\omega_4 \gamma_{15}\eta_8^2}{(\omega_4^2 + \omega^2)^2}) a_{20}^2 + \frac{1}{8} (2\alpha_4 - \frac{\gamma_{13}\eta_7}{\omega_3^2 + \omega^2} - \frac{\omega_3 \gamma_{14}\eta_7}{\omega_3^2 + \omega^2} - \frac{2\gamma_{16}\eta_8}{\omega_4^2 + \omega^2}) a_{10}^2 + \frac{1}{8} (-\alpha_4 + \alpha_7 - \frac{2\omega_3 \gamma_{12}\eta_7^2}{(\omega_3^2 + \omega^2)^2} - \frac{\gamma_{13}\eta_7}{\omega_3^2 + \omega^2} + \frac{\omega_3 \gamma_{14}\eta_7}{\omega_3^2 + \omega^2}) a_{10}^2 \cos(2\phi_{20} - 2\phi_{10}) + \frac{1}{8} (\frac{\alpha_2}{\omega} - \alpha_5 \omega + \frac{(\omega_3^2 - \omega^2) \gamma_{12}\eta_7^2}{\omega(\omega_3^2 + \omega^2)^2} + \frac{\omega_3 \gamma_{13}\eta_7}{\omega(\omega_3^2 + \omega^2)} + \frac{\omega \gamma_{14}\eta_7}{\omega_3^2 + \omega^2}) a_{10}^2 \sin(2\phi_{20} - 2\phi_{10}) - \frac{1}{4\omega} \gamma_1 a_{20} b_{20} \sin(\phi_{40}) - \frac{1}{8\omega} \gamma_3 b_{20}^2 \sin(2\phi_{40}) + \frac{1}{4\omega} (\gamma_2 \omega - \frac{2\omega \gamma_8 \eta_8}{\omega_4^2 + \omega^2}) a_{20} b_{20} \cos(\phi_{40}) - \frac{1}{8\omega} (\frac{\omega \gamma_{10}\eta_7}{\omega_3^2 + \omega^2}) a_{20} b_{10} \cos(\phi_{30}) + \frac{1}{8\omega} (\frac{\omega_3 \gamma_{10}\eta_7}{\omega_3^2 + \omega^2}) a_{10} b_{10} \sin(\phi_{30}) + \frac{1}{8\omega} (\gamma_6 \omega - \frac{\omega \gamma_{10}\eta_7}{\omega_3^2 + \omega^2}) a_{10} b_{10} (\cos(2\phi_{20} - 2\phi_{10} - \phi_{30}) + \frac{1}{8\omega} (\gamma_4 + \frac{\omega_3 \gamma_{10}\eta_7}{\omega_3^2 + \omega^2}) a_{10} b_{10} \sin(2\phi_{20} - 2\phi_{10} - \phi_{30}) + \frac{1}{8\omega} \gamma_5 b_{10}^2 \sin(2\phi_{20} - 2\phi_{10} - 2\phi_{30}),$$

$$J_{23} = \frac{\partial F_2}{\partial b_{11}} = -\frac{1}{8\omega} (\frac{\omega \gamma_{10}\eta_7}{\omega_3^2 + \omega^2}) a_{20} a_{10} \cos(\phi_{30}) + \frac{1}{8\omega} (\frac{\omega_3 \gamma_{10}\eta_7}{\omega_3^2 + \omega^2}) a_{20} a_{10} \sin(\phi_{30}) + \frac{1}{8\omega} (\gamma_6 \omega - \frac{\omega \gamma_{10}\eta_7}{\omega_3^2 + \omega^2}) a_{20} a_{10} \cos(2\phi_{20} - 2\phi_{10} - \phi_{30}) + \frac{1}{8\omega} (\gamma_4 + \frac{\omega_3 \gamma_{10}\eta_7}{\omega_3^2 + \omega^2}) a_{20} a_{10} \sin(2\phi_2 - 2\phi_1 - \phi_3) + \frac{1}{4\omega} \gamma_5 a_{20} b_{10} \sin(2\phi_{20} - 2\phi_{10} - 2\phi_{30}),$$

$$J_{24} = \frac{\partial F_2}{\partial b_{21}} = \left(-\frac{1}{2\omega}\eta_3 - \frac{1}{8\omega}\gamma_1 a_{20}^2 - \frac{1}{4\omega}\gamma_7 a_{10}^2\right) \sin(\phi_{40}) - \frac{1}{4\omega}\gamma_3 a_{20} b_{20} \sin(2\phi_{40}) + \frac{1}{8\omega}\left(\gamma_2 \omega - \frac{2\omega\gamma_8 \eta_8}{\omega_4^2 + \omega^2}\right) a_{20}^2 \cos(\phi_{40}) + \frac{1}{8\omega}\gamma_7 a_{10}^2 \sin(2\phi_{20} - 2\phi_{10} + \phi_{40}),$$

$$J_{25} = \frac{\partial F_2}{\partial \phi_{11}} = \frac{1}{4}\left(-\alpha_4 + \alpha_7 - \frac{2\omega_3\gamma_{12}\eta_7^2}{(\omega_3^2 + \omega^2)^2} - \frac{\gamma_{13}\eta_7}{\omega_3^2 + \omega^2} + \frac{\omega_3\gamma_{14}\eta_7}{\omega_3^2 + \omega^2}\right) a_{20} a_{10}^2 \sin(2\phi_{20} - 2\phi_{10}) - \frac{1}{4}\left(\frac{\alpha_2}{\omega} - \alpha_5 \omega\right) + \frac{(\omega_3^2 - \omega^2)\gamma_{12}\eta_7^2}{\omega(\omega_3^2 + \omega^2)^2} + \frac{\omega_3\gamma_{13}\eta_7}{\omega(\omega_3^2 + \omega^2)} + \frac{\omega\gamma_{14}\eta_7}{\omega_3^2 + \omega^2} a_{20} a_{10}^2 \cos(2\phi_{20} - 2\phi_{10}) - \frac{1}{4\omega}\gamma_7 a_{10}^2 b_{20} \cos(2\phi_{20} - 2\phi_{10} + \phi_{40}) + \frac{1}{4\omega}\left(\gamma_6 \omega - \frac{\omega\gamma_{10}\eta_7}{\omega_3^2 + \omega^2}\right) a_{20} a_{10} b_{10} \sin(2\phi_{20} - 2\phi_{10} - \phi_{30}) - \frac{1}{4\omega}\left(\gamma_4 + \frac{\omega_3\gamma_{10}\eta_7}{\omega_3^2 + \omega^2}\right) a_{20} a_{10} b_{10} \cos(2\phi_{20} - 2\phi_{10} - \phi_{30}) - \frac{1}{4\omega}\gamma_5 a_{20} b_{10}^2 \cos(2\phi_{20} - 2\phi_{10} - 2\phi_{30}),$$

$$J_{26} = \frac{\partial F_2}{\partial \phi_{21}} = -\frac{1}{4}\left(-\alpha_4 + \alpha_7 - \frac{2\omega_3\gamma_{12}\eta_7^2}{(\omega_3^2 + \omega^2)^2} - \frac{\gamma_{13}\eta_7}{\omega_3^2 + \omega^2} + \frac{\omega_3\gamma_{14}\eta_7}{\omega_3^2 + \omega^2}\right) a_{20} a_{10}^2 \sin(2\phi_{20} - 2\phi_{10}) + \frac{1}{4}\left(\frac{\alpha_2}{\omega} - \alpha_5 \omega\right) + \frac{(\omega_3^2 - \omega^2)\gamma_{12}\eta_7^2}{\omega(\omega_3^2 + \omega^2)^2} + \frac{\omega_3\gamma_{13}\eta_7}{\omega(\omega_3^2 + \omega^2)} + \frac{\omega\gamma_{14}\eta_7}{\omega_3^2 + \omega^2} a_{20} a_{10}^2 \cos(2\phi_{20} - 2\phi_{10}) - \frac{1}{4\omega}\gamma_7 a_{10}^2 b_{20} \sin(2\phi_{20} - 2\phi_{10} + \phi_{40}) + \frac{1}{4\omega}\left(\gamma_6 \omega - \frac{\omega\gamma_{10}\eta_7}{\omega_3^2 + \omega^2}\right) a_{20} a_{10} b_{10} \cos(2\phi_{20} - 2\phi_{10} - \phi_{30}) + \frac{1}{4\omega}\left(\gamma_4 + \frac{\omega_3\gamma_{10}\eta_7}{\omega_3^2 + \omega^2}\right) a_{20} a_{10} b_{10} \cos(2\phi_{20} - 2\phi_{10} - \phi_{30}) + \frac{1}{4\omega}\gamma_5 a_{20} b_{10}^2 \cos(2\phi_{20} - 2\phi_{10} - 2\phi_{30}) + \frac{1}{2\omega}(\omega + \sigma)^2 f \sin(\phi_{20}),$$

$$J_{27} = \frac{\partial F_2}{\partial \phi_{31}} = \frac{1}{8\omega}\left(\frac{\omega\gamma_{10}\eta_7}{\omega_3^2 + \omega^2}\right) a_{20} a_{10} b_{10} \sin(\phi_3) + \frac{1}{8\omega}\left(\frac{\omega_3\gamma_{10}\eta_7}{\omega_3^2 + \omega^2}\right) a_{20} a_{10} b_{10} \cos(\phi_{30}) + \frac{1}{8\omega}(\gamma_6 \omega - \frac{\omega\gamma_{10}\eta_7}{\omega_3^2 + \omega^2}) a_{20} a_{10} b_{10} \sin(2\phi_{20} - 2\phi_{10} - \phi_{30}) - \frac{1}{8\omega}\left(\gamma_4 + \frac{\omega_3\gamma_{10}\eta_7}{\omega_3^2 + \omega^2}\right) a_{20} a_{10} b_{10} \cos(2\phi_{20} - 2\phi_{10} - \phi_{30}) - \frac{1}{8\omega}\gamma_5 a_{20} b_{10}^2 \cos(2\phi_{20} - 2\phi_{10} - 2\phi_{30}),$$

$$J_{28} = \frac{\partial F_2}{\partial \phi_{41}} = \left(-\frac{1}{2\omega}\eta_3 b_{20} - \frac{1}{8\omega}\gamma_1 a_{20}^2 b_{20} - \frac{1}{4\omega}\gamma_7 a_{10}^2 b_{20}\right) \cos(\phi_{40}) - \frac{1}{4\omega}\gamma_3 a_{20} b_{20}^2 \cos(2\phi_{40}) - \frac{1}{8\omega}(\gamma_2 \omega - \frac{2\omega\gamma_8 \eta_8}{\omega_4^2 + \omega^2}) a_{20}^2 b_{20} \sin(\phi_{40}) + \frac{1}{8\omega}\gamma_7 a_{10}^2 b_{20} \cos(2\phi_{20} - 2\phi_{10} + \phi_{40}),$$

$$J_{31} = \frac{\partial F_3}{\partial a_{11}} = \frac{1}{2(\omega + \sigma_1)} \eta_5 \sin(\phi_{30}),$$

$$J_{32} = \frac{\partial F_3}{\partial a_{21}} = 0,$$

$$J_{33} = \frac{\partial F_3}{\partial b_{11}} = -\mu_1,$$

$$J_{34} = \frac{\partial F_3}{\partial b_{21}} = 0,$$

$$J_{35} = \frac{\partial F_3}{\partial \phi_{11}} = 0,$$

$$J_{37} = \frac{\partial F_3}{\partial \phi_{31}} = \frac{1}{2(\omega + \sigma_1)} \eta_5 a_{10} \cos(\phi_{30}),$$

$$J_{38} = \frac{\partial F_3}{\partial \phi_{41}} = 0,$$

$$J_{41} = \frac{\partial F_4}{\partial a_{11}} = 0,$$

$$J_{42} = \frac{\partial F_4}{\partial a_{21}} = \frac{1}{2(\omega + \sigma_2)} \eta_6 \sin(\phi_{40}),$$

$$J_{43} = \frac{\partial F_4}{\partial b_{11}} = 0,$$

$$J_{44} = \frac{\partial F_4}{\partial b_{21}} = -\mu_2,$$

$$J_{45} = \frac{\partial F_4}{\partial \phi_{11}} = 0,$$

$$J_{46} = \frac{\partial F_4}{\partial \phi_{21}} = 0,$$

$$J_{47} = \frac{\partial F_4}{\partial \phi_{31}} = 0,$$

$$J_{48} = \frac{\partial F_4}{\partial \phi_{41}} = \frac{1}{2(\omega + \sigma_2)} \eta_6 a_{20} \cos(\phi_{40}),$$

$$J_{51} = \frac{\partial F_5}{\partial a_{11}} = \frac{1}{4\omega} (3\alpha_1 + \alpha_6 \omega^2 + \frac{2\omega_3 \beta_{11} \eta_7}{\omega_3^2 + \omega^2} + \frac{(\omega_3^2 - \omega^2) \beta_{15} \eta_7^2}{(\omega_3^2 + \omega^2)^2}) a_{10} + (\frac{-1}{2a_{10}^2} \eta_1 b_{10} + \frac{3}{8} \beta_1 b_{10} - \frac{1}{4a_{10}^2} \beta_7 a_2^2 b_{10} + \frac{1}{4} \frac{\omega_3 \beta_8 \eta_7}{\omega_3^2 + \omega^2} b_{10}) \frac{\cos(\phi_{30})}{\omega} - \frac{1}{8} \frac{\beta_8 \eta_7}{\omega_3^2 + \omega^2} b_{10} \sin(\phi_{30}) - \frac{1}{8} \beta_2 b_{10} \sin(\phi_{30}) - \frac{1}{8\omega a_{10}^2} \beta_7 a_2^2 b_{10} \cos(2\phi_{10} - 2\phi_{20} + \phi_{30}) - \frac{1}{2\omega a_{10}^2} (\omega + \sigma)^2 f \cos(\phi_{10}),$$

$$J_{52} = \frac{\partial F_5}{\partial a_{21}} = \frac{1}{4\omega} (2\alpha_2 + 2\alpha_5 \omega^2 + \frac{\omega_4 \beta_{13} \eta_8}{\omega_4^2 + \omega^2} - \frac{\omega^2 \beta_{14} \eta_8}{\omega_4^2 + \omega^2} + \frac{2\omega_3 \beta_{16} \eta_7}{\omega_3^2 + \omega^2}) a_{20} + \frac{1}{4\omega} (\alpha_2 - \alpha_5 \omega^2 + \frac{(\omega_4^2 - \omega^2) \beta_{12} \eta_8^2}{(\omega_4^2 + \omega^2)^2} + \frac{\omega_4 \beta_{13} \eta_8}{\omega_4^2 + \omega^2} + \frac{\omega^2 \beta_{14} \eta_8}{\omega_4^2 + \omega^2}) a_{20} \cos(2\phi_{10} - 2\phi_{20}) + \frac{1}{4\omega} (\alpha_4 \omega - \alpha_7 \omega + \frac{2\omega_4 \omega \beta_{12} \eta_8^2}{(\omega_4^2 + \omega^2)^2} + \frac{\omega \beta_{13} \eta_8}{\omega_4^2 + \omega^2} - \frac{\omega_4 \omega \beta_{14} \eta_8}{\omega_4^2 + \omega^2}) a_{20} \sin(2\phi_{10} - 2\phi_{20}) + \frac{1}{4} \frac{\beta_7 a_2^2 b_1}{\omega a_1} \cos(\phi_{30}) + \frac{1}{8\omega} (2\beta_4 + \frac{\omega_4 \beta_{10} \eta_8}{\omega_4^2 + \omega^2}) b_{20} \cos(\phi_{40}) + \frac{1}{8} (-2\beta_6 + \frac{\beta_{10} \eta_8}{\omega_4^2 + \omega^2}) b_{20} \sin(\phi_{40}) + \frac{1}{4\omega a_{10}} \beta_7 a_{20} b_{10} \cos(2\phi_{10} - 2\phi_{20} + \phi_{30}) + \frac{1}{8\omega} (\beta_4 + \frac{\omega_4 \beta_{10} \eta_8}{\omega_4^2 + \omega^2}) b_2 \cos(2\phi_{10} - 2\phi_{20} - \phi_{40}) + \frac{1}{8\omega} (-\beta_6 \omega + \frac{\omega \beta_{10} \eta_8}{\omega_4^2 + \omega^2}) b_2 \sin(2\phi_{10} - 2\phi_{20} - \phi_{40}),$$

$$J_{53} = \frac{\partial F_5}{\partial b_{11}} = \frac{1}{2\omega} \beta_3 b_{10} + (\frac{1}{2} \eta_1 + \frac{3}{8} \beta_1 a_{10}^2 + \frac{1}{4} \beta_7 a_{20}^2 + \frac{1}{4} \frac{\omega_3 \beta_8 \eta_7}{\omega_3^2 + \omega^2} a_{10}^2) \frac{\cos(\phi_{30})}{\omega a_{10}} + \frac{1}{4\omega} \beta_3 b_{10} \cos(2\phi_{30}) - \frac{1}{8} \frac{\beta_8 \eta_7}{\omega_3^2 + \omega^2} a_{10} \sin(\phi_{30}) - \frac{1}{8} \beta_2 a_{10} \sin(\phi_{30}) + \frac{1}{8\omega a_{10}} \beta_7 a_{20}^2 \cos(2\phi_{10} - 2\phi_{20} + \phi_{30}),$$

$$J_{54} = \frac{\partial F_5}{\partial b_{21}} = \frac{1}{2\omega} \beta_5 b_{20} + \frac{1}{8\omega} (2\beta_4 + \frac{\omega_4 \beta_{10} \eta_8}{\omega_4^2 + \omega^2}) a_{20} \cos(\phi_{40}) + \frac{1}{8} (-2\beta_6 + \frac{\beta_{10} \eta_8}{\omega_4^2 + \omega^2}) a_{20} \sin(\phi_{40}) + \frac{1}{8\omega} (\beta_4 + \frac{\omega_4 \beta_{10} \eta_8}{\omega_4^2 + \omega^2}) a_{20} \cos(2\phi_{10} - 2\phi_{20} - \phi_{40}) + \frac{1}{8\omega} (-\beta_6 \omega + \frac{\omega \beta_{10} \eta_8}{\omega_4^2 + \omega^2}) a_{20} \sin(2\phi_{10} - 2\phi_{20} - \phi_{40}) + \frac{1}{4\omega} \beta_5 b_{20} \cos(2\phi_{10} - 2\phi_{20} - 2\phi_{40}),$$

$$J_{55} = \frac{\partial F_5}{\partial \phi_{11}} = -\frac{1}{4\omega} (\alpha_2 - \alpha_5 \omega^2 + \frac{(\omega_4^2 - \omega^2) \beta_{12} \eta_8^2}{(\omega_4^2 + \omega^2)^2} + \frac{\omega_4 \beta_{13} \eta_8}{\omega_4^2 + \omega^2} + \frac{\omega^2 \beta_{14} \eta_8}{\omega_4^2 + \omega^2}) a_{20}^2 \sin(2\phi_{10} - 2\phi_{20}) + \frac{1}{4\omega} (\alpha_4 \omega - \alpha_7 \omega + \frac{2\omega_4 \omega \beta_{12} \eta_8^2}{(\omega_4^2 + \omega^2)^2} + \frac{\omega \beta_{13} \eta_8}{\omega_4^2 + \omega^2} - \frac{\omega_4 \omega \beta_{14} \eta_8}{\omega_4^2 + \omega^2}) a_{20}^2 \cos(2\phi_{10} - 2\phi_{20}) - \frac{1}{4\omega a_{10}} \beta_7 a_{20}^2 b_{10} \sin(2\phi_{10} - 2\phi_{20} + \phi_{30}) - \frac{1}{4\omega} (\beta_4 + \frac{\omega_4 \beta_{10} \eta_8}{\omega_4^2 + \omega^2}) a_{20} b_{20} \sin(2\phi_{10} - 2\phi_{20} - \phi_{40}) + \frac{1}{4\omega} (-\beta_6 \omega + \frac{\omega \beta_{10} \eta_8}{\omega_4^2 + \omega^2}) a_{20} b_{20} \cos(2\phi_{10} - 2\phi_{20} - \phi_{40}) - \frac{1}{4\omega} \beta_5 b_{20}^2 \sin(2\phi_{10} - 2\phi_{20} - 2\phi_{40}) - \frac{1}{2\omega a_{10}} (\omega + \sigma)^2 f \sin(\phi_{10}),$$

$$J_{56} = \frac{\partial F_5}{\partial \phi_{21}} = \frac{1}{4\omega} (\alpha_2 - \alpha_5 \omega^2 + \frac{(\omega_4^2 - \omega^2) \beta_{12} \eta_8^2}{(\omega_4^2 + \omega^2)^2} + \frac{\omega_4 \beta_{13} \eta_8}{\omega_4^2 + \omega^2} + \frac{\omega^2 \beta_{14} \eta_8}{\omega_4^2 + \omega^2}) a_{20}^2 \sin(2\phi_{10} - 2\phi_{20}) - \frac{1}{4\omega} (\alpha_4 \omega - \alpha_7 \omega + \frac{2\omega_4 \omega \beta_{12} \eta_8^2}{(\omega_4^2 + \omega^2)^2} + \frac{\omega \beta_{13} \eta_8}{\omega_4^2 + \omega^2} - \frac{\omega_4 \omega \beta_{14} \eta_8}{\omega_4^2 + \omega^2}) a_{20}^2 \cos(2\phi_{10} - 2\phi_{20}) + \frac{1}{4\omega a_{10}} \beta_7 a_{20}^2 b_{10} \sin(2\phi_{10} - 2\phi_{20} + \phi_{30}) + \frac{1}{4\omega} (\beta_4 + \frac{\omega_4 \beta_{10} \eta_8}{\omega_4^2 + \omega^2}) a_{20} b_{20} \sin(2\phi_{10} - 2\phi_{20} - \phi_{40}) - \frac{1}{4\omega} (-\beta_6 \omega + \frac{\omega \beta_{10} \eta_8}{\omega_4^2 + \omega^2}) a_{20} b_{20} \cos(2\phi_{10} - 2\phi_{20} - \phi_{40}) + \frac{1}{4\omega} \beta_5 b_{20}^2 \sin(2\phi_{10} - 2\phi_{20} - 2\phi_{40}),$$

$$\begin{aligned}
J_{57} &= \frac{\partial F_5}{\partial \phi_{31}} = -\frac{1}{\omega a_{10}} \left( \frac{1}{2} \eta_1 b_{10} + \frac{3}{8} \beta_1 a_{10}^2 b_{10} + \frac{1}{4} \beta_7 a_{20}^2 b_{10} + \frac{1}{4} \frac{\omega_3 \beta_8 \eta_7}{\omega_3^2 + \omega^2} a_{10}^2 b_{10} \right) \sin(\phi_{30}) - \frac{1}{4\omega} \beta_3 b_{10}^2 \sin(2\phi_{30}) \\
&\quad - \frac{1}{8} \frac{\beta_8 \eta_7}{\omega_3^2 + \omega^2} a_{10} b_{10} \cos(\phi_{30}) - \frac{1}{8} \beta_2 a_{10} b_{10} \cos(\phi_{30}) - \frac{1}{8\omega a_{10}} \beta_7 a_{20}^2 b_{10} \sin(2\phi_{10} - 2\phi_{20} + \phi_{30}), \\
J_{58} &= \frac{\partial F_5}{\partial \phi_{41}} = -\frac{1}{8\omega} (2\beta_4 + \frac{\omega_4 \beta_{10} \eta_8}{\omega_4^2 + \omega^2}) a_{20} b_{20} \sin(\phi_{40}) + \frac{1}{8} (-2\beta_6 + \frac{\beta_{10} \eta_8}{\omega_4^2 + \omega^2}) a_{20} b_{20} \cos(\phi_{40}) + \frac{1}{8\omega} (\beta_4 \\
&\quad + \frac{\omega_4 \beta_{10} \eta_8}{\omega_4^2 + \omega^2}) a_{20} b_{20} \sin(2\phi_{10} - 2\phi_{20} - \phi_{40}) - \frac{1}{8\omega} (-\beta_6 \omega + \frac{\omega \beta_{10} \eta_8}{\omega_4^2 + \omega^2}) a_{20} b_{20} \cos(2\phi_{10} - 2\phi_{20} - \phi_{40}) \\
&\quad + \frac{1}{4\omega} \beta_5 b_{20}^2 \sin(2\phi_{10} - 2\phi_{20} - 2\phi_{40}), \\
J_{61} &= \frac{\partial F_6}{\partial a_{11}} = \frac{1}{4\omega} (2\alpha_2 + 2\alpha_5 \omega^2 + \frac{\omega_3 \gamma_{13} \eta_7}{\omega_3^2 + \omega^2} - \frac{\omega^2 \gamma_{14} \eta_7}{\omega_3^2 + \omega^2} + \frac{2\omega_4 \gamma_{16} \eta_8}{\omega_4^2 + \omega^2}) a_{10} + \frac{1}{4\omega} (\alpha_2 - \alpha_5 \omega^2 + \frac{(\omega_3^2 - \omega^2) \gamma_{12} \eta_7^2}{(\omega_3^2 + \omega^2)^2} + \frac{\omega_3 \gamma_{13} \eta_7}{\omega_3^2 + \omega^2} \\
&\quad + \frac{\omega^2 \gamma_{14} \eta_7}{\omega_3^2 + \omega^2}) a_{10} \cos(2\phi_{20} - 2\phi_{10}) + \frac{1}{4\omega} (\alpha_4 \omega - \alpha_7 \omega + \frac{2\omega_3 \omega \gamma_{12} \eta_7^2}{(\omega_3^2 + \omega^2)^2} - \frac{\omega \gamma_{13} \eta_7}{\omega_3^2 + \omega^2} + \frac{\omega_3 \omega \gamma_{14} \eta_7}{\omega_3^2 + \omega^2}) a_{10} \sin(2\phi_{20} - 2\phi_{10}) \\
&\quad + \frac{1}{2} \gamma_7 a_{10} b_{20} \frac{\cos(\phi_{40})}{\omega a_{20}} + \frac{1}{8\omega} (2\gamma_4 + \frac{\omega_3 \gamma_{10} \eta_7}{\omega_3^2 + \omega^2}) b_{10} \cos(\phi_{30}) + \frac{1}{8} (-2\gamma_6 + \frac{\gamma_{10} \eta_7}{\omega_3^2 + \omega^2}) b_{10} \sin(\phi_{30}) \\
&\quad + \frac{1}{4\omega a_{20}} \gamma_7 a_{10} b_{20} \cos(2\phi_{20} - 2\phi_{10} + \phi_{40}) + \frac{1}{8\omega} (\gamma_4 + \frac{\omega_3 \gamma_{10} \eta_7}{\omega_3^2 + \omega^2}) b_{10} \cos(2\phi_{20} - 2\phi_{10} - \phi_{30}) + \frac{1}{8} (-\gamma_6 \\
&\quad + \frac{\gamma_{10} \eta_7}{\omega_3^2 + \omega^2}) b_{10} \sin(2\phi_{20} - 2\phi_{10} - \phi_{30}), \\
J_{62} &= \frac{\partial F_6}{\partial a_{21}} = \frac{1}{4\omega} (3\alpha_1 + \alpha_6 \omega^2 + \frac{2\omega_4 \gamma_{11} \eta_8}{\omega_4^2 + \omega^2} + \frac{(\omega_4^2 - \omega^2) \gamma_{15} \eta_8^2}{(\omega_4^2 + \omega^2)^2}) a_{20} + (\frac{-1}{2a_{20}} \eta_3 b_{20} + \frac{3}{8} \gamma_1 b_{20} - \frac{1}{4a_{20}^2} \gamma_7 a_{10}^2 b_{20} \\
&\quad + \frac{1}{4} \frac{\omega_4 \gamma_8 \eta_8}{\omega_4^2 + \omega^2} b_{20}) \frac{\cos(\phi_{40})}{\omega} - \frac{1}{8} \frac{\gamma_8 \eta_8}{\omega_4^2 + \omega^2} b_{20} \sin(\phi_{40}) - \frac{1}{8} \gamma_2 b_{20} \sin(\phi_{40}) - \frac{1}{8\omega a_{20}^2} \gamma_7 a_{10}^2 b_{20} \cos(2\phi_{20} - 2\phi_{10} + \phi_{40}) \\
&\quad - \frac{1}{2\omega a_{20}^2} (\omega + \sigma)^2 f \sin(\phi_{20}), \\
J_{63} &= \frac{\partial F_6}{\partial b_{11}} = \frac{1}{2\omega} \gamma_5 b_{10} + \frac{1}{8\omega} (2\gamma_4 + \frac{\omega_3 \gamma_{10} \eta_7}{\omega_3^2 + \omega^2}) a_{10} \cos(\phi_{30}) + \frac{1}{8} (-2\gamma_6 + \frac{\gamma_{10} \eta_7}{\omega_3^2 + \omega^2}) a_{10} \sin(\phi_{30}) + \frac{1}{8\omega} (\gamma_4 \\
&\quad + \frac{\omega_3 \gamma_{10} \eta_7}{\omega_3^2 + \omega^2}) a_{10} \cos(2\phi_{20} - 2\phi_{10} - \phi_{30}) + \frac{1}{8} (-\gamma_6 + \frac{\gamma_{10} \eta_7}{\omega_3^2 + \omega^2}) a_{10} \sin(2\phi_{20} - 2\phi_{10} - \phi_{30}) \\
&\quad + \frac{1}{4\omega} \gamma_5 b_{10} \cos(2\phi_{20} - 2\phi_{10} - 2\phi_{30}), \\
J_{64} &= \frac{\partial F_6}{\partial b_{21}} = \frac{1}{2\omega} \gamma_3 b_{20} + (\frac{1}{2} \eta_3 + \frac{3}{8} \gamma_1 a_{20}^2 + \frac{1}{4} \gamma_7 a_{10}^2 + \frac{1}{4} \frac{\omega_4 \gamma_8 \eta_8}{\omega_4^2 + \omega^2} a_{20}^2) \frac{\cos(\phi_{40})}{\omega a_{20}} + \frac{1}{4\omega} \gamma_3 b_{20} \cos(2\phi_{40}) \\
&\quad - \frac{1}{8} \frac{\gamma_8 \eta_8}{\omega_4^2 + \omega^2} a_{20} \sin(\phi_{40}) - \frac{1}{8} \gamma_2 a_{20} \sin(\phi_{40}) + \frac{1}{8\omega a_{20}} \gamma_7 a_{10}^2 \cos(2\phi_{20} - 2\phi_{10} + \phi_{40}), \\
J_{65} &= \frac{\partial F_6}{\partial \phi_{11}} = \frac{1}{4\omega} (\alpha_2 - \alpha_5 \omega^2 + \frac{(\omega_3^2 - \omega^2) \gamma_{12} \eta_7^2}{(\omega_3^2 + \omega^2)^2} + \frac{\omega_3 \gamma_{13} \eta_7}{\omega_3^2 + \omega^2} + \frac{\omega^2 \gamma_{14} \eta_7}{\omega_3^2 + \omega^2}) a_{10}^2 \sin(2\phi_{20} - 2\phi_{10}) - \frac{1}{4\omega} (\alpha_4 \omega - \alpha_7 \omega \\
&\quad + \frac{2\omega_3 \omega \gamma_{12} \eta_7^2}{(\omega_3^2 + \omega^2)^2} - \frac{\omega \gamma_{13} \eta_7}{\omega_3^2 + \omega^2} + \frac{\omega_3 \omega \gamma_{14} \eta_7}{\omega_3^2 + \omega^2}) a_{10}^2 \cos(2\phi_{20} - 2\phi_{10}) + \frac{1}{4\omega a_2} \gamma_7 a_{10}^2 b_{20} \sin(2\phi_{20} - 2\phi_{10} + \phi_{40}) \\
&\quad + \frac{1}{4\omega} (\gamma_4 + \frac{\omega_3 \gamma_{10} \eta_7}{\omega_3^2 + \omega^2}) a_{10} b_{10} \sin(2\phi_{20} - 2\phi_{10} - \phi_{30}) - \frac{1}{4} (-\gamma_6 + \frac{\gamma_{10} \eta_7}{\omega_3^2 + \omega^2}) a_{10} b_{10} \cos(2\phi_{20} - 2\phi_{10} - \phi_{30}) \\
&\quad + \frac{1}{4\omega} \gamma_5 b_{10}^2 \sin(2\phi_{20} - 2\phi_{10} - 2\phi_{30}), \\
J_{66} &= \frac{\partial F_6}{\partial \phi_{21}} = \frac{1}{4\omega} (\alpha_2 - \alpha_5 \omega^2 + \frac{(\omega_3^2 - \omega^2) \gamma_{12} \eta_7^2}{(\omega_3^2 + \omega^2)^2} + \frac{\omega_3 \gamma_{13} \eta_7}{\omega_3^2 + \omega^2} + \frac{\omega^2 \gamma_{14} \eta_7}{\omega_3^2 + \omega^2}) a_{10}^2 \sin(2\phi_{20} - 2\phi_{10}) + \frac{1}{4\omega} (\alpha_4 \omega - \alpha_7 \omega \\
&\quad + \frac{2\omega_3 \omega \gamma_{12} \eta_7^2}{(\omega_3^2 + \omega^2)^2} - \frac{\omega \gamma_{13} \eta_7}{\omega_3^2 + \omega^2} + \frac{\omega_3 \omega \gamma_{14} \eta_7}{\omega_3^2 + \omega^2}) a_{10}^2 \cos(2\phi_{20} - 2\phi_{10}) - \frac{1}{4\omega a_2} \gamma_7 a_{10}^2 b_{20} \sin(2\phi_{20} - 2\phi_{10} + \phi_{40}) \\
&\quad - \frac{1}{4\omega} (\gamma_4 + \frac{\omega_3 \gamma_{10} \eta_7}{\omega_3^2 + \omega^2}) a_{10} b_{10} \sin(2\phi_{20} - 2\phi_{10} - \phi_{30}) + \frac{1}{4} (-\gamma_6 + \frac{\gamma_{10} \eta_7}{\omega_3^2 + \omega^2}) a_{10} b_{10} \cos(2\phi_{20} - 2\phi_{10} - \phi_{30}) \\
&\quad - \frac{1}{4\omega} \gamma_5 b_{10}^2 \sin(2\phi_{20} - 2\phi_{10} - 2\phi_{30}) + \frac{1}{2\omega a_{20}} (\omega + \sigma)^2 f \cos(\phi_{20}), \\
J_{67} &= \frac{\partial F_6}{\partial \phi_{31}} = -\frac{1}{8\omega} (2\gamma_4 + \frac{\omega_3 \gamma_{10} \eta_7}{\omega_3^2 + \omega^2}) a_{10} b_{10} \sin(\phi_{30}) + \frac{1}{8} (-2\gamma_6 + \frac{\gamma_{10} \eta_7}{\omega_3^2 + \omega^2}) a_{10} b_{10} \cos(\phi_{30}) \\
&\quad + \frac{1}{4\omega} \gamma_5 b_{10}^2 \sin(2\phi_{20} - 2\phi_{10} - 2\phi_{30}) + \frac{1}{8\omega} (\gamma_4 + \frac{\omega_3 \gamma_{10} \eta_7}{\omega_3^2 + \omega^2}) a_{10} b_{10} \sin(2\phi_{20} - 2\phi_{10} - \phi_{30}) \\
&\quad - \frac{1}{8} (-\gamma_6 + \frac{\gamma_{10} \eta_7}{\omega_3^2 + \omega^2}) a_{10} b_{10} \cos(2\phi_{20} - 2\phi_{10} - \phi_{30}),
\end{aligned}$$

$$J_{68} = \frac{\partial F_6}{\partial \phi_{41}} = -\left(\frac{1}{2}\eta_3 b_{20} + \frac{3}{8}\gamma_1 a_{20}^2 b_{20} + \frac{1}{4}\gamma_7 a_{10}^2 b_{20} + \frac{1}{4}\frac{\omega_4 \gamma_8 \eta_8}{\omega_4^2 + \omega^2} a_{20}^2 b_{20}\right) \frac{\sin(\phi_{40})}{\omega a_{20}} - \frac{1}{4\omega} \gamma_{30} b_{20}^2 \sin(2\phi_{40}) - \frac{1}{8}\frac{\gamma_8 \eta_8}{\omega_4^2 + \omega^2} a_{20} b_{20} \cos(\phi_{40}) - \frac{1}{8}\gamma_2 a_{20} b_{20} \cos(\phi_{40}) - \frac{1}{8\omega a_2} \gamma_7 a_{10}^2 b_{20} \sin(2\phi_{20} - 2\phi_{10} + \phi_{40}),$$

$$J_{71} = \frac{\partial F_7}{\partial a_{11}} = \frac{1}{2(\omega + \sigma_1) b_{10}} \eta_5 \cos(\phi_{30}) - \frac{1}{4\omega} (3\alpha_1 + \alpha_6 \omega^2 + \frac{2\omega_3 \beta_{11} \eta_7}{\omega_3^2 + \omega^2} + \frac{(\omega_3^2 - \omega^2) \beta_{15} \eta_7^2}{(\omega_3^2 + \omega^2)^2}) a_{10} - (-\frac{1}{2a_{10}^2} \eta_1 b_{10} + \frac{3}{8}\beta_1 b_{10} + \frac{1}{4}\beta_7 b_{10} + \frac{1}{4}\frac{\omega_3 \beta_8 \eta_7}{\omega_3^2 + \omega^2} b_{10}) \frac{\cos(\phi_{30})}{\omega} + \frac{1}{8}\frac{\beta_8 \eta_7}{\omega_3^2 + \omega^2} b_{10} \sin(\phi_{30}) - \frac{1}{8}\beta_2 b_{10} \sin(\phi_{30}) - \frac{1}{2\omega a_{10}^2} (\omega + \sigma)^2 f \cos(\phi_{10}),$$

$$J_{72} = \frac{\partial F_7}{\partial a_{21}} = -\frac{1}{4\omega} (2\alpha_2 + 2\alpha_5 \omega^2 + \frac{\omega_4 \beta_{13} \eta_8}{\omega_4^2 + \omega^2} - \frac{\omega^2 \beta_{14} \eta_8}{\omega_4^2 + \omega^2} + \frac{2\omega_3 \beta_{16} \eta_7}{\omega_3^2 + \omega^2}) a_{20} - \frac{1}{4\omega} (\alpha_2 - \alpha_5 \omega^2 + \frac{(\omega_4^2 - \omega^2) \beta_{12} \eta_8^2}{(\omega_4^2 + \omega^2)^2} + \frac{\omega_4 \beta_{13} \eta_8}{\omega_4^2 + \omega^2} + \frac{\omega^2 \beta_{14} \eta_8}{\omega_4^2 + \omega^2}) a_{20} \cos(2\phi_{10} - 2\phi_{20}) - \frac{1}{4\omega} (\alpha_4 \omega - \alpha_7 \omega + \frac{2\omega_4 \omega \beta_{12} \eta_8^2}{(\omega_4^2 + \omega^2)^2} + \frac{\omega \beta_{13} \eta_8}{\omega_4^2 + \omega^2} - \frac{\omega_4 \omega \beta_{14} \eta_8}{\omega_4^2 + \omega^2}) a_{20} \sin(2\phi_{10} - 2\phi_{20}) - \frac{1}{2}\beta_7 a_{20} b_{10} \frac{\cos(\phi_{30})}{\omega a_{10}} - \frac{1}{8\omega} (2\beta_4 + \frac{\omega_4 \beta_{10} \eta_8}{\omega_4^2 + \omega^2}) b_{20} \cos(\phi_{40}) - \frac{1}{8} (-2\beta_6 + \frac{\beta_{10} \eta_8}{\omega_4^2 + \omega^2}) b_{20} \sin(\phi_{40}) - \frac{1}{4\omega a_{10}} \beta_7 a_{20} b_{10} \cos(2\phi_{10} - 2\phi_{20} + \phi_{30}) - \frac{1}{8\omega} (\beta_4 + \frac{\omega_4 \beta_{10} \eta_8}{\omega_4^2 + \omega^2}) b_{20} \cos(2\phi_{10} - 2\phi_{20} - \phi_{40}) - \frac{1}{8\omega} (-\beta_6 \omega + \frac{\omega \beta_{10} \eta_8}{\omega_4^2 + \omega^2}) b_{20} \sin(2\phi_{10} - 2\phi_{20} - \phi_{40}),$$

$$J_{73} = \frac{\partial F_7}{\partial b_{11}} = -\frac{1}{2(\omega + \sigma_1) b_{10}^2} \eta_5 a_{10} \cos(\phi_{30}) - \frac{1}{2\omega} \beta_3 b_{10} - (\frac{1}{2}\eta_1 + \frac{3}{8}\beta_1 a_{10}^2 + \frac{1}{4}\beta_7 a_{20}^2 + \frac{1}{4}\frac{\omega_3 \beta_8 \eta_7}{\omega_3^2 + \omega^2} a_{10}^2) \frac{\cos(\phi_{30})}{\omega a_{10}} - \frac{1}{4\omega} \beta_3 b_{10} \cos(2\phi_{30}) + \frac{1}{8}\frac{\beta_8 \eta_7}{\omega_3^2 + \omega^2} a_{10} \sin(\phi_3) - \frac{1}{8}\beta_2 a_{10} \sin(\phi_{30}) - \frac{1}{8\omega a_{10}} \beta_7 a_{20}^2 \cos(2\phi_{10} - 2\phi_{20} + \phi_{30}),$$

$$J_{74} = \frac{\partial F_7}{\partial b_{21}} = -\frac{1}{2\omega} \beta_5 b_{20} - \frac{1}{8\omega} (2\beta_4 + \frac{\omega_4 \beta_{10} \eta_8}{\omega_4^2 + \omega^2}) a_{20} \cos(\phi_{40}) - \frac{1}{8} (-2\beta_6 + \frac{\beta_{10} \eta_8}{\omega_4^2 + \omega^2}) a_{20} \sin(\phi_{40}) - \frac{1}{8\omega} (\beta_4 + \frac{\omega_4 \beta_{10} \eta_8}{\omega_4^2 + \omega^2}) a_{20} \cos(2\phi_{10} - 2\phi_{20} - \phi_{40}) - \frac{1}{8\omega} (-\beta_6 \omega + \frac{\omega \beta_{10} \eta_8}{\omega_4^2 + \omega^2}) a_{20} \sin(2\phi_{10} - 2\phi_{20} - \phi_{40}) - \frac{1}{4\omega} \beta_5 b_{20} \cos(2\phi_{10} - 2\phi_{20} - 2\phi_{40}),$$

$$J_{75} = \frac{\partial F_7}{\partial \phi_{11}} = \frac{1}{4\omega} (\alpha_2 - \alpha_5 \omega^2 + \frac{(\omega_4^2 - \omega^2) \beta_{12} \eta_8^2}{(\omega_4^2 + \omega^2)^2} + \frac{\omega_4 \beta_{13} \eta_8}{\omega_4^2 + \omega^2} + \frac{\omega^2 \beta_{14} \eta_8}{\omega_4^2 + \omega^2}) a_{20}^2 \sin(2\phi_{10} - 2\phi_{20}) - \frac{1}{4\omega} (\alpha_4 \omega - \alpha_7 \omega + \frac{2\omega_4 \omega \beta_{12} \eta_8^2}{(\omega_4^2 + \omega^2)^2} + \frac{\omega \beta_{13} \eta_8}{\omega_4^2 + \omega^2} - \frac{\omega_4 \omega \beta_{14} \eta_8}{\omega_4^2 + \omega^2}) a_{20}^2 \cos(2\phi_{10} - 2\phi_{20}) + \frac{1}{4\omega a_1} \beta_7 a_{20}^2 b_{10} \sin(2\phi_{10} - 2\phi_{20} + \phi_{30}) + \frac{1}{4\omega} (\beta_4 + \frac{\omega_4 \beta_{10} \eta_8}{\omega_4^2 + \omega^2}) a_{20} b_{20} \sin(2\phi_{10} - 2\phi_{20} - \phi_{40}) - \frac{1}{4\omega} (-\beta_6 \omega + \frac{\omega \beta_{10} \eta_8}{\omega_4^2 + \omega^2}) a_{20} b_{20} \cos(2\phi_{10} - 2\phi_{20} - \phi_{40}) + \frac{1}{4\omega} \beta_5 b_{20}^2 \sin(2\phi_{10} - 2\phi_{20} - 2\phi_{40}) + \frac{1}{2\omega a_{10}} (\omega + \sigma)^2 f \sin(\phi_{10}),$$

$$J_{76} = \frac{\partial F_7}{\partial \phi_{21}} = -\frac{1}{4\omega} (\alpha_2 - \alpha_5 \omega^2 + \frac{(\omega_4^2 - \omega^2) \beta_{12} \eta_8^2}{(\omega_4^2 + \omega^2)^2} + \frac{\omega_4 \beta_{13} \eta_8}{\omega_4^2 + \omega^2} + \frac{\omega^2 \beta_{14} \eta_8}{\omega_4^2 + \omega^2}) a_{20}^2 \sin(2\phi_{10} - 2\phi_{20}) + \frac{1}{4\omega} (\alpha_4 \omega - \alpha_7 \omega + \frac{2\omega_4 \omega \beta_{12} \eta_8^2}{(\omega_4^2 + \omega^2)^2} + \frac{\omega \beta_{13} \eta_8}{\omega_4^2 + \omega^2} - \frac{\omega_4 \omega \beta_{14} \eta_8}{\omega_4^2 + \omega^2}) a_{20}^2 \cos(2\phi_{10} - 2\phi_{20}) - \frac{1}{4\omega a_1} \beta_7 a_{20}^2 b_{10} \sin(2\phi_{10} - 2\phi_{20} + \phi_{30}) - \frac{1}{4\omega} (\beta_4 + \frac{\omega_4 \beta_{10} \eta_8}{\omega_4^2 + \omega^2}) a_{20} b_{20} \sin(2\phi_{10} - 2\phi_{20} - \phi_{40}) + \frac{1}{8\omega} (-\beta_6 \omega + \frac{\omega \beta_{10} \eta_8}{\omega_4^2 + \omega^2}) a_{20} b_{20} \cos(2\phi_{10} - 2\phi_{20} - \phi_{40}) - \frac{1}{8\omega} \beta_5 b_{20}^2 \sin(2\phi_{10} - 2\phi_{20} - 2\phi_{40}),$$

$$J_{77} = \frac{\partial F_7}{\partial \phi_{31}} = (\frac{1}{2}\eta_1 b_{10} + \frac{3}{8}\beta_1 a_{10}^2 b_{10} + \frac{1}{4}\beta_7 a_{20}^2 b_{10} + \frac{1}{4}\frac{\omega_3 \beta_8 \eta_7}{\omega_3^2 + \omega^2} a_{10}^2 b_{10}) \frac{\sin(\phi_{30})}{\omega a_{10}} + \frac{1}{4\omega} \beta_3 b_{10}^2 \sin(2\phi_{30}) + \frac{1}{8}\frac{\beta_8 \eta_7}{\omega_3^2 + \omega^2} a_{10} b_{10} \cos(\phi_{30}) - \frac{1}{8}\beta_2 a_{10} b_{10} \cos(\phi_{30}) + \frac{1}{8\omega a_{10}} \beta_7 a_{20}^2 b_{10} \sin(2\phi_{10} - 2\phi_{20} + \phi_{30}),$$

$$J_{78} = \frac{\partial F_7}{\partial \phi_{41}} = \frac{1}{8\omega} (2\beta_4 + \frac{\omega_4 \beta_{10} \eta_8}{\omega_4^2 + \omega^2}) a_{20} b_{20} \sin(\phi_{40}) - \frac{1}{8} (-2\beta_6 + \frac{\beta_{10} \eta_8}{\omega_4^2 + \omega^2}) a_{20} b_{20} \cos(\phi_{40}) - \frac{1}{8\omega} (\beta_4 + \frac{\omega_4 \beta_{10} \eta_8}{\omega_4^2 + \omega^2}) a_{20} b_{20} \sin(2\phi_{10} - 2\phi_{20} - \phi_{40}) + \frac{1}{8\omega} (-\beta_6 \omega + \frac{\omega \beta_{10} \eta_8}{\omega_4^2 + \omega^2}) a_{20} b_{20} \cos(2\phi_{10} - 2\phi_{20} - \phi_{40}) + \frac{1}{4\omega} \beta_5 b_{20}^2 \sin(2\phi_{10} - 2\phi_{20} - 2\phi_{40}),$$

$$\begin{aligned}
J_{81} = \frac{\partial F_8}{\partial a_{11}} = & -\frac{1}{4\omega} (2\alpha_2 + 2\alpha_5\omega^2 + \frac{\omega_3\gamma_{13}\eta_7}{\omega_3^2+\omega^2} - \frac{\omega^2\gamma_{14}\eta_7}{\omega_3^2+\omega^2} + \frac{2\omega_4\gamma_{16}\eta_8}{\omega_4^2+\omega^2}) a_{10} - \frac{1}{4\omega} (\alpha_2 - \alpha_5\omega^2 + \frac{(\omega_3^2-\omega^2)\gamma_{12}\eta_7^2}{(\omega_3^2+\omega^2)^2} \\
& + \frac{\omega_3\gamma_{13}\eta_7}{\omega_3^2+\omega^2} + \frac{\omega^2\gamma_{14}\eta_7}{\omega_3^2+\omega^2}) a_{10} \cos(2\phi_{20} - 2\phi_{10}) - \frac{1}{4\omega} (\alpha_4\omega - \alpha_7\omega + \frac{2\omega_3\omega\gamma_{12}\eta_7^2}{(\omega_3^2+\omega^2)^2} - \frac{\omega\gamma_{13}\eta_7}{\omega_3^2+\omega^2} \\
& + \frac{\omega_3\omega\gamma_{14}\eta_7}{\omega_3^2+\omega^2}) a_{10} \sin(2\phi_{20} - 2\phi_{10}) - \frac{1}{2}\gamma_7 a_{10} b_{20} \frac{\cos(\phi_{40})}{\omega a_{20}} - \frac{1}{8\omega} (2\gamma_4 + \frac{\omega_3\gamma_{10}\eta_7}{\omega_3^2+\omega^2}) b_{10} \cos(\phi_{30}) - \frac{1}{8} (-2\gamma_6 \\
& + \frac{\gamma_{10}\eta_7}{\omega_3^2+\omega^2}) b_{10} \sin(\phi_{30}) - \frac{1}{4\omega a_2} \gamma_7 a_{10} b_{20} \cos(2\phi_{20} - 2\phi_{10} + \phi_{40}) - \frac{1}{8\omega} (\gamma_4 + \frac{\omega_3\gamma_{10}\eta_7}{\omega_3^2+\omega^2}) b_{10} \cos(2\phi_{20} - 2\phi_{10} - \phi_{30}) \\
& - \frac{1}{8} (-\gamma_6 + \frac{\gamma_{10}\eta_7}{\omega_3^2+\omega^2}) b_{10} \sin(2\phi_{20} - 2\phi_{10} - \phi_{30}),
\end{aligned}$$

$$\begin{aligned}
J_{82} = \frac{\partial F_8}{\partial a_{21}} = & \frac{1}{2(\omega+\sigma_2)b_{20}} \eta_6 \cos(\phi_{40}) - \frac{1}{4\omega} (3\alpha_1 + \hat{\alpha}_6\omega^2 + \frac{2\omega_4\gamma_{11}\eta_8}{\omega_4^2+\omega^2} + \frac{(\omega_4^2-\omega^2)\gamma_{15}\eta_8^2}{(\omega_4^2+\omega^2)^2}) a_{20} - (-\frac{1}{2a_{20}^2} \eta_3 b_{20} + \frac{3}{8}\gamma_1 b_{20} \\
& - \frac{1}{4a_{20}^2} \gamma_7 a_{10}^2 b_{20} + \frac{1}{4} \frac{\omega_4\gamma_8\eta_8}{\omega_4^2+\omega^2} b_{20}) \frac{\cos(\phi_{40})}{\omega} + \frac{1}{8} \frac{\gamma_8\eta_8}{\omega_4^2+\omega^2} b_{20} \sin(\phi_{40}) + \frac{1}{8}\gamma_2 b_{20} \sin(\phi_{40}) \\
& + \frac{1}{8\omega a_{20}^2} \gamma_7 a_{10}^2 b_{20} \cos(2\phi_{20} - 2\phi_{10} + \phi_{40}) + \frac{1}{2\omega a_{20}^2} (\omega + \sigma)^2 f \sin(\phi_{20}),
\end{aligned}$$

$$\begin{aligned}
J_{83} = \frac{\partial F_8}{\partial b_{11}} = & -\frac{1}{2\omega} \gamma_5 b_{10} - \frac{1}{8\omega} (2\gamma_4 + \frac{\omega_3\gamma_{10}\eta_7}{\omega_3^2+\omega^2}) a_{10} \cos(\phi_{30}) - \frac{1}{8} (-2\gamma_6 + \frac{\gamma_{10}\eta_7}{\omega_3^2+\omega^2}) a_{10} \sin(\phi_{30}) - \frac{1}{8\omega} (\gamma_4 \\
& + \frac{\omega_3\gamma_{10}\eta_7}{\omega_3^2+\omega^2}) a_{10} \cos(2\phi_{20} - 2\phi_{10} - \phi_{30}) - \frac{1}{8} (-\gamma_6 + \frac{\gamma_{10}\eta_7}{\omega_3^2+\omega^2}) a_{10} \sin(2\phi_{20} - 2\phi_{10} - \phi_{30}) \\
& - \frac{1}{4\omega} \gamma_5 b_{10} \cos(2\phi_{20} - 2\phi_{10} - 2\phi_{30}),
\end{aligned}$$

$$\begin{aligned}
J_{84} = \frac{\partial F_8}{\partial b_{21}} = & \frac{-1}{2(\omega+\sigma_2)b_{20}^2} \eta_6 a_{20} \cos(\phi_{40}) - \frac{1}{2\omega} \gamma_3 b_{20} - (\frac{1}{2}\eta_3 + \frac{3}{8}\gamma_1 a_{20}^2 + \frac{1}{4}\gamma_7 a_{10}^2 + \frac{1}{4} \frac{\omega_4\gamma_8\eta_8}{\omega_4^2+\omega^2} a_{20}^2) \frac{\cos(\phi_{40})}{\omega a_{20}} \\
& - \frac{1}{4\omega} \gamma_3 b_{20} \cos(2\phi_{40}) + \frac{1}{8} \frac{\gamma_8\eta_8}{\omega_4^2+\omega^2} a_{20} \sin(\phi_{40}) + \frac{1}{8}\gamma_2 a_{20} \sin(\phi_{40}) - \frac{1}{8\omega a_{20}} \gamma_7 a_{10}^2 \cos(2\phi_{20} - 2\phi_{10} + \phi_{40}),
\end{aligned}$$

$$\begin{aligned}
J_{85} = \frac{\partial F_8}{\partial \phi_{11}} = & -\frac{1}{4\omega} (\alpha_2 - \alpha_5\omega^2 + \frac{(\omega_3^2-\omega^2)\gamma_{12}\eta_7^2}{(\omega_3^2+\omega^2)^2} + \frac{\omega_3\gamma_{13}\eta_7}{\omega_3^2+\omega^2} + \frac{\omega^2\gamma_{14}\eta_7}{\omega_3^2+\omega^2}) a_{10}^2 \sin(2\phi_{20} - 2\phi_{10}) + \frac{1}{4\omega} (\alpha_4\omega - \alpha_7\omega \\
& + \frac{2\omega_3\omega\gamma_{12}\eta_7^2}{(\omega_3^2+\omega^2)^2} - \frac{\omega\gamma_{13}\eta_7}{\omega_3^2+\omega^2} + \frac{\omega_3\omega\gamma_{14}\eta_7}{\omega_3^2+\omega^2}) a_{10}^2 \cos(2\phi_{20} - 2\phi_{10}) - \frac{1}{4\omega a_{20}} \gamma_7 a_{10}^2 b_{20} \sin(2\phi_{20} - 2\phi_{10} + \phi_{40}) \\
& - \frac{1}{4\omega} (\gamma_4 + \frac{\omega_3\gamma_{10}\eta_7}{\omega_3^2+\omega^2}) a_{10} b_{10} \sin(2\phi_{20} - 2\phi_{10} - \phi_{30}) + \frac{1}{4} (-\gamma_6 + \frac{\gamma_{10}\eta_7}{\omega_3^2+\omega^2}) a_{10} b_{10} \cos(2\phi_{20} - 2\phi_{10} - \phi_{30}) \\
& - \frac{1}{4\omega} \gamma_5 b_{10}^2 \sin(2\phi_{20} - 2\phi_{10} - 2\phi_{30}),
\end{aligned}$$

$$\begin{aligned}
J_{86} = \frac{\partial F_8}{\partial \phi_{21}} = & \frac{1}{4\omega} (\alpha_2 - \alpha_5\omega^2 + \frac{(\omega_3^2-\omega^2)\gamma_{12}\eta_7^2}{(\omega_3^2+\omega^2)^2} + \frac{\omega_3\gamma_{13}\eta_7}{\omega_3^2+\omega^2} + \frac{\omega^2\gamma_{14}\eta_7}{\omega_3^2+\omega^2}) a_{10}^2 \sin(2\phi_{20} - 2\phi_{10}) - \frac{1}{4\omega} (\alpha_4\omega - \alpha_7\omega \\
& + \frac{2\omega_3\omega\gamma_{12}\eta_7^2}{(\omega_3^2+\omega^2)^2} - \frac{\omega\gamma_{13}\eta_7}{\omega_3^2+\omega^2} + \frac{\omega_3\omega\gamma_{14}\eta_7}{\omega_3^2+\omega^2}) a_{10}^2 \cos(2\phi_{20} - 2\phi_{10}) + \frac{1}{4\omega a_2} \gamma_7 a_{10}^2 b_{20} \sin(2\phi_{20} - 2\phi_{10} + \phi_{40}) \\
& + \frac{1}{4\omega} (\gamma_4 + \frac{\omega_3\gamma_{10}\eta_7}{\omega_3^2+\omega^2}) a_{10} b_{10} \sin(2\phi_{20} - 2\phi_{10} - \phi_{30}) - \frac{1}{4} (-\gamma_6 + \frac{\gamma_{10}\eta_7}{\omega_3^2+\omega^2}) a_{10} b_{10} \cos(2\phi_{20} - 2\phi_{10} - \phi_{30}) \\
& + \frac{1}{4\omega} \gamma_5 b_{10}^2 \sin(2\phi_{20} - 2\phi_{10} - 2\phi_{30}) - \frac{1}{2\omega a_{20}} (\omega + \sigma)^2 f \cos(\phi_{20}),
\end{aligned}$$

$$\begin{aligned}
J_{87} = \frac{\partial F_8}{\partial \phi_{31}} = & \frac{1}{8\omega} (2\gamma_4 + \frac{\omega_3\gamma_{10}\eta_7}{\omega_3^2+\omega^2}) a_{10} b_{10} \sin(\phi_{30}) - \frac{1}{8} (-2\gamma_6 + \frac{\gamma_{10}\eta_7}{\omega_3^2+\omega^2}) a_{10} b_{10} \cos(\phi_{30}) - \frac{1}{8\omega} (\gamma_4 + \\
& \frac{\omega_3\gamma_{10}\eta_7}{\omega_3^2+\omega^2}) a_{10} b_{10} \sin(2\phi_{20} - 2\phi_{10} - \phi_{30}) + \frac{1}{8} (-\gamma_6 + \frac{\gamma_{10}\eta_7}{\omega_3^2+\omega^2}) a_{10} b_{10} \cos(2\phi_{20} - 2\phi_{10} - \phi_{30}) \\
& - \frac{1}{4\omega} \gamma_5 b_{10}^2 \sin(2\phi_{20} - 2\phi_{10} - 2\phi_{30}),
\end{aligned}$$

$$\begin{aligned}
J_{88} = \frac{\partial F_8}{\partial \phi_{41}} = & (\frac{1}{2}\eta_3 b_{20} + \frac{3}{8}\gamma_1 a_{20}^2 b_{20} + \frac{1}{4}\gamma_7 a_{10}^2 b_{20} + \frac{1}{4} \frac{\omega_4\gamma_8\eta_8}{\omega_4^2+\omega^2} a_{20}^2 b_{20}) \frac{\sin(\phi_{40})}{\omega a_{20}} + \frac{1}{4\omega} \gamma_3 b_{20}^2 \sin(2\phi_{40}) \\
& + \frac{1}{8} \frac{\gamma_8\eta_8}{\omega_4^2+\omega^2} a_{20} b_{20} \cos(\phi_{40}) + \frac{1}{8}\gamma_2 a_{20} b_{20} \cos(\phi_{40}) + \frac{1}{8\omega a_2} \gamma_7 a_{10}^2 b_{20} \sin(2\phi_{20} - 2\phi_{10} + \phi_{40}).
\end{aligned}$$

## References

1. Ji, J.C.; Yu, L.; Leung, A.Y.T. Bifurcation behavior of a rotor supported by active magnetic bearings. *J. Sound Vib.* **2000**, *235*, 133–151. [[CrossRef](#)]
2. Saeed, N.A.; Awwad, E.M.; El-Meligy, M.A.; Nasr, E.S.A. Radial Versus Cartesian Control Strategies to Stabilize the Non-linear Whirling Motion of the Six-Pole Rotor-AMBs. *IEEE Access* **2020**, *8*, 138859–138883. [[CrossRef](#)]

3. Ji, J.C.; Hansen, C.H. Non-linear oscillations of a rotor in active magnetic bearings. *J. Sound Vib.* **2001**, *240*, 599–612. [[CrossRef](#)]
4. Ji, J.C.; Leung, A.Y.T. Non-linear oscillations of a rotor-magnetic bearing system under superharmonic resonance conditions. *Int. J. Non-Linear Mech.* **2003**, *38*, 829–835. [[CrossRef](#)]
5. El-Shourbagy, S.M.; Saeed, N.A.; Kamel, M.; Raslan, K.R.; Abouel Nasr, E.; Awrejcewicz, J. On the Performance of a Non-linear Position-Velocity Controller to Stabilize Rotor-Active Magnetic-Bearings System. *Symmetry* **2021**, *13*, 2069. [[CrossRef](#)]
6. Saeed, N.A.; Mahrous, E.; Abouel Nasr, E.; Awrejcewicz, J. Non-linear dynamics and motion bifurcations of the rotor active magnetic bearings system with a new control scheme and rub-impact force. *Symmetry* **2021**, *13*, 1502. [[CrossRef](#)]
7. Zhang, W.; Zhan, X.P. Periodic and chaotic motions of a rotor-active magnetic bearing with quadratic and cubic terms and time-varying stiffness. *Nonlinear Dyn.* **2005**, *41*, 331–359. [[CrossRef](#)]
8. Zhang, W.; Yao, M.H.; Zhan, X.P. Multi-pulse chaotic motions of a rotor-active magnetic bearing system with time-varying stiffness. *Chaos Solitons Fractals* **2006**, *27*, 175–186. [[CrossRef](#)]
9. Zhang, W.; Zu, J.W.; Wang, F.X. Global bifurcations and chaos for a rotor-active magnetic bearing system with time-varying stiffness. *Chaos Solitons Fractals* **2008**, *35*, 586–608. [[CrossRef](#)]
10. Zhang, W.; Zu, J.W. Transient and steady non-linear responses for a rotor-active magnetic bearings system with time-varying stiffness. *Chaos Solitons Fractals* **2008**, *38*, 1152–1167. [[CrossRef](#)]
11. Li, J.; Tian, Y.; Zhang, W.; Miao, S.F. Bifurcation of multiple limit cycles for a rotor-active magnetic bearings system with time-varying stiffness. *Int. J. Bifurc. Chaos* **2008**, *18*, 755–778. [[CrossRef](#)]
12. Li, J.; Tian, Y.; Zhang, W. Investigation of relation between singular points and number of limit cycles for a rotor-AMBs system. *Chaos Solitons Fractals* **2009**, *39*, 1627–1640. [[CrossRef](#)]
13. El-Shourbagy, S.M.; Saeed, N.A.; Kamel, M.; Raslan, K.R.; Aboudaif, M.K.; Awrejcewicz, J. Control Performance, Stability Conditions, and Bifurcation Analysis of the Twelve-pole Active Magnetic Bearings System. *Appl. Sci.* **2021**, *11*, 10839. [[CrossRef](#)]
14. Saeed, N.A.; Kandil, A. Two different control strategies for 16-pole rotor active magnetic bearings system with constant stiffness coefficients. *Appl. Math. Model.* **2021**, *92*, 1–22. [[CrossRef](#)]
15. Wu, R.; Zhang, W.; Yao, M.H. Analysis of non-linear dynamics of a rotor-active magnetic bearing system with 16-pole legs. In Proceedings of the International Design Engineering Technical Conferences and Computers and Information in Engineering Conference, Cleveland, OH, USA, 6–9 August 2017. [[CrossRef](#)]
16. Wu, R.Q.; Zhang, W.; Yao, M.H. Non-linear dynamics near resonances of a rotor-active magnetic bearings system with 16-pole legs and time varying stiffness. *Mech. Syst. Signal Process.* **2018**, *100*, 113–134. [[CrossRef](#)]
17. Zhang, W.; Wu, R.Q.; Siriguleng, B. Non-linear Vibrations of a Rotor-Active Magnetic Bearing System with 16-Pole Legs and Two Degrees of Freedom. *Shock. Vib.* **2020**, *2020*, 5282904.
18. Ma, W.S.; Zhang, W.; Zhang, Y.F. Stability and multi-pulse jumping chaotic vibrations of a rotor-active magnetic bearing system with 16-pole legs under mechanical-electric-electro-magnetic excitations. *Eur. J. Mech. A/Solids* **2021**, *85*, 104120. [[CrossRef](#)]
19. Ishida, Y.; Inoue, T. Vibration suppression of non-linear rotor systems using a dynamic damper. *J. Vib. Control.* **2007**, *13*, 1127–1143. [[CrossRef](#)]
20. Saeed, N.A.; Awwad, E.M.; El-Meligy, M.A.; Nasr, E.S.A. Sensitivity analysis and vibration control of asymmetric non-linear rotating shaft system utilizing 4-pole AMBs as an actuator. *Eur. J. Mech. A/Solids* **2021**, *86*, 104145. [[CrossRef](#)]
21. Saeed, N.A.; Eissa, M. Bifurcation analysis of a transversely cracked non-linear Jeffcott rotor system at different resonance cases. *Int. J. Acoust. Vib.* **2019**, *24*, 284–302. [[CrossRef](#)]
22. Saeed, N.A.; Awwad, E.M.; El-Meligy, M.A.; Nasr, E.S.A. Analysis of the rub-impact forces between a controlled non-linear rotating shaft system and the electromagnet pole legs. *Appl. Math. Model.* **2021**, *93*, 792–810. [[CrossRef](#)]
23. Srinivas, R.S.; Tiwari, R.; Kannababu, C. Application of active magnetic bearings in flexible rotordynamic systems—A state-of-the-art review. *Mech. Syst. Signal Processing* **2018**, *106*, 537–572. [[CrossRef](#)]
24. Shan, J.; Liu, H.; Sun, D. Slewing and vibration control of a single-link flexible manipulator by positive position feedback (PPF). *Mechatronics* **2005**, *15*, 487–503. [[CrossRef](#)]
25. Ahmed, B.; Pota, H.R. Dynamic compensation for control of a rotary wing UAV using positive position feedback. *J. Intell. Robot. Syst.* **2011**, *61*, 43–56. [[CrossRef](#)]
26. Warminski, J.; Bochenski, M.; Jarzyna, W.; Filipek, P.; Augustylnak, M. Active suppression of non-linear composite beam vibrations by selected control algorithms. *Commun. Nonlinear Sci. Numer. Simul.* **2011**, *16*, 2237–2248. [[CrossRef](#)]
27. Omid, E.; Mahmoodi, S.N. Non-linear vibration suppression of flexible structures using non-linear modified positive position feedback approach. *Nonlinear Dyn.* **2015**, *79*, 835–849. [[CrossRef](#)]
28. Saeed, N.A.; Kandil, A. Lateral vibration control and stabilization of the quasiperiodic oscillations for rotor-active magnetic bearings system. *Nonlinear Dyn.* **2019**, *98*, 1191–1218. [[CrossRef](#)]
29. Diaz, I.M.; Pereira, E.; Reynolds, P. Integral resonant control scheme for cancelling human-induced vibrations in light-weight pedestrian structures. *Struct. Control Health Monit* **2012**, *19*, 55–69. [[CrossRef](#)]
30. Al-Mamun, A.; Keikha, E.; Bhatia, C.S.; Lee, T.H. Integral resonant control for suppression of resonance in piezoelectric micro-actuator used in precision servomechanism. *Mechatronics* **2013**, *23*, 1–9. [[CrossRef](#)]
31. Omid, E.; Mahmoodi, S.N. Non-linear integral resonant controller for vibration reduction in non-linear systems. *Acta Mech. Sin* **2016**, *32*, 925–934. [[CrossRef](#)]



32. MacLean, J.D.J.; Sumeet, S.A. A modified linear integral resonant controller for suppressing jump phenomenon and hysteresis in micro-cantilever beam structures. *J. Sound Vib.* **2020**, *480*, 115365. [[CrossRef](#)]
33. Omid, E.; Mahmoodi, S.N. Sensitivity analysis of the Non-linear Integral Positive Position Feedback and Integral Resonant controllers on vibration suppression of non-linear oscillatory systems. *Commun. Nonlinear Sci. Numer. Simul.* **2015**, *22*, 149–166. [[CrossRef](#)]
34. Saeed, N.A.; El-Shourbagy, S.M.; Kamel, M.; Raslan, K.R.; Aboudaif, M.K. Nonlinear Dynamics and Static Bifurcations Control of the 12-Pole Magnetic Bearings System Utilizing the Integral Resonant Control strategy. *J. Low Freq. Noise Vib. Act. Control* **2022**. [[CrossRef](#)]
35. Saeed, N.A.; Moatimid, G.M.; Elsabaa, F.M.; Ellabban, Y.Y.; Elagan, S.K.; Mohamed, M.S. Time-Delayed Non-linear Integral Resonant Controller to Eliminate the Non-linear Oscillations of a Parametrically Excited System. *IEEE Access* **2021**, *9*, 74836–74854. [[CrossRef](#)]
36. Saeed, N.A.; Mohamed, M.S.; Elagan, S.K.; Awrejcewicz, J. Integral Resonant Controller to Suppress the Non-linear Oscillations of a Two-Degree-of-Freedom Rotor Active Magnetic Bearing System. *Processes* **2022**, *10*, 271. [[CrossRef](#)]
37. Ishida, Y.; Yamamoto, T. *Linear and Non-Linear Rotordynamics: A Modern Treatment with Applications*, 2nd ed.; Wiley-VCH Verlag GmbH & Co. KGaA: New York, NY, USA, 2012.
38. Schweitzer, G.; Maslen, E.H. *Magnetic Bearings: Theory, Design, and Application to Rotating Machinery*; Springer: Berlin/Heidelberg, Germany, 2009.
39. Nayfeh, A.H.; Mook, D.T. *Non-Linear Oscillations*; Wiley: New York, NY, USA, 1995.
40. Nayfeh, A.H. Resolving Controversies in the Application of the Method of Multiple Scales and the Generalized Method of Averaging. *Nonlinear Dyn.* **2005**, *40*, 61–102. [[CrossRef](#)]
41. Vlase, S.; Năstac, C.; Marin, M.; Mihălcică, M. A method for the study of the vibration of mechanical bars systems with symmetries. *Acta Tech. Napoc.* **2017**, *60*, 539–544.
42. Slotine, J.-J.E.; Li, W. *Applied Non-Linear Control*; Prentice Hall: Englewood Cliffs, NJ, USA, 1991.
43. Yang, W.Y.; Cao, W.; Chung, T.; Morris, J. *Applied Numerical Methods Using Matlab*; John Wiley & Sons, Inc.: Hoboken, NJ, USA, 2005.